PhD THESIS

PROGRAMA DE DOCTORADO EN BIOLOGÍA MOLECULAR Y BIOMEDICINA

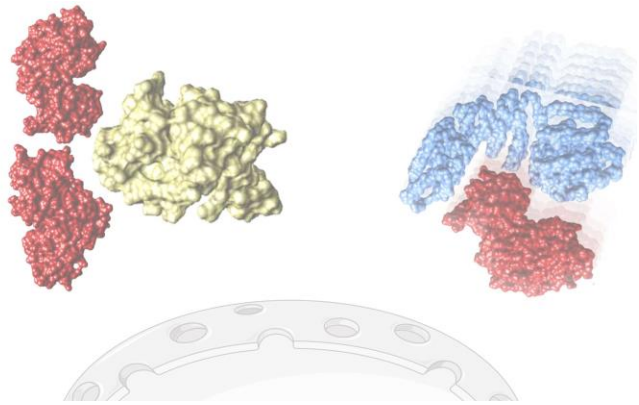

Serine 284 as a regulator of ERK2 dimerization and cellular localization

---

Serina 284 como regulador de la dimerización y de la localización celular de ERK2

VINCENZO CAPPITELLI | Santander, 2020

Dirigida por: **PIERO CRESPO BARAJA y BERTA CASAR MARTÍNEZ**

UNIVERSIDAD DE CANTABRIA

ESCUELA DE DOCTORADO DE LA UNIVERSIDAD DE CANTABRIA

UNIVERSIDAD DE CANTABRIA

PROGRAMA DE DOCTORADO EN BIOLOGÍA MOLECULAR Y BIOMEDICINA

TESIS DOCTORAL

Serina 284 como regulador de la dimerización y de la localización celular de ERK2

PhD THESIS

Serine 284 as a regulator of ERK2 dimerization and cellular localization

Realizada por: **Vincenzo Cappitelli**

Dirigida por: **Piero Crespo Baraja y Berta Casar Martínez**

Escuela de Doctorado de la Universidad de Cantabria| Santander, 2020

El Dr. PIERO CRESPO BARAJA, Profesor de Investigación del Consejo Superior de Investigaciones Científicas (CSIC) en el laboratorio de Regulación espacial de las señales RAS/ERK en cáncer en el departamento de Señalización celular y molecular ubicado en el Instituto de Biomedicina y Biotecnología de Cantabria (IBBTEC), como Tutor/Director de esta Tesis y la Dra. BERTA CASAR MARTÍNEZ, Investigadora del Consejo Superior de Investigaciones Científicas (CISC) en el mismo instituto, como co-Directora de esta Tesis

CERTIFICAN:

Que VINCENZO CAPPITELLI ha realizado bajo su dirección el presente trabajo de Tesis Doctoral en el Instituto de Biomedicina y Biotecnología de Cantabria (IBBTEC) titulado:

Serina 284 como regulador de la dimerización y de la localización celular de ERK2

Serine 284 as a regulator of ERK2 dimerization and cellular localization

Que consideran que dicho trabajo se encuentra terminado y reúne los requisitos necesarios para su presentación como Memoria de Doctorado al objeto de poder optar al grado de Doctor en Biología Molecular y Biomedicina por la Universidad de Cantabria.

Y para que conste y surta los efectos oportunos, expiden el presente certificado en Santander a 12 de marzo de 2020.

Fdo. Piero Crespo Baraja

Fdo. Berta Casar Martínez

La presente Tesis Doctoral titulada “Serine 284 as a regulator of ERK2 dimerization and cellular localization” ha sido realizada en el Instituto de Biomedicina y Biotecnología de Cantabria (IBBTEC) en el laboratorio de Regulación espacial de las señales RAS/ERK en cáncer gracias a la Ayuda para contratos predoctorales para la formación de doctores de la agencia estatal consejo superior de investigaciones científicas (BES-2016-077555) y a los proyectos financiados por:

Durante el presente trabajo Vincenzo Cappitelli ha realizado una estancia predoctoral de 3 meses y medio en el laboratorio del Dr. Adam Hurlstone en la Faculty of Biology, Medicine and Health de la Universidad de Manchester, Reino Unido, gracias a la ayuda para la realización de estancias en otros centros de i+d del ministerio de economía, industria y competitividad (BES-2016-077555).

Alla mia famiglia

RESUMEN

1. Introducción

La ruta de señalización mediada por las MAP quinasas ERK1 y 2 desempeña un papel esencial en el control de la proliferación, diferenciación y supervivencia celular, en condiciones fisiológicas. Esta ruta es activada en respuesta a una gran variedad de estímulos mitogénicos, como por ejemplo el factor de crecimiento EGF. La unión de EGF al receptor de membrana RTK, con actividad tirosina quinasa, conlleva la activación de RAS. Las proteínas RAS unen nucleótidos de guanina y actúan como interruptores moleculares. Una vez activada, RAS media la activación de RAF (MAPKKK), la cual desencadena el mecanismo de activación secuencial, por fosforilación, de MEK1/2 (MAPKK) y finalmente de ERK1/2 (MAPK), que se fosforila en treonina 185 y tirosina 187.

Las proteínas ERK1/2, una vez activadas en el citoplasma, dimerizan y regulan la activación de un gran número de sustratos, citoplasmáticos y nucleares (más de 400). Las señales de ERK están reguladas por varios tipos de proteínas reguladoras, como por ejemplo las proteínas "scaffold". Dichas proteínas ensamblan a los distintos componentes de la cascada en un complejo multi-enzimático, mediante el cual regulan y afinan la intensidad, amplitud y duración de las señales. Además, estas proteínas tienen un papel importante en la regulación espacio-temporal de la señalización de ERK. Estudios previos en nuestro laboratorio han demostrado que las proteínas scaffold regulan de manera sitio-especifica la activación de la cascada de señalización MAP Kinasa, uniéndose a dímeros de ERK. De esta forma la dimerización de ERK sería un punto crítico para la activación de los substratos citoplasmáticos y su retención en el citoplasma. Por otro lado, se ha descrito el mecanismo de translocación de ERK al núcleo. Según este modelo, ERK una vez fosforilada en dos serinas (motivo SPS) entra al núcleo a través de los poros nucleares unido a la Importina 7.

Un gran número de estudios demuestran incuestionablemente la implicación de la ruta de señalización RAS-ERK en la aparición y progresión de muchos tumores. Aproximadamente el 40% de los tumores humanos portan mutaciones activadoras en algún miembro de la cascada de señalización RAS-ERK, en

particular RAS G12V y B-RAF V600E. En melanoma, esta cifra es aún más alta, con un 15-20% de melanomas que presentan mutaciones N-RAS, mientras que el oncogén B-RAF aparece mutado en el 50-60% de los casos. Consecuentemente, en los últimos años, tanto la investigación básica como la industria farmacéutica, han dedicado un enorme esfuerzo en la búsqueda y desarrollo de fármacos destinados a bloquear las señales oncogénicas que fluyen a través de la ruta RAS-ERK. Los inhibidores de las quinasas B-RAF y MEK se destacan como agentes terapéuticos muy prometedores para el tratamiento del melanoma. Los inhibidores de RAF, como el Vemurafenib (PLX4032), han mostrado una espectacular eficacia clínica en melanomas con mutaciones en BRAF V600E. Además, se han testado, con mucho éxito clínico, los inhibidores alostéricos de MEK1/2, como el trametinib (GSK 1120212) y se ha visto que son más efectivos en pacientes con mutaciones B-RAF. En ambos casos, la eficacia terapéutica es proporcional al grado de supresión de actividad de ERK. Si bien estos fármacos logran importantes remisiones en pacientes con melanoma (B-RAF V600E), la respuesta es muy variable y las remisiones completas son raras. De hecho, la mejoría es breve y los pacientes tratados con dichos inhibidores desarrollan resistencia, con lo que la enfermedad acaba progresando fatalmente. En melanoma, los mecanismos de resistencia por sí solos conllevan una reactivación aberrante de la señalización de ERK. Por lo tanto, números estudios se están centrando en la inhibición de la activación de ERK o en la combinación de diferentes inhibidores que puedan actuar a distintos niveles de la cascada de señalización. En este sentido, se está revelando de especial importancia la inhibición de la interacción proteína-proteína. De esta forma, se inhibe la proteína de interés sin afectar completamente a su actividad kinasa, y además de manera compartimental. Es decir, inhibiendo ERK de manera que active solo substratos nucleares o citoplásmicos, se evitan los fenómenos de resistencia asociados al efecto rebote que surgiría inhibiendo completamente su actividad kinasa. Es el caso del péptido EPE, que bloqueando la unión de ERK y la IMP7 inhibe la entrada de ERK al núcleo y por lo tanto la activación de substratos nucleares, causando apoptosis en células de melanoma con mutación B-RAF. Siguiendo la misma línea, en nuestro laboratorio, se ha demostrado la eficacia de DEL22379, un potente inhibidor, capaz de inhibir la dimerización de ERK2, sin afectar su

fosforilación. DEL22379 induce apoptosis en líneas celulares de melanoma y de cáncer de colon que presentan mutaciones activadoras en BRAF y en RAS. Además, se ha visto que DEL22379 no está afectado por los mecanismos de resistencia que se han descrito en otros inhibidores.

En nuestro estudio hicimos la sorprendente observación de que DEL22379 no afectaba la dimerización de ERK en el modelo de embriones de pollos usado para estudiar el melanoma. A raíz de este hallazgo, nuestros análisis posteriores desvelaron que la dimerización de ERK es especifica de mamíferos, lo que sugiere una diferencia evolutiva en cuanto a la dimerización de ERK se refiere. Además, se demostró como esta capacidad de dimerizar no depende del contexto celular si no que de la característica de las proteínas de ERK en las distintas especies. Sabiendo que la dimerización de ERK es esencial para la activación de substratos citoplásmicos era muy interesantes estudiar cuales fuesen las diferencias de ERK en las distintas especies e intentar elucidar un poco más a fondo los mecanismos que regulan su distribución celular.

2. Objetivos:

1. Estudiar el papel de la fosforilación de la Ser284 en la dimerización de ERK y su localización célular.
2. Elucidar los procesos bioquímicos y los efectos biológicos derivados de la fosforilación de ERK2 en Ser284.
3. Determinar la relevancia de la fosforilación de ERK2 en Ser284 en procesos de carcinogénesis y establecer su uso como un diagnostico de prognosis en melanoma.

3. Materiales y Métodos

Para estudiar el papel de la Ser284 en la dimerización de ERK2 se generaron mutantes de ERK2 en dichos residuos, sustituyendo la serina por una prolina (S>P), un aspártico (S>D) o un glutámico (S>E). Se analizó la dimerización de estos mutantes tanto por geles nativos como por “Philipova & Witaker” PAGE.

Se generó un anticuerpo fosfoespecífico frente al residuo Ser284 de ERK2 para analizar su fosforilación.

Para la identificación de la kinasa responsable de la fosforilación en dicho residuo se hizo un silenciamiento de todas las Ser/Thr kinasas conocidas usando RNA de interferencia y se corroboró su efectiva actividad por ensayo kinasa *in vitro.*

Para estudiar la localización de dicho residuo se efectuaron tantos ensayos de fraccionamientos núcleo/citoplasma como de análisis de inmunofluorescencias.

Para analizar el papel de las kinasas y cómo influyen la interación de ERK con los scaffolds se realizaron ensayos de co-inmunoprecipitación, tras silenciamiento con RNAi o usando inhibidores especifico frente a la kinasa involucrada.

Para estudiar las funciones bioquímicas de la Serina284 se hicieron estudios de la cinética de fosforilación de ERK en los residuos canónicos y se analizó su actividad kinasa por western blot, tras inmunoprecipitar los distinctos constructos. Para analizar la implicación biológica de la Ser284 se generaron líneas estables de MEF ERK1-/-; ERK2 flox/flox y se analizó su actividad proliferativa por método colorimétrico. Además, mediante el uso de la tecnología de CRISPR/Cas9, se generaron ratones donde se substituyó la Ser284 por una prolina, generando un modelo animal donde ERK2 no dimeriza. Símilmente se está intentando generar un modelo de pez cebra donde ERK2 dimeriza, substituyendo la prolina por la Ser284.

Para establecer la relación entre fosforilación en Ser284 y susceptibilidad a Vemurafenib en melanoma se analizó el patrón de p-Ser284 en distintas líneas de melanoma con mutaciones activadoras en B-RAF y N-RAS, así como se compararon los niveles de p-Ser284 en líneas de melanoma B-RAF sensibles o resistentes al tratamiento con Vemurafenib. Finalmente se analizaron los niveles de p-Ser284 en muestras de pacientes de melanoma por inmunohistoquímica.

4. Resultados y Discusión

En este estudio hemos encontrado que la diferencia entre mamíferos y otras especies, en términos de secuencia aminoacídica, reside en el cambio de tan solo un aminoácido: habiendo una serina en aquellas especies donde ERK2 dimeriza (Ser284 en humano) y una prolina en las especies dónde ERK2 no dimeriza. Por tanto, la Ser284 en ERK2 podría tener un papel importante en su dimerización. Para dilucidar este asunto, hemos generado mutantes de ERK2 cambiando dicha serina por una prolina (S>P) y dos mutantes fosfomiméticos (S>E/D). Analizado la dimerización de dichos mutantes, observamos que el mutante S>P pierde su capacidad de dimerización mientras que los fosfomiméticos dimerizan, pero solamente tras estimulación por EGF, lo cual indica que la fosforilación de este residuo es necesaria pero no suficiente. Siendo un residuo fosforilable de ERK hemos generado un anticuerpo fosfo-específico y hemos encontrado que ERK2, únicamente en su estado dimérico, está fosforilado en dicho residuo y que además tanto p-Ser284, como los dimeros de ERK2, tienen localización exclusivamente citoplasmática. Por tanto, la fosforilación en Ser284 constituye un marcador inequívoco de los niveles de ERK activado en citoplasma. Además, hemos descubierto que para la dimerización se necesita que los dos monómeros de ERK estén fosforilados en Ser284.

Para identificar las kinasas implicadas en la fosforilación de las Ser284 hemos hecho un screening de silenciamiento por RNAi de todas las Ser/Thr kinasa del genoma humano. Hemos identificado que tanto MEK1 como AKT1 fosforilan este residuo y que se trata de una fosforilación directa, como indican los resultados de ensayo kinasa *in vitro*. Este hallazgo abre el abanico de sustratos fosforilados por MEK y por AKT1, rompiendo de alguna manera la especificidad dual de MEK1, siendo una Thr/Tyr kinasa. Símilmente, aunque Ser284 por su secuencia consenso y ERK misma, no es un substrato de AKT1, nuestros resultados demuestran que AKT fosforila la Ser284, añadiendo así un nuevo sito de fosforilación mediado por AKT.

Hemos demostrado que el residuo Ser284 es importante para la localización citoplásmica de ERK en condiciones de reposo. Además, hemos comprobado

que la fosforilación de la Ser284 aumenta la afinidad con proteínas scaffold, como por ejemplo KSR1. Por tanto, este residuo es un importante regulador de la distribución subcelular de ERK. El trasportador que regula los niveles basales de ERK en el núcleo podría ser la Importina7, aunque no se descartan que existan otros tipos de transportadores que regulan la entrada de ERK al núcleo bajo estímulatión. De hecho, como se evidencia en el análisis de microscopía (*time lapse*) en células viva, la fosforilación de este residuo no está implicada en la cinética de entrada de ERK al núcleo.

Hemos analizado como este residuo puede afectar la fosforilación de ERK en los residuos canónicos y actividad kinasa. Para ello hemos comparado la fosforilación en el motivo TEY de los distintos mutantes de ERK obteniendo que no existe una diferencia significativa entre los distintos mutantes. De la misma manera, se ha analizado la actividad kinasa de ERK analizando su capacidad de fosforilación de MBP y como esa dependa de la presencia de la Ser284. Observamos una ligera diferencia significativa, entre el mutante que no dimeriza (S>P) y el WT, siendo más intensa la actividad del ERK WT. Además, se ha estudiado la secuencia de eventos que llevan a la dimerización de ERK y su fosforilación en TEY y en Ser284, observando que dichas fosforilaciones ocurren de forma simultánea, indicando que tanto la dimerización como la fosforilación en Ser284 ocurren al mismo tiempo.

Se ha estudiado la dependencia de la fosforilación en Ser284 en términos de viabilidad celular. Los resultados muestran una reducción de la viabilidad de las células MEF ERK S>P, aunque esta reducción podría ser atribuible al hecho que dicho mutante tiene un nivel de expresión más bajo, comparado con los demás. Similarmente, hemos generado unos ratones modificado genéticamente, donde ERK2 no dimeriza, habiendo substituido la Serina284 por una Prolina. Actualmente no parece que dicha substitución esté afectando la viabilidad ni el normal desarrollo de estos ratones. Cabiendo la posibilidad de que ERK1 esté enmascarando el fenotipo derivante por la substitución S>P, nuestro próximo objetivo será cruzar estos ratones con ratones ERK1-/-, de manera que la única isoforma de ERK presente sea la de ERK2 S>P. Para intentar dilucidar las ventajas, si así se tratara, derivantes de la dimerización de

ERK, estamos intentando generar unos peces cebra donde ERK dimeriza. Estos modelos nos darán respuestas de que ventaja tiene la dimerización de ERK, además de servir como modelo para dilucidar el papel de la dimerización en procesos de carcinogénesis, como por ejemplo el melanoma.

Finalmente, sabiendo que la susceptibilidad al tratamiento con Vemurafenib de pacientes con melanoma portadores de la mutación B-RAF V600E se correlaciona con los niveles de ERK activada en citoplasma, mejor que con los niveles totales de ERK fosforilada y considerando que la fosforilación del residuo Ser284 es un marcador univoco de ERK fosforilada en el citoplasma, nuestro propósito ha sido dilucidar si los niveles de Ser284 fosforilada podrían establecerse como un marcador de susceptibilidad y de respuesta a Vemurafenib, más fiable que los niveles de ERK fosforilada en los residuos canónicos. Para ellos hemos comparado distintas líneas celulares de melanoma, con mutaciones activadoras en B-RAF y N-RAS, así como clones celulares B-RAF tanto resistentes como sensibles al tratamiento con Vemurafenib. Hemos comprobado que la fosforilación de ERK en Ser284 es más alta en aquellas células que resultan ser más sensibles al tratamiento con el inhibidor de B-RAF, pudiendo ser un marcador de sensibilidad a este tipo de tratamiento. Con respecto a esto, hemos analizado los niveles de fosforilación de Ser284 en muestras de pacientes. Los resultados, si bien preliminares, indican que existe dicha correlación y por lo tanto este análisis de fosforilación en Ser284 podría incluirse como marcador de sensibilidad al tratamiento con Vemurafenib en aquellos pacientes de Melanoma con mutación B-RAF. De ser así, se podría hacer una estratificación precoz para identificar aquellos pacientes que sí responderán al tratamiento, frente a aquellos que serán resistentes, ahorrando inútiles efectos indeseados, tiempo y dinero. Además, este tipo de diagnóstico podría extenderse no solo a la detección de pacientes con melanoma sensibles al tratamiento, sino que también a pacientes que padecen otros tipos de tumores portadores de la mutación B-RAF.

5. Conclusiones

1. La fosforilación en Ser284 es necesaria pero no suficiente para la dimerización de ERK2.
2. Ambos monómeros de ERK2 tienen que estar fosforilados en Ser284 para que ERK2 dimerice.
3. AKT1 and MEK1 son las principales kinasas responsables de fosforilar el residuo Ser284 en ERK2.
4. La fosforilación de la Ser284 de ERK2 tiene localización exclusivamente citoplásmica.
5. La fosforilación Ser284 aumenta la afinidad de ERK2 por la proteína scaffold KSR1. Por lo contrario, disminuye la afinidad para transportadores nucleares como la importina 7.
6. La sensibilidad al tratamiento con Vemurafenib de las células de melanoma portadoras de la mutación BRAF se correlacionan con unos niveles más altos de fosfo-Ser284. Por lo tanto, los niveles de p-Ser284 podrían ser utilizados como un biomarcador de susceptibilidad al tratamiento con Vemurafenib en pacientes con melanoma portadores de BRAF mutado.

INDEX

INDEX

ABBREVIATIONS

Abbreviation

AKT	Protein Kinase B
APE	End of Activation Segment
Arg, R	Arginine
Asp, D	Aspartate
ATP	Adenosine triphosphate
BBS	Borate Buffered Saline
BSA	Bovine Serum Albumin
BSU	Biological Service Unit
CD	Common domain. MAP kinase D-recruitment domain
cDNA	Complementary DNA
CFP	Cyan Fluorescent Protein
CK2	Casein kinase 2
Co-IP	Co-ImmunoPrecipitacion
cPLA2	Cytosolic Phospholipase A2
CRD	Cysteine-Rich Domain
CRISPR	clustered regularly interspaced short palindromic repeats
CRM1	Chromosomal Maintenance 1
Cys, C	Cysteine
D/H pf	Day/Hour post-fertilization
DAB	Diaminobenzidine
DAPK	Death-associated protein kinase
DFG	Beginning of Activation Segment
DTT	Dithiothreitol
DUSP	Dual Specificity Phosphatase
DVD	Domain of Variable Docking
ECL	Enhanced chemiluminescent system
EDTA	Ethylenediaminetetraacetic acid
EGF	Epidermal Growth Factor
EGFR	Epidermal Growth Factor Receptor
EGTA	Ethylene glycol-bis(β-aminoethyl ether)-N,N,N′,N′-tetraacetic acid
ERK	Extracellular Signal-Regulated kinase
FBS	Fetal bovine serum
GAP	GTPase Activating Protein
Gbr2	Growth Factor Receptor-Bound Protein 2
Glu, E	Glutamate
GTP	Guanosine Triphosphate
HDR	ERK Catalytic loop
HDR	Homology-directed repair
HEPES	N-(2-Hydroxyethyl)piperazine-N'-(2-ethanesulfonic acid)
His, H	Histidine
HRP	Horseradish Peroxidase
IMP	E3 ubiquitin ligase
IMP7	Importin7
IPTG	isopropyl-β-d-thiogalactopyranoside
IQGAP	Ras GTPase-activating-like protein
JNKs	c-Jun amino (N)-terminal kinases
Kd	Dissociation Constant

KIM	kinase interaction motif
KSR	kinase suppressor of Ras
LB	Luria-Bertani Broth
Leu, L	Leucine
LFQ	Label Free Quantification
Lys, K	Lysine
MAGI1	Membrane Associated Guanylate Kinase
MAP2	Microtubule-Associated Protein Kinase 2
MAPK	Mitogen-Activated Protein Kinase
MBP	Myelin Basic Protein
MEK	Mitogen-Activated Protein Kinase Kinase
MKP	MAP Kinase Phosphatase
MLK	Mixed Lineage Kinase
MP1	MEK partner 1
MS	Mass Spectrometry
MS22	ethyl 3-aminobenzoate methanesulfonate
NES	Nuclear Exportation Signals
NGF	Nerve growth factor
NLS	Nuclear Localization Signal
NMR	Nuclear magnetic resonance
NTS	Nuclear Translocation Signal
NUPs	Nucleoporines
O/N	overnight
PAK1	p21-Activated Kinase 1
PAM	Protospacer adjacent motif
PBS	Phosphate-Buffered Saline
PCR	Polymerase Chain Reaction
PDGF	Platelet-Derived Growth Factor
PEA15	Phosphoprotein-Enriched in Astrocytes 15
PEI	Polyethylenimine
PFA	Paraformaldehyde
Phe, F	Phenylalanine
PI3K	Phosphatidylinositol-3 Kinase
PKA	Protein kinase A
PKC	Protein Kinase C
PNPP	p-nitrophenyl phosphate disodium
PP2A	Protein Phosphatase 2A
Pro, P	Proline
PTEN	Phosphatase and Tensin Homolog
PTP	Protein-Tyrosine Phosphatases
PTPrK	Protein Tyrosine Phosphates Receptor-type k
PVC	Polyvynilchloride
RAF	Rapidly Accelerated Fibrosarcoma
Ran GTP	Ras-Like Nuclear GTP
RAS	Small GTPase Protein
RAS GEF	Ras Guanine Nucleotide Exchange Factor
RBD	RAS-binding domain
RKIP	RAF Kinase Inhibitor Protein
RTK	Tyrosine Kinase Receptor
SDS	Sodium dodecyl sulfate

SEF	Similar expression to FGF protein
Ser, S	Serine
sgRNA	Single guide RNA
SHC	SH2-Containg Protein
SOS	Son of Sevenless. RAS GEF
ssODN	single-stranded donor oligonucleotides
STEP	Striatal-Enriched Tyrosine Phosphatases
TAE	Tris-acetate-EDTA
TBS-T	Tris Buffered Saline-Tween
Thr, T	Threonine
Tm5NM1	Tropomyosin isoform 5 non-muscle 1
Tyr, Y	Tyrosine
Val, V	Valine

1. INTRODUCTION

1.1 MAP KINASES: a general overview

Protein kinases are a class of enzymes capable to phosphorylating specific substrates, thereby regulating their activity. To regulate their substrates, the enzyme catalyses the transfer of a phosphoryl group (PO3-) from a donor molecule, such as ATP, to a protein. Depending on the aminoacid acting as the phospho-acceptor, these kinases are classified as protein-serine/threonine kinases or protein-tyrosine kinases. It has been estimated that about 2% of the human genome encodes for protein kinases, 518 human protein kinases genes having been identified (Roskoski, 2012a).

Within the protein kinases, the MAPK (Mitogen-Activated Protein Kinase) family is one of the best studied. This family is evolutionary conserved, being present in all eukaryotes, and under the control of different extracellular stimuli, it can regulate fundamental cellular processes such as proliferation, differentiation, survival and apoptosis. (Cargnello and Roux, 2011).

The MAPK family has been divided into four subfamilies: the extracellular signal-regulated kinases; c-Jun amino (N)-terminal kinases, stress-activated protein kinases; p38; and ERK5. These subfamilies share the common characteristic of being activated by a three-tier kinase core formed by: MAPKKKs, which are Ser/Thr kinases; these activate MAPKKs, which are dual-specificity kinases, that once activated phosphorylate MAPKs on Thr and Tyr (TXY motif). Once activated, MAPKs exert their functions by phosphorylating multiple cytoplasmatic and nuclear substrates (Fig.1.1). These MAPK modules are activated at their origin by small GTPase of the RAS family (Cargnello and Roux, 2011; Plotnikov et al., 2011; Roskoski, 2012a; Turjanski et al., 2007).

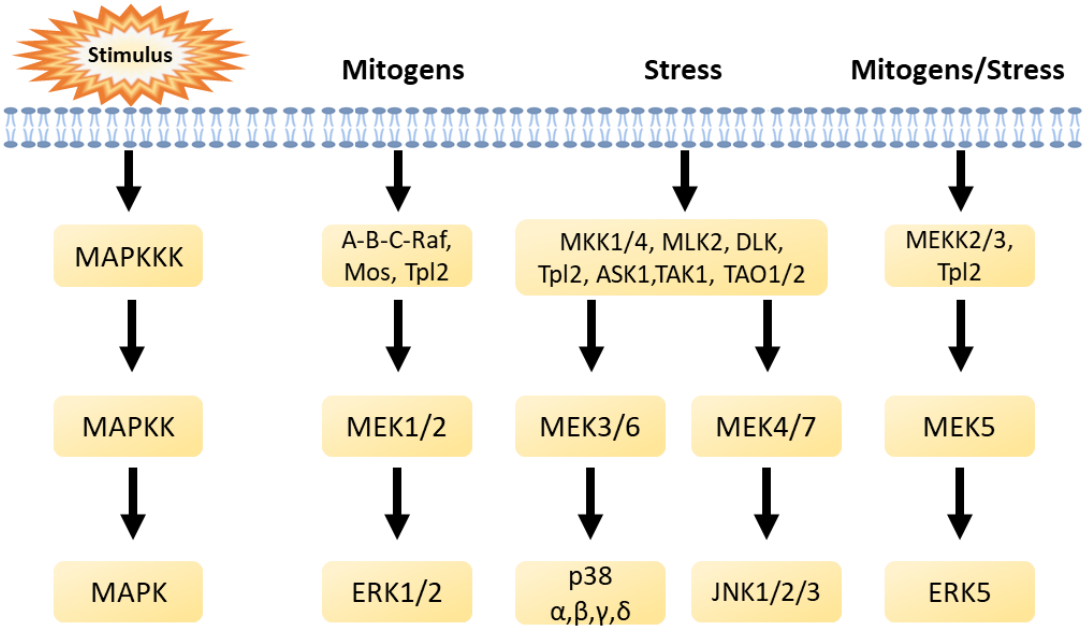

Figure 1.1. General scheme of the four classical MAPK signalling pathways. Each cascade is represented as a three-tiered kinase which include a MAP kinase kinase kinase (MAPKKK), a MAP kinase kinase (MAPKK) and the MAPK. Depending on the pathway, activated MAPK regulates different biological outcomes.

- **ERKs** (Extracellular signal regulated kinases) ERK1/2, also known as p44 and p42 respectively, due to their molecular weight. They were the first MAPKs to be identified and cloned (Boulton et al., 1991). Members of this family are mainly activated by growth factors. The two isoforms are ubiquitously expressed, with high levels in brain, muscle, thymus and heart. Two ERK1 alternative splicing isoforms have been described: ERK1b and ERK1c. There is also an ERK2 splicing isoform, named ERK2b (Cargnello and Roux, 2011). All of the above mentioned ERKs share a common phosphorylation motif, TEY, in the activation loop.
- **JNKs** (c-Jun (N)-terminal Kinases) are also known as Stress Activated Protein kinases (SAPKs) since were originally identified as mediators of intra- and extra-cellular stress (Davis, 1994). Three JNK isoforms (JNK 1, 2 and 3) have been identified encoded by three different genes, which express up to 10 different splicing isoforms. The JNK isoforms become active when phosphorylated in their TPY motif in response to various form of cellular stress (Cargnello and Roux, 2011).

- **p38 MAPKs**. p38, also known as CSBP, mHOG1, RK and SAPK2, it was described for the first time by three groups (Han and Ulevitch, 1994; Lee et al., 1994; Rouse et al., 1994). Structurally, they share 50% of aminoacidic identity with ERK2. Four p38 isoforms have been identified: p38 α and p38 β, which are ubiquitously distributed and p38 γ and p38 δ, which, by contrast, have a more restricted expression pattern. In mammals, p38 kinases are activated in response to stress signals and inflammatory cytokines, by phosphorylation on their TGY motif (Cargnello and Roux, 2011).

  Besides the classical p38 isoforms, there have been described other isoforms of p38, encoded by alternative splicing. This is the case of Mxi2 (Zervos et al., 1995), a p38 isoform where the last 80 C-terminal aminoacids are replaced by 17 amino acids not found in the classic isoforms, which gives it unique characteristics and different functions (Sanz-Moreno et al., 2003).

- **ERK5/BMK1** is also known as big MAP kinase 1, due to its size. In fact, ERK5 is twice bigger (110 kDa) than other MAPKs. In spite of being structurally similar to ERK2, sharing approximately 50% of its sequence, ERK5 shows a long C-terminal domain, with no similarity with other MAPKs. Actually, the C-terminal domain contains a nuclear localization signal (NLS) and a proline-rich domain (Lee JD, Ulevitch RJ, 1995). ERK5 is mainly activated by growth factors, oxidative stress and hyperosmolarity (Wang et al., 2006). The phosphorylation motif is TEY, like ERK MAPKs.

1.2 The RAS-ERK signalling pathway

The RAS-ERK pathway is certainly one of the best-characterized signalling cascades. This is likely due to its relevant role in essential functions within cells. In fact, in response to multiple stimuli, this signalling pathway regulates pivotal functions, such as proliferation, differentiation, apoptosis, among others (Roskoski, 2012a). The interest for investigating this pathway not only arises from its implications in the regulation of physiological processes. This pathway appears dysregulated in a large variety of diseases, where cancer holds the main position.

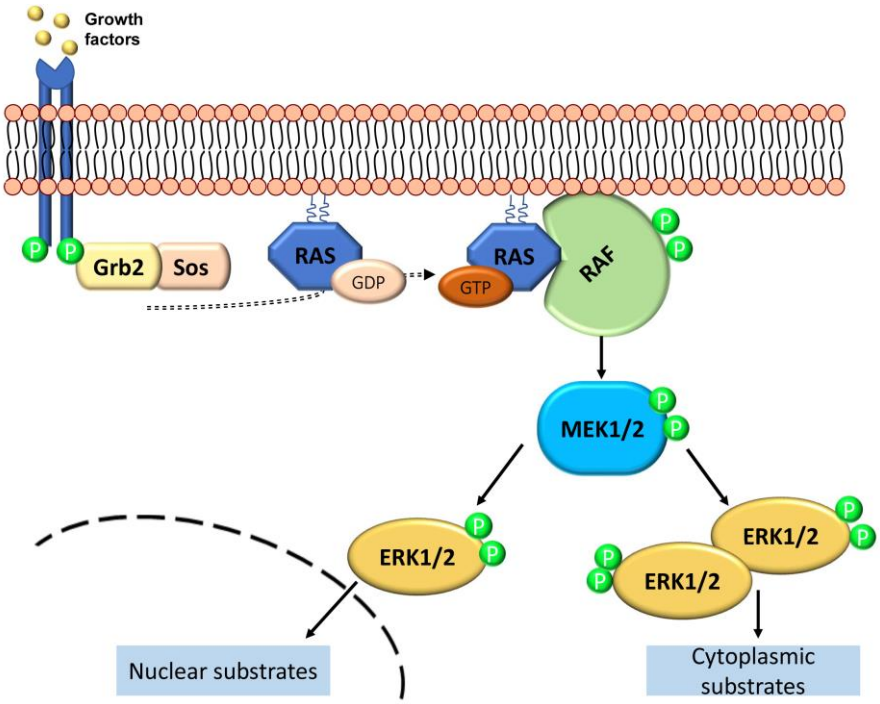

Figure 1.2. RAS-ERK signalling pathway. Upon stimulation mediated by growth factors, receptor tyrosine kinase auto-phosphorylates on its tyrosine residues and dimerize. This allows the recruitment of Grb2, which in turn bind to the guanine nucleotide exchange factor (GEF) SOS. SOS operates on RAS, inducing the interchange of GDP (inactive form) for GTP (active form). GTP-RAS recruits RAF to the membrane where it is activated. RAF phosphorylates MEK1/2 which, in turn, phosphorylates ERK1/2. Activated ERK, may dimerize and phosphorylate a large variety of cytoplasmic substrates or it can translocate into the nucleus as a monomer where it activates transcription factors. P stands for phosphoryl group.

RAS activation is triggered by the interaction of growth factors (such as EGF, PDGF, among others) with cell-surface receptors. The binding of these agonists

to their cognate receptors, mainly tyrosine kinase receptor (RTKs), induces their dimerization and, subsequently, their autophosphorylation on tyrosine residues.

Phosphorylated receptors recruit SHC (SH2-containg protein) and Gbr2 (growth factor receptor-bound protein 2) adapter proteins to the plasma membrane. Gbr2 is constitutively bound to the RAS guanine nucleotide exchange factor, SOS (son of sevenless), which is designed to interchange GDP for GTP. The Grb2/SOS complex promotes RAS activation at the plasma membrane. RAS is a small GTPase that by interchanging GDP for GTP becomes active. Active RAS has several downstream effector pathways, including the ERK1/2 pathway (Wortzel and Seger, 2011). RAS-GTP go through a conformational change which make it able to bind RAF (MAPKKK) at the plasma membrane contributing to its activation (Liu et al., 2018).

Phosphorylated RAF propagates the activation signal to its downstream substrate, by phosphorylating MEK1/2 (MAPKK), which in turn phosphorylates and activates ERK1/2 (MAPK).

Activated ERKs can dimerize and regulate the activity of an huge number of cytoplasmic substrates. Alternatively, activated ERK monomers can enter the nucleus where they carry out regulatory functions on nuclear substrates (Casar et al., 2009; Ünal et al., 2017).

1.2.1 RAF

RAF family proteins are the first kinases involved in the propagation of signals through the RAS-ERK pathway.

The *v-raf* (rat fibrosarcoma) oncogene was identified in the oncogenic mouse sarcoma virus. *V-raf,* together with the homologue avian virus oncogene, *v-mil*, were described as proteins showing Ser/Thr kinase activity (Moelling et al., 1984). The first human RAF proto-oncogene identified was C-RAF or RAF1 (Vdzina et al., 1984). Subsequentially, two other mammalian isoforms were described, named A-RAF (Huebner et al., 1986) and B-RAF (Ikawa et al., 1988).

The three RAF isoforms are structurally similar, sharing three conserved regions (CR1-3) (Fig.1.3). The first region (CR1), located at the N-terminus, has two domains: the cysteine-rich domain (CRD), a regulatory region, and the RAS-binding domain (RBD), essential for its interaction with RAS. The second one (CR2) is composed of a long sequence rich in Ser and Thr residues, involved in the inhibition of RAF activation and its binding to RAS. The third conserved region (CR3) corresponds with the kinase domain, whose phosphorylation is essential for its kinase activity (Migliaccio et al., 2013).

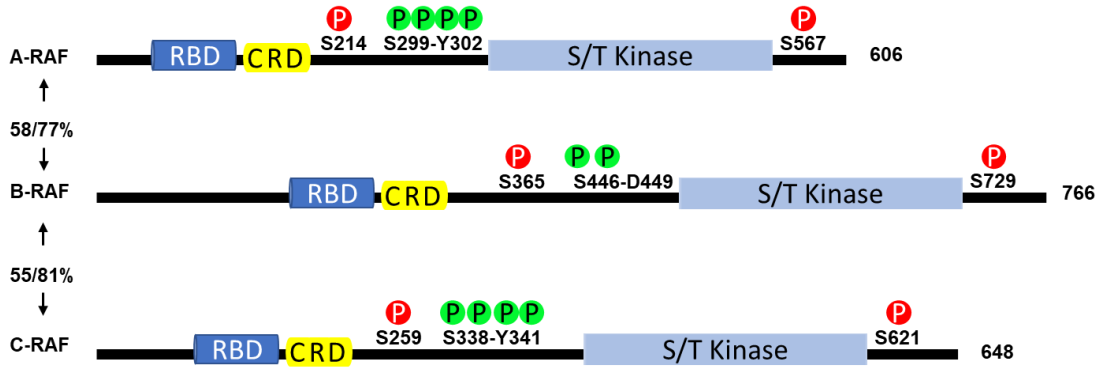

Figure 1.3 Representation of the three RAF isoforms. (%/%) refer to the total protein and kinase domain sequence identity. RBD stands for RAS binding domain, indicating the first conserved region of RAF, together with the CRB (cysteine-rich domain). Phosphorylatable residues are represented by P coloured circle. Red circles indicate negative regulator residues whereas green circles show activator residues. Adapted from (Ryan et al., 2015).

In resting cells, RAF is in an auto-inhibited state, where the N-terminal regulatory region is folded over the catalytic region, repressing its activity. This process involves the phosphorylation of C-RAF at Ser 259 (or its equivalent site, Ser 365, in B-RAF) and it is mediated by Protein kinase A (PKA) (Dhillon et al., 2002) and AKT (Moelling, 1999). RAF is also negatively regulated by 14-3-3 proteins, which bind to RAF upon Ser259/Ser621 phosphorylation, and whose interaction stabilizes C-RAF in its inactive form (Michaud et al., 1995; Procaccia et al., 2017).

RAF activation is a multi-step process. The recruitment of RAF to the plasma membrane is the first step and it is mediated by RAS-GTP. RAF

interacts with RAS through its RBD domain. In addition, the CRD (cysteine rich-domain) domain also seems to be crucial for C-RAF anchoring to the plasma membrane (Bondeva et al., 2002). RAS binding also promotes the dephosphorylation of the inhibitory 14-3-3 binding sites, a process that involves two protein phosphatases (PP2A and PP1) (Jaumot and Hancock, 2001). This dephosphorylation promotes the release of 14-3-3 from RAF N-terminus, allowing its recruitment to the plasma membrane.

Another regulatory mechanism in RAF activation involves the dimerization of active B-RAF and C-RAF, also mediated by RAS (Rushworth et al., 2006). B-RAF and C-RAF homodimers have also been described, even though they are less stable than heterodimers. The dimerization and activation of RAF proteins is mediated by KSR (kinase suppressor of RAS) interaction. Crystallographic structural analysis highlight that the interaction between human B-RAF kinase domain and KSR1 is “side-to-side”, being B-RAF Arg509 residue at the heart of this interface, establishing a network of hydrogen bonds between the two proteins. In this regard, point mutations in Arg509 have highlighted the relevance of this residue, since Arg509His disrupts RAF dimerization reducing its kinase activity (Rajakulendran et al., 2009).

RAF, to be fully active, requires the phosphorylation on three main areas: the negatively charged N-terminus; the activation segment; and the C-terminal domain for 14-3-3 binding. The N-terminal primary sequence is different among the three RAF family members, giving them particular regulatory properties. In the specific cases of A-RAF and C-RAF, the phosphorylation domain is composed of a SSYY motif (residues 338-341 in C-RAF and 299-302 in A-RAF). All of these residues need to be phosphorylated for complete activation. This process seems to be undertaken by CK2 and PAK kinases. By contrast, the phosphorylation domain of B-RAF only contains two serine residues (SSDD motif), here phosphomimetic aspartic aminoacids contribute to enhance its basal activity (Lavoie and Therrien, 2015).

The phosphorylation of the activation segment also seems to be important for RAF activation. Here, two conserved residues have been described to be functionally relevant for catalysis in the different RAF isoforms:

Thr452 and Thr455 in A-RAF (Baljuls et al., 2008), Thr599 and Ser602 in B-RAF (Zhang, 2000) and Thr491 and Ser494 in C-RAF (Chong et al., 2001).

Finally, the phosphorylation on Ser621 at C-RAF C-terminus is required for preventing 14-3-3 protein binding. This would stabilize RAF dimers and increase the affinity for ATP (Dhillon et al., 2009).

The activating phosphorylation events described above, induce a conformational change in the kinase domain of RAF, switching the αC helix domain from the inactive state to the active state, enabling the phosphorylation and activation of its main substrate, the MEK kinase (Yaeger and Corcoran, 2019).

1.2.2 MEK

Mitogen-Activated Protein Kinase Kinase 1 and 2, also known as MEK1 and 2, are two isoforms encoded by *map2k1* and *map2k2* genes, which display an 80% aminoacidic identity (Fig. 1.4) (Lefloch et al., 2009). These proteins are located downstream of the RAF proteins, which activate MEK by phosphorylation in their activation loop sequence. MEK1/2 can also be phosphorylated by other MAPKKKs, such as Tlp2 (Banerjee et al., 2006), Mos (Haccard and Jessus, 2006), MLKs (Marusiak et al., 2014) and PAKs (Frost et al., 1997).

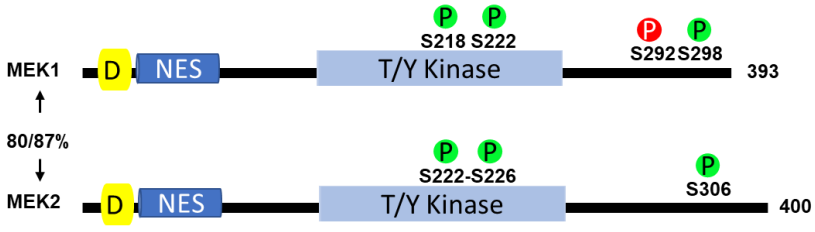

Figure 1.4. Representation of the two MEK isoforms. (%/%) refer to the total protein and kinase domain sequence identity. The D in yellow indicates the D-domain of MEK whereby it interacts with its substrates. NES stands for Nuclear export signals. Green P circles indicate activating phosphorylation residues. Red P circles are negative regulatory residues.

MEK1/2 are dual specificity kinases. To be activated, they require the phosphorylation of two contiguous serine residues localized in their activation

loop, within the typical MAPKKs motif Ser-Xaa-Ala-Xaa-Ser/Thr. In the case of Human MEK1, these residues are Ser218 and Ser222 (Alessi et al., 1994). Phosphorylation on both residues is required to fully activate the enzyme (Zheng and Guan, 1994). Once activated, MEK interacts through its basic N-terminal D-domain, with the CD (common docking) site of ERK1/2, phosphorylating them in their TEY residues (Bardwell et al., 2003; Crews et al., 1992; Roskoski, 2012b).

Another important domain is the Domain of Variable docking (DVD). This domain, conserved among all MAPKKs, is composed by a stretch of 20 aminoacids positioned just downstream of MEK activation segment. This domain is essential for the interaction between MEK and its upstream activator RAF (Takekawa et al., 2005). Intriguingly, MEK would also mediate in B-RAF activation, independently of its catalytic activation. In this mechanism is involved the KSR scaffold, whose ability to stimulate the catalytic activity of B-RAF is mediated by MEK. In this regard, Therrien and Collaborators, using the MEK F311S mutant, unable to bind KSR, demonstrate that the priming of MEK-KSR binding is essential for B-RAF-KSR heterodimerization, and this complex would promote B-RAF activation, and the final phosphorylation of free MEK molecules (Lavoie et al., 2018).

MEK activation is also dependent on the phosphorylation of Ser298, which is mediated by p21-activated kinase 1 (PAK1), a downstream kinase of the PI3K pathway (Frost et al., 1997). This residue is in another important regulatory region: the proline-rich domain (PRD) (Dang et al., 1998). This domain has been described to be crucial for MP1 (MEK partner 1) interaction (Schaeffer, 1998). The phosphorylation of Ser298 enhances MEK kinase activity toward ERK and, at the same time, stimulates a negative feedback loop mediated by active ERK. In other words, MEK activity is counteracted by a retro-phosphorylation on Thr292, in the PRD, undertaken by ERK (Eblen et al., 2004).

The MEK PRD domain is also implicated in the regulation of the PI3K-AKT pathway. In particular, MEK Thr292 phosphorylation, but not MEK1 kinase activity, is responsible of recruiting PTEN to the plasma membrane, decreasing

in such way PI3PK activation (Zmajkovicova et al., 2013). This crosstalk between the two pathways, highlights that the ERK and PI3K pathways are continuously regulating each other.

Another evidence of the crosstalk among the two pathways comes from Seger's lab: AKT activation is mediated by the PRD of MEK1/2 and depends on the reciprocal AKT-mediated phosphorylation of Ser298 in MEK1 or Ser306 in MEK2 (Procaccia et al., 2017).

Like other members of the RAS-ERK pathway, MEK1/2 are also able to dimerize. This dimerization plays an important role not only in MEK activation mediated by RAF, but also in its regulatory activity. As mentioned before, the ERK-induced phosphorylation of Thr292 mediates MEK inactivation. This residue, located in the unique proline-rich domain, is absent in MEK2. Thus, MEK1/2 heterodimerization is essential to achieve the negative-regulatory loop, induced by ERK (Catalanotti et al., 2009).

Another MEK function is to anchor ERK in the cytoplasm. In fact, the N-terminal domain of MEK1 contains three lysine residues neighboured by hydrophobic residues, named NES (nuclear export signal), which serves as a platform for holding ERK1/2 in the cytoplasm, under resting conditions (Fukuda et al., 1997b). Upon stimulation, MEK1 translocates to the nucleus, but it is immediately exported to the cytoplasm. In this mechanism is involved the CRM1 nuclear export protein, which recognizes the MEK-NES motif. In this way, CRM1 shuttles MEK back to the cytoplasm, carrying with it ERK back to the cytoplasm. (Fukuda et al., 1997a). ERK nuclear export is inhibited by leptomycin B, an inhibitor of CRM1 (Adachi et al., 2000).

1.2.3 ERK1/2

ERK1 and ERK2 are two proteins of 44 and 42 kDa, respectively. The acronym ERK stands for extracellular signal-regulated protein kinase. It was coined by Boulton et al. when they cloned, for the first time, ERK1 cDNA sequence (Boulton et al., 1990) and subsequently the cDNA ERK2 sequence from rat (Boulton et al., 1991). This designation replaced the previous name MAP2 (microtubule-associated protein 2 kinase) described firstly as an insulin-

stimulated protein (Ray and Sturgill, 1987), as these proteins were activated by a wide range of extracellular signals.

For a long time, it has been though that ERK1 and ERK2 could have specific functions. In agreement with this concept, several works demonstrated that ERK1 knock-out animals were perfectly viable while ERK2 knock-out animals were not viable (Blasco et al., 2011; Hatano et al., 2003; Krens et al., 2008; Pagès et al., 1999; Saba-El-Leil et al., 2003). However, these studies didn't consider global ERK1/2 expression. In fact, since ERK1/2 are differentially expressed in cell lines and tissues, and being the ERK2 isoform the higher expressed isoform (Buscà et al., 2015; Frémin et al., 2015), it was conceivable that the deleterious effects were a consequence of the depletion of the most expressed isoform (Lefloch et al., 2009; Saba-El-Leil et al., 2016; Voisin et al., 2010). In this regard, it has been recently shown that overexpression of ERK1 can compensate for ERK2 deficiency during development, indicating that both proteins share similar functions and that a minimum ERK threshold is required for their physiological activity (Frémin et al., 2015).

Structurally, ERK1/2 display a high similarity with other MAPKs. They are composed by a small N-terminal lobe and a large C-terminal lobe, connected by a linker. The small lobe is composed by five antiparallel β sheet-strands. In this region is contained a conserved αC helix whose orientation, in or out, contributes to the activation of the protein (Roskoski, 2012a).

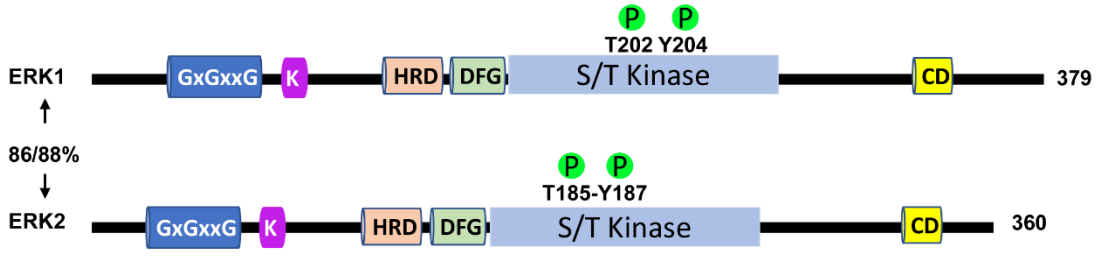

Figure 1.5. Organization of Human ERK1 and ERK2. (%/%) refer to the total protein and kinase domain sequence identity. The N-terminal GxGxxG sequence represents the glycine-rich domain. K is Lysine54, important for coordinating ATP phosphate groups. HDR sequence corresponds to ERK catalytic domain. DFG sequence marks the beginning of the activation segment, comprising the activation lip including by threonine and tyrosine residues. The C-terminal docking domain (CD) is an essential site for the interaction with MEK, substrates and phosphatases. Adapted from (Ryan et al., 2015).

Besides its high conservation, ERK2 shows unique characteristics, such as: an insertion at the N-terminus; and a C- terminal extension that lies on the surface of the molecule. ERK2 displays a four-amino acid insertion in the N-terminal lobe, between β4 and β5 strands; and a 31-residue insertion between G- and H-helix that contacts with the phosphorylation lip containing the Thr185 and Tyr187 phosphorylation sites. The C-terminal extension (315-358) forms part of the kinase domain interface and the αL16 helix which makes contact with the N-terminal lobe. (Roskoski, 2012a; Zhang et al., 1994).

The N-terminal lobe contains a glycine-rich loop (GxGxxG), which is the most flexible part (Fig.1.5) (Zhang et al., 1994). This loop allocates the β- and γ-phosphates groups of the ATP in the right orientation for catalysis; while a conserved valine (V56/V39 in human ERK1/2) (h will indicate human hereafter), next to the glycine loop, is in charge of making a hydrophobic contact with the adenine of ATP. The β3-strand contains an important lysine (K71/54 hERK1/2) which connects the α and β phosphate of ATP to a conserved glutamate (E88/71) of the αC-helix. This interaction is essential for catalysis. Mutation of K54 to arginine abolishes ERK catalytic activity, obtaining the dead-kinase mutant (K54R) (Canagarajah et al., 1997). The formation of a salt-bridge among the β3-lysine and the αC-glutamate is a pre-requisite for the formation of the activated state, corresponding with the “αC-in” conformation (Roskoski, 2012a).

The large C-terminal lobe contains six conserved α helixes (αD-αI) and four short β-strands (β6-β9). Most of the catalytic residues in charge of transferring ATP to the substrates occupy these strands. The HDR sequence marks the beginning of the ERK catalytic loop in the β6 strand (Fig. 1.5). The aspartate (D169/149 in hERK1/2) residue of the HDR motif extracts the proton from the -OH group of the protein substrate, enhancing its nucleophilicity, thereby facilitating the nucleophilic attack of the oxygen on the γ-Phosphorous atom of Mg-ATP (Fig. 1.6).

The main ERK regulatory region is the activation segment. This sequence is comprised between the DFG and the APE motifs. The aspartate D186/167 (ERK1/2) in the DFG motif binds Mg^{2+} ions, which in turn coordinate the three phosphate groups of ATP. The activation loop, also known as the activation lip,

is located within the activation segment. This lip contains two phosphorylatable residues, a threonine and a tyrosine, spaced out by a glutamate (TEY motif). The lip is located close to the magnesium-binding loop, the HDR catalytic loop and the N-terminal αC-helix. This large lobe typically binds the peptide/protein substrates, where the negative charges of the phosphates generate an optimal grove for positioning in the right orientation the proline P+1 present in all ERK substrates. Thus, ERK being a proline-directed kinase (Canagarajah et al., 1997; Zhang et al., 1994).

ERK catalytic site is in the cleft between the small and the large lobes. In the catalytic-inactive state, also termed as open conformation, the two lobes are slightly angled away from each other. As a result, the catalytic residues are misaligned. In addition, the P+1 substrate-binding region is blocked, preventing substrate entrance (Canagarajah et al., 1997). By contrast, in the closed, catalytically active conformation, the two lobes rotate 5.4º closer. After the Mg^{2+}-ATP and substrate binding, an additional movement of the lobes allows ATP to transfer the phosphoryl-group on the substrate. Two already mentioned structures contribute to the final activation of the protein. The αC-helix in the N-small lobe, whose rotation in the position “in”, induces the formation of a salt-bridge among the glutamate (E71 of hERK2) of the αC-helix and K54 in the β3-strand. The second, but not less important event, involves the aspartate (E164) movement of the DFG motif. In this regard, the D-residue of the DFG motif, move in facing the ATP-binding pocket, thereby coordinating with Mg^{2+}, while the bulky phenylalanine residue moves out. (Roskoski, 2012a).

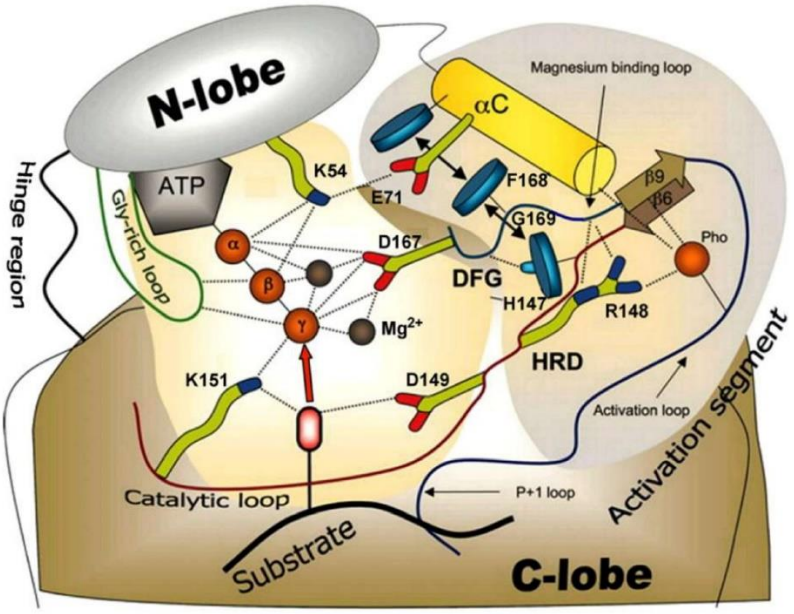

Figure 1.6. Representation of molecular interactions between the human ERK2 kinase catalytic core residues, ATP, and the protein substrates. Catalytically residues that interact with ATP and the protein substrate are in the light khaki background on the left. Secondary structures and residues that participate in the regulation of catalytic activity occur within the gray background on the right. Hydrophobic interactions between the HRD motif (the first D of K/D/D), the DFG motif (the second D of K/D/D), and the αC-helix are indicated by double arrows while polar contacts are depicted as dashed lines. Pho, represented by a red circle, is the phosphate attached to Thr185. Adapted from (Roskoski, 2012a).

1.2.3.1 ERK activation and regulation

The conversion from inactive to active ERK, requires the phosphorylation of two residues located within the activation lip, namely the TEY motif. The phosphorylation of these two residues is mediated by MEK; even though a basal amount of phosphorylated ERK on Tyr187 has been detected when it is overexpressed in bacteria. This finding suggests ERK ability to auto-phosphorylate (Robbins et al., 1993; Rossomando et al., 1992). Phosphorylation on the TEY residues is essential for the right molecular organization, which end up in ERK activation. Replacement of the Thr185 by alanine, or Tyr187 by phenylalanine, in the case of ERK2 AEF mutant, eliminates completely its kinase activity. Moreover, attempting to generate a phospho-mimetic active mutant, namely the EEY, where a glutamate substitutes the threonine, results in a 10% of activity, compared to the wild-type form. This is because, upon phosphorylation, p-Thr185 makes essential ionic contacts with

the N-terminal domain, contributing to the enzyme closure, which otherwise would be lost (Canagarajah et al., 1997).

Specific residues in the C-terminal L16 segment of ERK display a key role in the docking of ERK with substrates, phosphatases, and also with MEKs. This region has been named CD (common docking). Mutational analysis reveals three residues, namely Asp316, Asp319 and Glu320 in rat ERK2, which are essential for the interaction with MEK D-domain (Robinson et al., 2002). However, since the TEY motif is buried in the inactive ERKs, additional interactions between ERK N-terminus and MEK seem to cooperate in order to expose the phosphorylatable ERK residues to MEK. Since these sites are located in different position of the molecule, it is likely that more than one MEK molecule are involved is this process (Adachi et al., 2000; Chuderland and Seger, 2005; Robinson et al., 2002). The phosphorylation on TEY by MEK increases ERK kinase activity by 1000-fold (Eblen, 2018; Robbins et al., 1993).

Upon phosphorylation, the biggest conformational changes occur at the activation lip and L16 helix (Pegram et al., 2019). In such a way, p-Thr185 interacts directly with three arginine residues, Arg70 in the αC-helix, Arg148 in the catalytic loop, Arg172 in the lip and, indirectly, with the Arg67 in the αC-helix (Canagarajah et al., 1997). The interaction among the p-Thr185 and Arg67/70 in the αC helix, may stabilize the active form (Xiao and Al., 2014) (Fig. 1.7).

Other interactions occur at the C-terminal extension L16 (from Pro311 to Arg 360), where the loop is further folded forming a 3/10 helix. Phosphorylated Thr185 forms two additional hydrogen bonds with L16 residue. In this way, Thr185 contacting with both N- and C-terminus, directly influences the

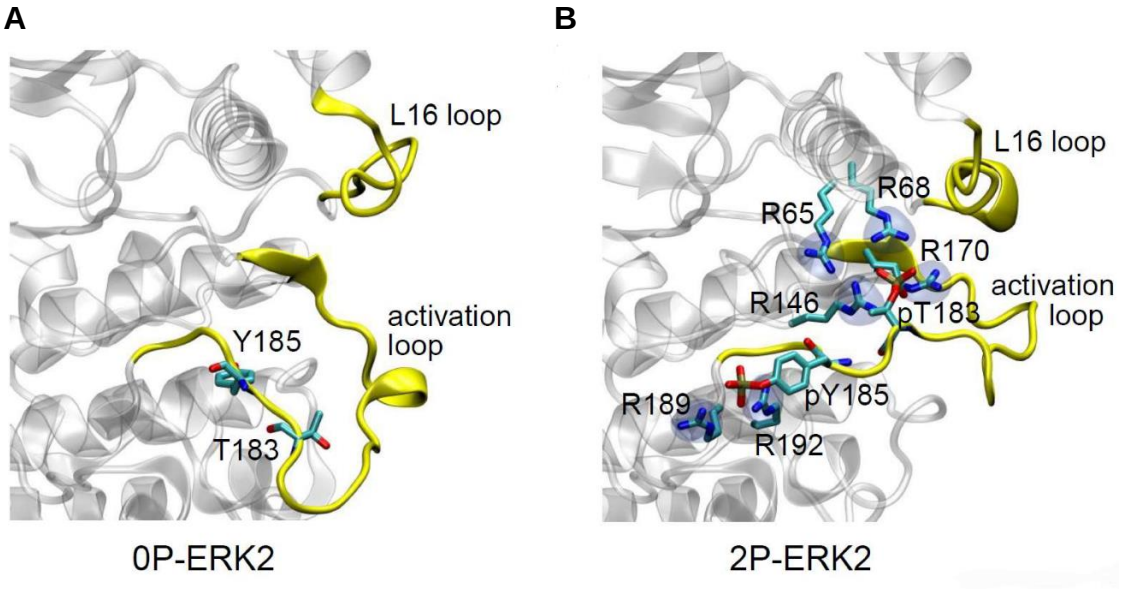

Figure 1.7. ERK2 crystal structure. Upon Thr183 and Tyr185 (mouse numeration) the biggest conformation changes occurs at the activation loop and L16 loop. **A)** It is shown the two disconnected regions in unphosphorylated ERK2 (0P). **B)** In phosphorylated ERK2 (2P), the p-Thr183 and p-Tyr185 establish several interactions with multiple Arginine residues, while the L16 loop is further folded into a 3/10 helix. Adapted from (Pegram et al., 2019).

orientation of the two domains and promotes a tighter interaction among the two domains, resulting in the final closed conformation of activated ERK (Canagarajah et al., 1997).

On the other hand, the phosphorylation of Tyr187 promotes a conformational change in the P+1 site, enhancing ERK substrate specificity. In addition, p-Tyr187 interactions with Arg191 and Arg194 contributes to place the proline substrate in the right position (Canagarajah et al., 1997) (Fig. 1.7).

The process of ERK activation mediated by MEK has been controversial. Two models of ERK activation have been proposed so far. Initially, the mechanism of ERK activation was thought to follow a switch-like manner (Fig.1.8 A). In fact, Ferrel and co-worker have established that, in *Xenopus* oocytes, upon increasing concentration of a stimulus, ERK activation followed a kinetics of “all

or none", which corresponds to a "distributive activation" mode. In their *in vitro* model, a MEK molecule would first phosphorylate ERK at Tyr187. Soon after, MEK will dissociate from p-TyrERK and only after its re-binding, ERK will be fully activated after Thr185 phosphorylation (Ferrell and Bhatt, 1997). Nevertheless, this model cannot be applied to all biological system. In fact, this model cannot explain the "graded response" observed in the mammalian HeLa cells upon EGF stimulation (Fig. 1.8 A) (Aoki et al., 2011).

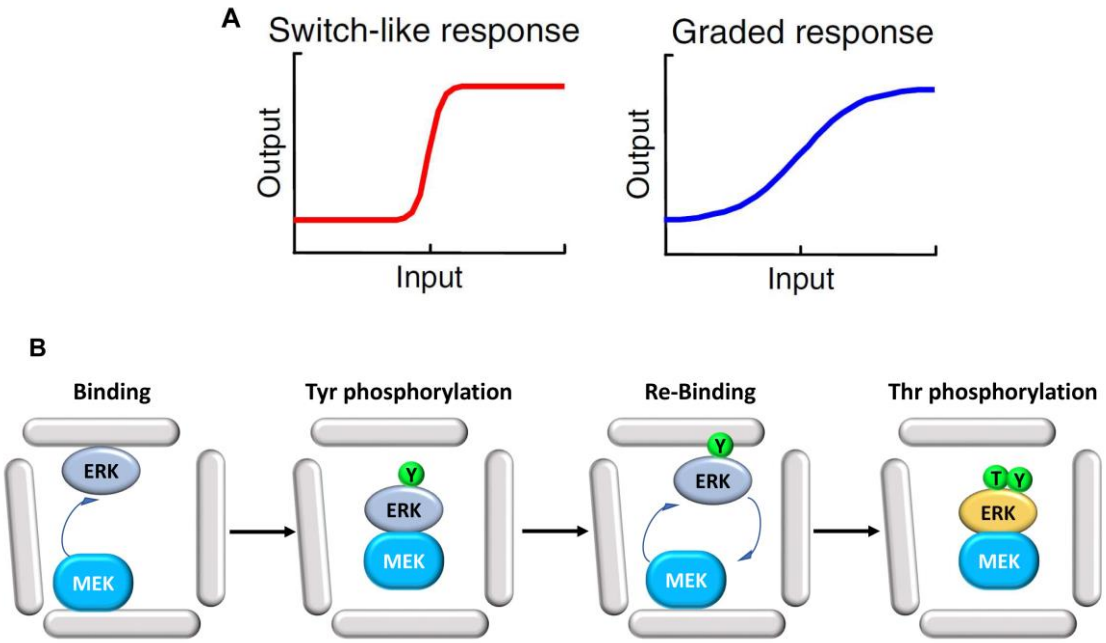

Figure 1.8. Representation of the input-output response of ERK MAP kinase. A) Comparison between distributive phosphorylation model, which occur in vitro, leading to a switch-like response, and graded response, observed in mammals. **B)** Quasi-processive model of ERK activation. Under molecular crowding condition, MEK phosphorylates firstly ERK at Tyr187 (pY-ERK), dissociates from ERK and re-binds with high probability to p-TyrERK in order to activate completely ERK (pT-pY-ERK). Adapted from (Aoki et al., 2011).

It was hypothesized that these differences could be attributed to scaffold proteins, whose interaction with ERK would change the activation response from a switch-like mode to a processive manner. In this other model, MEK binds to ERK and only after having phosphorylated both residues in the TEY, it dissociates away. However, MEK-ERK does not form such as stable complex in order to completely satisfy this model (Burack and Sturgill, 1997). For these reasons, Matzuda and collaborators proposed the "quasi-processive" model

(Fig.1.8 B). In this model, MEK first phosphorylates ERK at the tyrosine residue (p-TyrERK) and then dissociates from the product. The discrepant results between the *in vitro* model and HeLa cells was attributed to a molecular crowding effect, which restricts the molecules movements. Thus, due to molecular crowding, the two molecules do not have enough space for moving away from each other, thereby MEK re-binds ERK and re-phosphorylates p-TyrERK with high probability. Apparently, none of the scaffold proteins contribute to changing the phosphorylation process from distributive to quasi-processive. However, these findings cannot exclude the possibility that scaffold proteins could play the role of increasing molecular crowding withing the cells, rather than scaffolding per se (Aoki et al., 2011).

1.2.3.1.1 ERK dephosphorylation

In order to maintain cell physiological homeostasis, activated ERK1/2 undergo a dephosphorylation process which regulates the magnitude and duration of its activation. To do so, protein phosphatases, removing one or both phosphates from its activation lip, play the relevant task of switching off the signal conveyed through the Ras-ERK pathway (Anderson et al., 1990).

Three groups of protein phosphatases have been identified: the protein Ser/Thr phosphatases (S/T PPs); protein Tyr phosphatases (PTPs); and dual specificity phosphatases (DUSPs) (Chuderland and Seger, 2005).

The dual-specificity mitogen-activated protein kinase phosphatases (DUSPs), also known as MAP Kinase Phosphatases (MKPs), are able to remove phosphates both from tyrosine and threonine residues in their substrates (Fig. 1.9). Depending on their substrate specificity and on their localization, these enzymes can be further subdivided into three classes. i) The dual phosphatases class I enzymes, namely: DUSP 1, 2, 4 and 5, whose expression is induced by ERK. Phosphatases belonging to this class, have a nuclear localization signal (NLS) in their amino terminal which retains them at the nucleus. DUSP 5 specifically dephosphorylates and anchors ERK in the nucleus (Kidger et al., 2017). ii) By contrast, the DUSP 6, 7 and 9 belonging to the class II, contain a leucine-rich NES sequence (nuclear export signal) thereby, their activity is

restricted to the cytoplasm. i) The class III enzymes (DUSP 8, 10 and 16), are located in both cellular compartment and are more promiscuous than the previous two classes, also inactivating other MAPKs, such as p38 and JNK (Roskoski, 2012a).

All the members of this group contain a conserved N-terminal domain, the kinase interaction motif (KIM), which is essential for the interaction with its substrates, and a C-terminal domain with phosphatase activity. The interaction among MKPs and ERK occurs through the positive and hydrophobic MAPK binding domain (KIM) and the MAP kinase D-recruitment domain (CD). DUSP6 (also known as MKP3) is an ERK2 specific phosphatase. Disruption of DUSP catalytic motif, by using the DUSP Cys293Ser mutant, impairs ERK inactivation (Farooq et al., 2001). Mutations on ERK2 common docking site, such as the substitutions E322K or D321N, have been found in many pathological conditions, including cancer. These mutations reduce DUSP inhibitory activity, by preventing its binding to ERK. Altering ERK regulation, leading to its overactivation (Taylor et al., 2019).

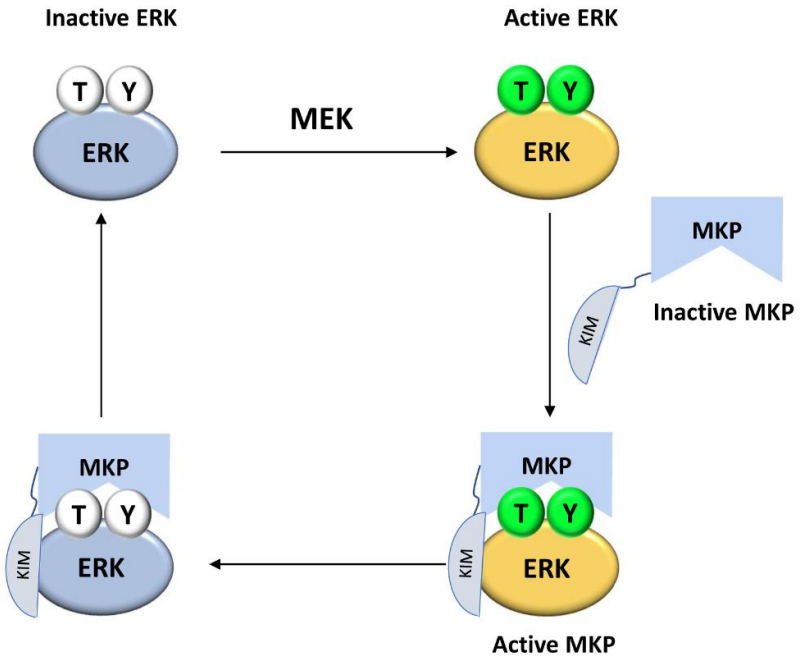

Figure 1.9. Representation of ERK inactivation mediated by phosphatases. Active ERK (yellow) induces the activation of MKP (MAP Kinase Phosphatase), which in turn bind to ERK, through its Kinase Insert Motif (KIM). The latter event is the dephosphorylation of ERK and its subsequent inactivation.

In addition, upregulated levels of DUSP6 have been found in many types of cancers. These effects highlight the intricate role of phosphatases in the ERK regulation in cancer (Ahmad et al., 2018). There are evidences hinting the role of DUSP6 in ERK localization. In fact, in resting condition DUSP6 acts as anchor, retaining ERK at the cytoplasm (Karlsson et al., 2004).

The mechanism for removing phosphate groups from ERK activation lip is quite conserved among protein phosphatases (Fig. 1.9). The active site of DUSP phosphatases shows an enlarged cleft which can fit either a phosphotyrosine or a phosphothreonine residue, removing phosphate groups leads to ERK inactivation (Farooq and Zhou, 2004).

Another group of phosphatases involved in ERK inactivation are the protein-tyrosine phosphatases (PTP). This group of phosphatases specifically remove phosphate groups from tyrosine residues. Members of this group are the PTP-SL (STEP like) and PTP-STEP, where STEP stands for Striatal-Enriched Tyrosine Phosphatases. These phosphatases, to be catalytically active, are phosphorylated by activated ERK on threonine 360 (rat) and then dephosphorylate ERK Tyr187 (Pulido et al., 1998). These phosphatases interact with ERK D-site, via their kinase interacting motif (KIM), which determines their substrate specificity. Since they revert ERK action, members of this group may act as tumour-suppressors. It is the case of PTPrK, a receptor-type tyrosine-phosphate, whose action on C-RAF reduces ERK signalling, acting as tumour-suppressor in melanoma (Casar et al., 2018).

The Ser/Thr phosphatases (PPs) are proteins with the ability of removing phosphate group from serine and threonine residues (Alessi et al., 1995). Since most members of the RAS-ERK pathway contain several phospho- Ser and Thr residues, the protein PP2A, belonging to this group, has the ability to regulate ERK inactivation, or activation, at different step of the pathway. For instance, dephosphorylation of RAF-1 S259, mediated by PP1 and PP2A, releases the 14-3-3 inhibitor subunit from RAF, allowing its activation (Jaumot and Hancock, 2001). Dysregulation of PP1 has been found in cancer leading to an overactivation of RAF and subsequently of ERK (Chen et al., 2018).

1.2.3.1.2 Negative feedback loops

Another regulatory mechanism acting on the RAS-ERK pathway is represented by ERKs ability to directly phosphorylate nearly all of the components of its pathway, acting as a negative-regulator of the signalling through its own pathway (Fig. 1.10). MEK1 activation is negatively regulated by ERK-mediated phosphorylation on Ser292. This phosphorylation reduces MEK1/2 heterodimerization attenuating ERK activity (Catalanotti et al., 2009).

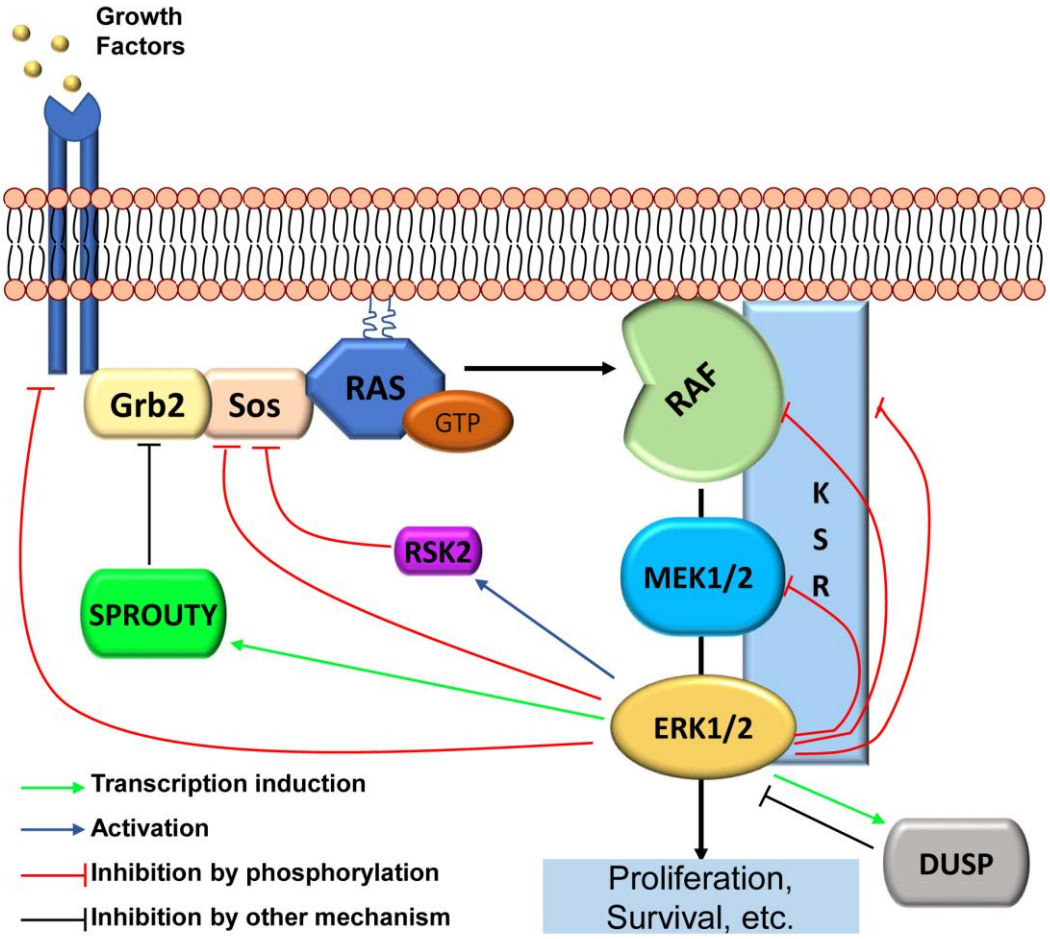

Figure 1.10. Regulation of Ras-ERK pathway by ERK mediated-negative feedback. Active ERK inhibits nearly all the component of the pathway. This is mediated by phosphorylation as well as by the activation of other modulators, by inducing their expression (DUSP and SPROUTY) or modulating its activation (RSK2). The red lines indicate the proteins targeted by the ERK inhibitory activity. Adapted from (Lake et al., 2016).

Moreover, the negative charge added by the phosphate group on Ser292 prevents the priming phosphorylation on Ser298 mediated by PAK1, which anticipates MEK phosphorylation on Ser218 and 222 (Eblen et al., 2004). To inhibit RAF activation, ERK phosphorylates RAF on several serine and

threonine residues. Phosphorylation on Ser151 prevents RAS-RAF association, whereas Thr401, Ser750 and Thr753 phosphorylation reduces B-RAF and C-RAF heterodimerization (Ritt et al., 2010). Another regulatory step affects RAS activation at the plasma-membrane. Active ERK phosphorylates epidermal growth factor receptor (EGFR) at Thr699 and, as a consequence of this negative feedback, prevents EGFR dimerization, attenuating its activation (Kluba et al., 2015). In addition to this, ERK can diminish RAS signals by phosphorylating the Ras guanine exchange factors, SOS1. ERK2-mediated phosphorylation of SOS1 on its proline-rich domain, blocks Grb2-SOS1 complex formation and EGFR-SOS1 association (Eblen, 2018). SOS1 is also inhibited by the ERK effector Ribosomal S6 Kinase 2 (RSK2) (Douville and Downward, 1997). Moreover, ERK can stimulate the activity of the regulatory protein SPROUTY. SPROUTY phosphorylation, having a docking site for Grb2, adds another negative regulatory event at the Ras core, blocking Grb2 function (Saei and Eichhorn, 2019). Activated ERK can also influence scaffold proteins activity. This is the case of KSR1, whose main function is to assemble members of the Ras-ERK pathway, in order to regulate ERK activation in a localization-specific fashion. ERK can phosphorylates KSR1 on Ser443, thereby reducing its ability to potentiate ERK activation (McKay et al., 2009).

Interestingly, the integrity of negative feedback loops plays a relevant function in determining ERK1/2 signalling outputs. In fact, disruption of the regulatory negative feedback loops reverts ERK activation from graded or “quasi-processive” to “switch-like” manner (Lake et al., 2016; Sturm et al., 2010).

1.2.3.2 ERK dimerization

The first evidence of ERK dimerization comes from the Cobb laboratory, when they solved the active ERK2 structure for the first time (Fig.1.11 A) (Canagarajah et al., 1997). Upon phosphorylation, ERKs dimerize. ERK1/2 homodimers show a higher stability, even though ERK1-ERK2 could hetero-dimerize. It has also been demonstrated that activated ERK can dimerize with non-phosphorylated ERK. However, the Kd of phosphorylated ERK2 dimers has

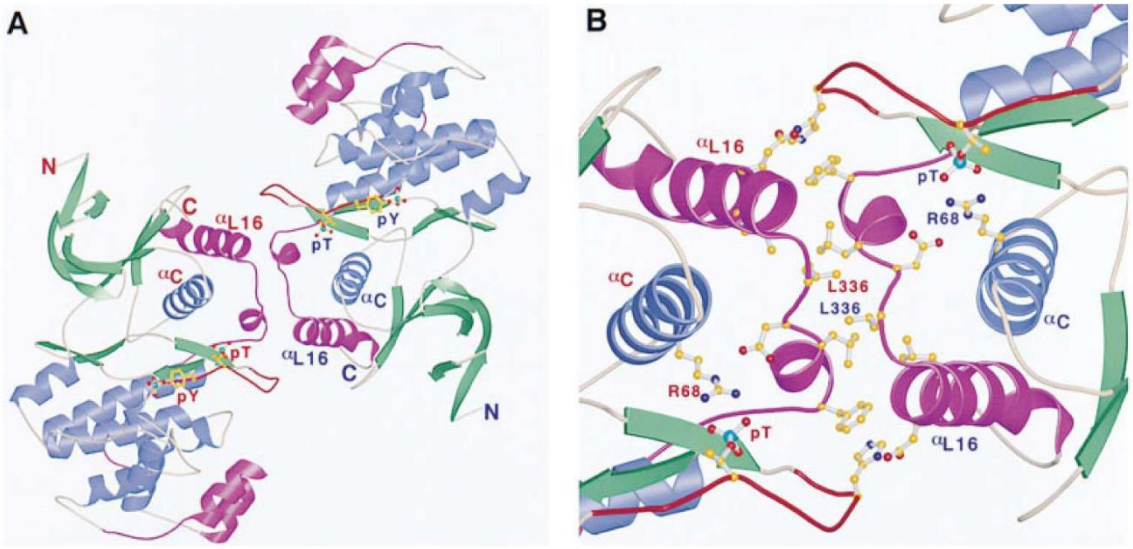

Figure 1.11. Structure of ERK2 dimers. A) Representation of a symmetric ERK2 dimer, having both activation lip and MAP kinase insertion domain completely accessible. The N-β strands are shown in green, the α helices in blue and the L16 and the MAP kinase insert in magenta. Phosphorylated Thr183 and Tyr185 are shown as pT and pY in yellow (mouse numeration). **B)** Representation of the hydrophobic zip composed by the Leucine residues 333, 336, and 344 in L16, contacting each other in the dimer. Moreover, an ionic bound is represented in red, bridging the H176 of the activation lip with E343 of the L16 of another molecule. Adapted from (Khokhlatchev et al., 1998).

been estimated to be 3000 times lower than the non-phosphorylated dimer. These findings hint that upon phosphorylation, the majority of activated ERKs homodimerize (Khokhlatchev et al., 1998). Canagarajah and collaborators have elucidated the molecular basis of ERK dimerization *in vitro* (Canagarajah et al., 1997). Upon phosphorylation of the lip, ERK molecules show the most dramatic conformational changes in the activation lip and in the C-terminal extension, known as L16 (from Pro309 to Arg358). In this regard, a shift of 25 Å in the activation loop provokes the exposure of three leucine residues (Leu333, Leu 336, Leu344) in the L16 C-terminus. As a result, this leucin-rich region is more exposed to the solvent, making hydrophobic interactions with another molecule

of ERK. Additionally, His176 in the activation lip makes ionic contacts with Glu343 in the L16 helix of another ERK partner, further stabilizing the interaction of the dimers (Fig.1.11 B). Thus, the two phosphorylated ERK2 oligomers bind through a hydrophobic zipper strengthened by two ion pairs, one on each side of the zipper (Canagarajah et al., 1997; Philipova and Whitaker, 2005).

Further evidence supporting the hypothesis that dimer formation requires both ionic and hydrophobic interactions, comes from Wilsbacher work, where chelating agents, such as EDTA, sequestering divalent cations, reduces ERK dimerization. Moreover, the ratio of dimers to monomers decreases proportionally as the salt concentration increases, in line with the evidence that a strong hydrophobic contribution is required for dimer formation (Wilsbacher et al., 2006). Mutational analysis confirms that five residues of the dimerization domain are essential for ERK dimerization. In fact, to obtain an ERK dimerization-impaired mutant, it is necessary to change simultaneously histidine176 to glutamate and four leucine (333,336, 341 and 344) to alanine, giving the ERK2 H176E L_4A mutant (Khokhlatchev et al., 1998). Functionally, ERK dimerization has been associated with a higher catalytic activity, endogenous ERK1 dimers being much more active than its monomers (Philipova and Whitaker, 2005).

It has been shown that ERK dimerization is a specific characteristic of mammals (Herrero et al., 2015). Regarding the dimerization domain, this region is conserved among all tetrapods. The only difference resides in the region around His176 residue, being PDHD in ERK2 and PEHD in ERK1, where the aspartic residue is replaced by a glutamic residue. Even though this bulky substitution could affect substrate interaction, this change does to not affect ERK dimerization indicating that further differences are required in order to explain ERK inability to dimerize in non-mammalians (Buscà et al., 2016).

Initially, ERK dimerization was proposed as a mechanism for ERK nuclear translocation, being the dimerization-deficient mutant (ERK2 H176E L_4A) impaired to translocate to the nucleus (Adachi et al., 1999; Khokhlatchev et al., 1998). Others, proposed that nuclear translocation occurred independently of

ERK dimerization, but dependent on the phosphorylation rate (Lidke et al., 2010). Conversely, in our laboratory we demonstrated that ERK2 dimerization occurs at the cytoplasm with the participation of scaffold proteins, and being essential for the activation of certain cytoplasmic substrates, such as the cytosolic phospholipase A_2 ($cPLA_2$) (Casar et al., 2008). These evidences suggested that phosphorylated ERKs dimerize using scaffold proteins as dimerization platforms. Contrarily, ERKs enter the nucleus as monomers. Moreover, blocking ERK dimerization, but not its phosphorylation, blocks tumour progression in animal models of tumour cells harbouring RAS and RAF mutations, opening the door to a new perspective of MAPK inhibitors (Casar et al., 2008; Herrero et al., 2015). This is the case of DEL22379, that functions blocking ERK dimerization. Predictive docking analysis revealed that DEL22379 docked on the cleft delimited by residues Pro174, Asp175, His176, Asp 177, Phe181 and Phe329. The interacting residues from the other monomer are: Pro 337, Lys338, Glu339, Lys340 and Glu343. Thus, binding to ERK2 at a groove in the dimerization interface, this compound prevents ERK2 dimerization. In such a way, DEL22379 reduces cytoplasmic but not nuclear ERK substrates activation (Herrero et al., 2015).

1.2.3.3 ERK nuclear translocation

ERK localization depends on its activation state. In resting cells, ERK is mainly localized at the cytoplasm, where specific cytoplasmic proteins act as ERK anchors (Chuderland and Seger, 2005). Altering ERKs physiological concentration, for instance by overexpression, enhances its entrance to the nucleus, leading to ERK mislocalization within the cell. By contrast, overexpressing ERK anchors, retains ERK at the cytoplasm, highlighting the importance of certain anchors for the correct ERK spatiotemporal dynamics (Costa et al., 2006).

MEK is one of ERK cytoplasmic anchors, it retains ERK at the cytoplasm in resting cells (Fukuda et al., 1997b). Considering that MEK concentration is much lower than ERK, it is conceivable to thing that other cytoplasmic anchors must also contribute to this retention (Yao and Seger, 2009). Other anchors, such as the scaffolds KSR1/2, MP1 and IQGAP or phosphatases (DUSP6 or

PTP-SL) (Caunt and Keyse, 2013) or even components of the cytoskeleton, serve as ERK retaining platforms in the cytoplasm in resting cells (Roskoski, 2012a).

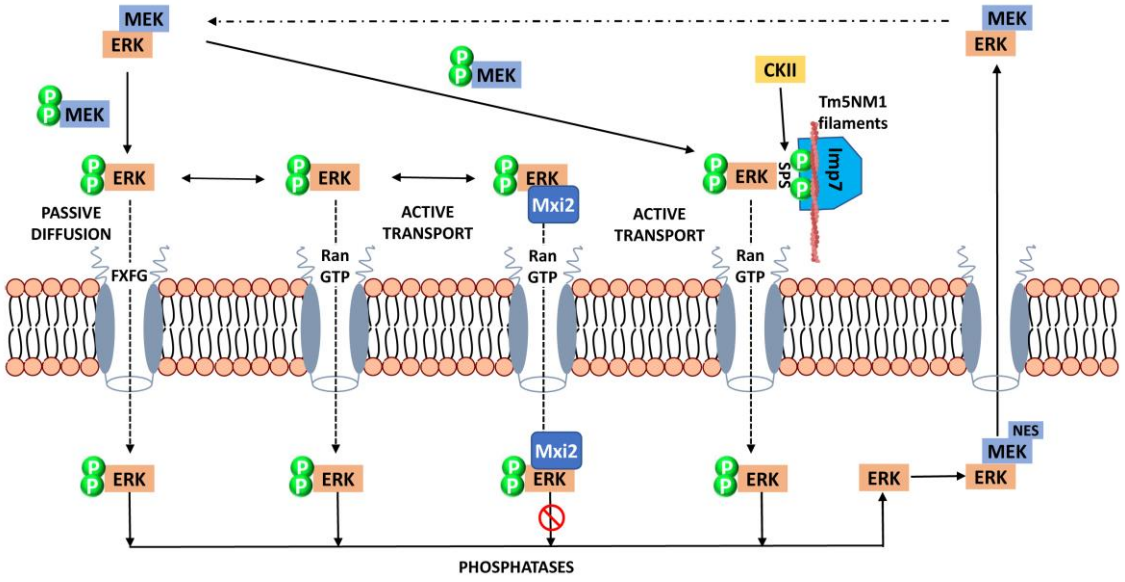

Figure 1.12. Schematic representation of all the possible mechanisms involved in ERK nuclear translocation. In resting cell, ERK is localized at the cytoplasm, anchored by cytoplasmic proteins, such as MEK. Upon phosphorylation, ERK detaches from its anchors and may translocate to the nucleus by passive diffusion, interacting with the FXFG regions of NUPs. This process can also be mediated by Importins α and β in an energy-dependent manner where RanGTP in implicated. Mxi2, a p38 isoform, may translocate escorting ERK to the nucleus, protecting it from phosphatases action. Imp7 can also translocate ERK to nucleus, after phosphorylation on ERK-SPS motif mediated by CKII. In this process Tm5NM1 actin filaments seem to contribute. Finally, dephosphorylated and inactive ERK is returned to the cytoplasm, shuttled by proteins, like MEK, harbouring nuclear export sequence (NES).

Upon stimulation, phosphorylated ERK dissociates from MEK and translocates immediately to the nucleus, acting on nuclear transcription factors (Adachi et al., 1999). ERK nuclear translocation influences several biological outcomes, depending on the transcriptional factors activated and on the durability of the activator stimulus. Activated ERK may translocate to the nucleus promoting cell proliferation and differentiation, among others. These different outcomes are orchestrated by differences in the duration and strength of the signal. The best example is PC12 cells, where EGF induces a transient ERK activation at the cytoplasm, which is essential for proliferation. By contrast, NGF stimulation

promotes ERK autophosphorylation, generating a sustained ERK activation, which implicates its nuclear translocation, resulting in neural differentiation (Cowley et al., 1994; Robinson et al., 1998; Traverse et al., 1992; Wu et al., 2015).

The process of nuclear translocation involves the crossing of the nuclear envelope, which functions as a barrier delimiting the cytoplasm from the nucleus (Fig.1.12). This membrane contains specific proteins that form pores, known as nucleoporines (NUPs), which allow the selective passage of proteins to and from the nucleus. Small proteins, with approximately less than 40 kDa molecular weight, ERK included, can pass through these pores by passive diffusion. The exact mechanism of ERK nuclear translocation is not completely clear, hinting that it can happen by diverse mechanisms. Active nuclear import typically involves a carrier, which recognizes a nuclear localization signal (NLS) on the cargo. The NLS consists of a cluster of basic aminoacid (Arg and Lys) of variable length, which bind to the polar and negatively charged aminoacids of importin α. Importin α and β families, also known as karyopherins, are two classes of shuttle proteins. The importin α family serves as an adaptor for the cargo proteins harbouring the NLS sequence, whereas importin β is the actual shuttle. The importin β in this ternary complex interacts with the FXFG sequences of NUPs, allowing the nuclear translocation of the complex. Once at the nucleus, the complex is disassembled in a process mediated by the hydrolysis of Ran-GTP, which is converted to Ran-GDP. Ran-GDP, together with importin α, moves back to the cytoplasm, where Ran GEFs re-activate it in order to repeat the process (Miyamoto et al., 2016; Roskoski, 2012a).

Adachi et al. demonstrated that a dominant negative Ran mutant (Ran Q69L) fails to block the nuclear translocation of wild type ERK, but inhibits the β-galactosidase-ERK2 entrance, too big for being uptaken by a simple passive mechanism. These evidences endorse the hypothesis that ERK can be translocated by both passive and active mechanisms (Adachi et al., 1999).

There are evidences supporting the idea that ERK could translocate independently of Ran active transport and even in a carrier-independent manner. In such a way, ERK, interacting directly with the FXFG sequence of

NUPs, forms a complex with the nuclear pore and translocates to the nucleus. This energy-independent process involves the nucleoporins 153 and 214, and can be inhibited by wheat germ agglutinin (WGA), a nuclear-pore blocker (Matsubayashi et al., 2001; Whitehurst et al., 2002).

Another protein involved in ERK translocation is Mxi2. Mxi2 is a splicing isoform of p38α, which is able to bind ERK, and increases ERK affinity for Nup153, promoting ERK nuclear translocation. This process requires both energy and Ran. Moreover, Mxi2 sequesters ERK at the nucleus, protecting it from nuclear phosphatases, without affecting its association with nuclear substrates (Casar et al., 2007).

It is important to mention that neither ERK nor MEK contain a NLS sequence, which, as mentioned before, is essential for importin α binding and the subsequent ternary complex formation. In this regard, Seger and collaborators have described a novel NLS-independent mechanism of nuclear translocation for ERK (Chuderland et al., 2008; Zehorai et al., 2010). These investigators identified a SPS (Ser244-Pro245-Ser246) sequence, within the ERK kinase insert domain, defined as a nuclear translocation signal (NTS). The phosphorylation of these residues allows the binding of ERK to importin β-like subtype 7 (IMP7, hereafter) and subsequently the nuclear translocation of the complex ERK-IMP7 (Flores and Seger, 2013). Going more deeply into the molecular events which lead to the phosphorylation of this novel motif, in resting cells ERK-SPS residues are hidden by MEK, thus impossible to be phosphorylated. Upon ERK phosphorylation on its canonical TEY residues, ERK is released from its anchors and exposes the SPS residues. The kinase responsible for phosphorylating the SPS motif is casein kinase II (CKII). This phosphorylation creates a negatively charged patch which is essential for IMP7 binding. CKII is a constitutively active Ser/Thr kinase whose minimal consensus phosphorylation site is Ser-Xaa-Xaa-Glu/Asp. The initial CKII-mediated phosphorylation of Ser246 is sufficient for ERK nuclear translocation, but phosphorylation of Ser244 accelerates the process. Moreover, since Ser244 is not a classical phosphorylation site for CKII, it cannot be excluded that ERK

autophosphorylates in this residue (Plotnikov et al., 2019; Zehorai et al., 2010). Once in the nucleus, the complex ERK-IMP7 is dissociated by Ran-GTP.

Interestingly, it has been reported that the tropomyosin Tm5NM1 improves IMP7-ERK interaction. The Tropomyosin isoform 5 non-muscle 1 (Tm5NM1), which is associated with actin filaments, might intervene to facilitate ERK-IMP7 interaction, therefore functioning as a scaffold, and also as a myosin motor moving the complex closer to the nucleus (Eblen, 2018; Schevzov et al., 2015).

Since the role of nuclear ERK is essential for cell proliferation, the inhibition of this process could be exploited as an anti-cancer therapy, especially when this pathway is upregulated. This is the case of the NTS-derived peptide which competing with IMP7 blocks ERK nuclear translocation without affecting ERK cytoplasmic function, having dramatic effects on melanoma cells harbouring B-RAF mutation. Therefore, these findings reveal a new antitumoral target in melanoma treatment (Plotnikov et al., 2015).

1.2.3.4 ERK substrates

Once ERK is phosphorylated on its activation lip, it becomes a powerful Ser/Thr kinase. Thus, it can phosphorylate a wide variety of substrates. Up to date, ERKs can interact with more than 400 substrates localized in the cytoplasm, nucleus and other cellular organelles (Hannen et al., 2017; Ünal et al., 2017; Von Kriegsheim et al., 2009; Yang et al., 2019; Yoon and Seger, 2006).

All ERK substrates possess a consensus phosphorylation sequence of Px(S/T)P, with a proline in the position +1/-1, though a minimal (S/T)P consensus sequence can also be phosphorylated. The presence of the proline in the substrate, at position +1 is an essential prerequisite given by the nature of the ERK binding site (P+1 pocket) (Canagarajah et al., 1997). In fact, upon activation, this region is remodelled in order to allocate the substrate in the right orientation for catalysis. Moreover, other docking regions exist, located outside of the ERK catalytic region, which are involved in the process of substrate recognition and binding, giving further substrate specificity. These regions are the D-recruitment site (DRS) and the F-recruitment site (FRS) (Fig. 1.13).

The ERK1/2 DRS is composed by negatively charged residues (Φchg), shown in blue, and hydrophobic aminoacids (Φhyd), shown in cyan (Fig 1.13). These regions, located on the side of the protein, comprise the residues T159, T160, D318, L115, L121, L157, H125 and Y128. The ERK DRS specifically interacts with the D-site in substrates. The D-site domain of ERK substrates is also known as DEJL (docking site for ERK and JNK, LXL) or KIM (kinase interaction motif) (Mace et al., 2013). The substrate hydrophobic domain (Φhyd) and the positively charged basic residues (Φchg) have the following consensus: $(R/K)_{2-3}$-X_{2-6}- Φhyd_A-X- Φhyd_B. The substrate D-site positively charged residues interact with those negatively charged in ERKs, specifically D318-D321. This region was firstly defined as “common docking” (CD), and it is also important for MEK and phosphatases interaction (Robinson et al., 2002; Taylor et al., 2019). The hydrophobic regions in substrates (Φ_A-X- Φ_B) connect with the ERKs DRS hydrophobic stretch Φhyd. Such docking motifs are present on several transcription factors, such as Elk1, TFII and, as previously mentioned, on ERK interacting molecules like MEK1, MKP3, STEP, MSK1, MNK1 and RSKs (Roskoski, 2012a; Zeke et al., 2015).

The other ERK recruitment site is the FRS (Fig 1.13). This motif, located nearby the activation segment, binds to the consensus sequence FXFP in substrates, known as the F-site or DEF motif. The FRS is in the opposite side of the DRS, below the activation lip. Interestingly, the FRS is fully formed only after ERK activation, which adds another level of specificity in terms of ERK fidelity toward its substrates (Piserchio et al., 2015).

Proteins containing the FXFP are Elk1, c-Fos, Sap1, Ksr1, C-RAF and the dual specificity phosphatases DUSP1 and 4 (Roskoski, 2012a). Thus, some ERK substrates, such as Elk1, contain both interacting domains. Contrarily, other ERK substrates, such as the transcription factor Ets-1 and the modulator protein PEA15, do not contain any canonical D- or F-site, nevertheless they interact with ERK through an hydrophobic region contacting with the DRS (Piserchio et al., 2011).

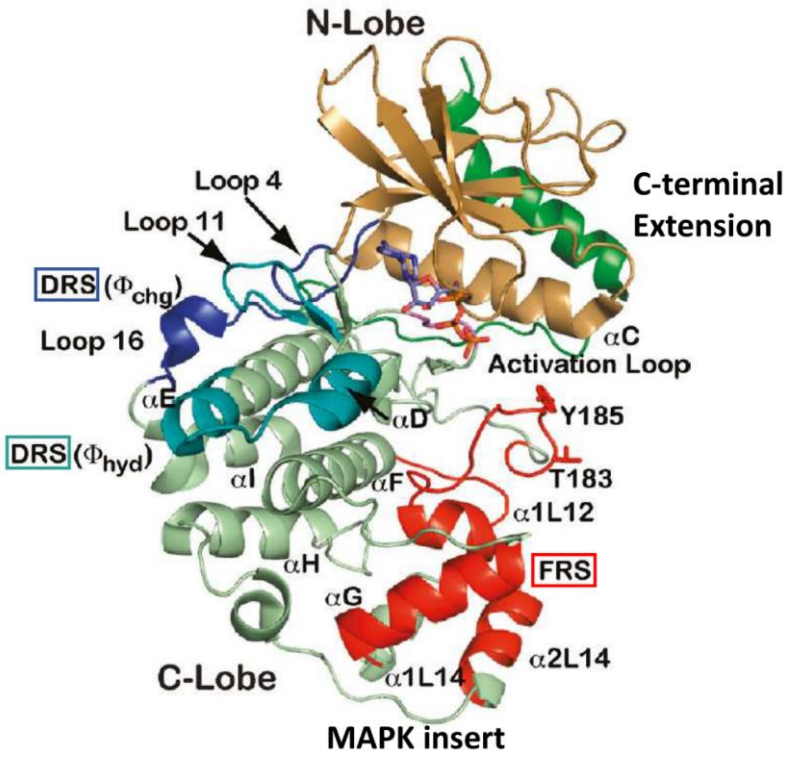

Figure 1.13. Visual representation of ERK2 structure. The activation loop, placing the catalytic Thr183 and Tyr185 (mouse numeration), is shown in stick representation. The F-recruitment site (FRS) is colored red. At the opposite side, the D-recruitment site (DRS) is shown in two colors; the Φchg subsite is blue, and the Φhyd subsite is cyan. Adapted from (Piserchio et al., 2011).

The combination of all these recruitment sites, together with the compartmentalization of ERK substrates, fine-tune substrate regulation to generate specific outcomes.

1.2.3.4.1 Nuclear substrates

To control the activation and the regulation of certain genes, active ERKs monomers translocate to the nucleus where they phosphorylate, directly or through the activation of other kinases (such as RSKs and MNKs), specific transcription factors. ERK phosphorylates transcription factors such as the TCFs type (ternary complex factors) like Ets1/2 and Elk1; the AP-1 family (activation protein-1) such as c-Fos and c-Jun (Murphy et al., 2002); and c-Myc and p53 (Hannen et al., 2017; Yoon and Seger, 2006). Another ERK target is FoxO3a, whose phosphorylation inactivates its inhibitory function, promoting cell survival (Yang et al., 2008). All these substrates are involved in the

regulation of proliferation and oncogenic transformation. Moreover, at the nucleus ERK phosphorylates pro-apoptotic proteins such as Bad (Bcl-2 associated death promoter), Bim or Caspase (Hannen et al., 2017)

1.2.3.4.2 Cytoplasmic substrates

Active ERK dimers can directly phosphorylate more than 70 cytoplasmic substrates. In addition to this, ERK phosphorylates and activates some MAPKAPKs proteins, that in turn increase significantly this number (Casar et al., 2009). The best known MAPKAPK proteins are the 90 kDa ribosomal S6 Kinase (RSKs) family. Activated RSK catalyses the phosphorylation of 35 nuclear and cytoplasmic proteins. Notably, ERK phosphorylates the RSK C-terminal domain, which leads to RSK-autophosphorylation. Nevertheless, to be fully activated, RSK requires an additional phosphorylation on its N-terminal domain by PDK1-mediated (Alexa et al., 2015). Active RSKs can independently translocate to the nucleus, regulating the expression of other genes. In fact, RSK can mediate cell survival, inactivating the pro-apoptotic protein Bad, or promote cell cycle progression, by inhibiting the cyclin-dependent kinase inhibitor p27 KIP (Roskoski, 2012a). In addition, ERK, as well as p38 α and β, activate other two MAPKAPKs, the MSKs (mitogen- and stress- activated kinase) and MNKs (MAP kinase-interacting kinases) (Yao and Seger, 2009).

Another well-established ERK substrate is the cytosolic phospholipase A2 ($cPLA_2$). Upon EGF stimulation, phosphorylated ERK dimers, in association with the scaffold KSR1, phosphorylate $cPLA_2$ on Ser505 (Casar et al., 2008; Lin et al., 1993).

Additionally, ERK can phosphorylate cytoskeletal proteins such as paxillin, which regulate focal adhesion kinase or actin-binding proteins like Palladin, regulating morphological and migratory cell behaviour (Roskoski, 2012a).

Moreover, as described in the previous section, ERK is able to phosphorylate most of the components of its pathway, like EGF, SOS, C-RAF or MEK, thereby modulating the intensity and the durability of the signalling conveyed through Ras-ERK pathway (Lake et al., 2016).

1.2.4 Scaffold proteins

A large number of studies have questioned the initial concept of RAS-ERK pathway linearity. In fact, the complexity of the biological outcomes raised by ERK activation cannot be explained by simple sequential phosphorylation events through a linear signalling route. Thus , additional levels of regulation might provide variability to ERK signals (Kolch, 2005). In this direction, many publications have highlighted the involvement of regulatory proteins known as scaffold proteins (Chol et al., 1994; Morrison, 2001; Therrien et al., 1996). According with the scaffold definition, these proteins simultaneously connect at least two components of the pathway (Fig 1.14 A), and in so doing they regulate amplitude and intensity, in addition to conferring spatial selectivity to ERKs signals (Dhanasekaran et al., 2007; McKay and Morrison, 2007).

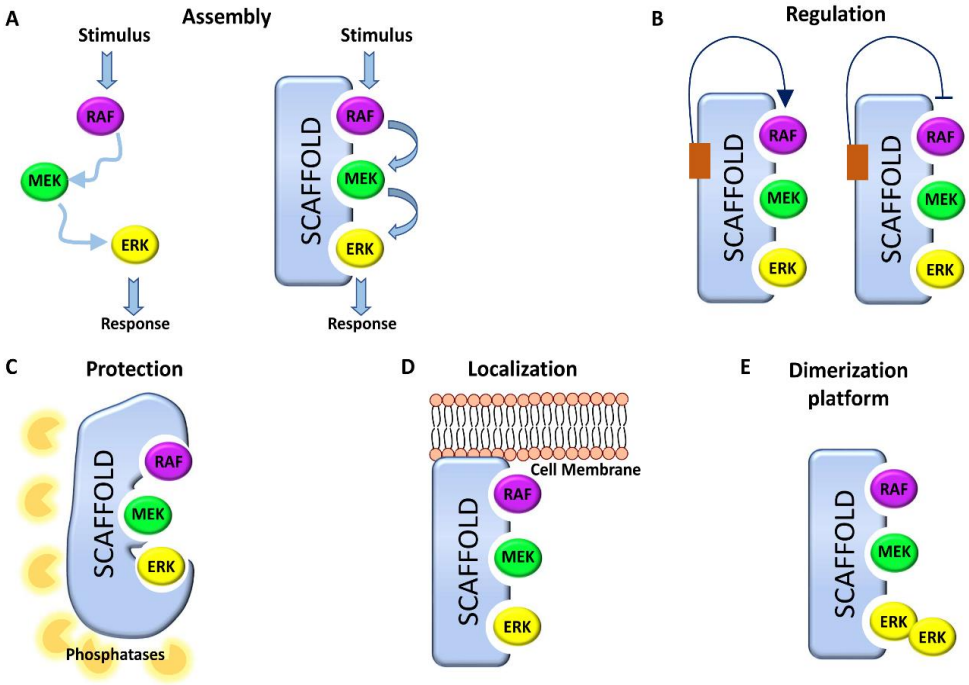

Figure1.14. Schematic representation of Scaffold functions. A) According to Scaffolds definition, their main function is serving as assembly platform, thereby connecting different components of the pathway. **B)** Scaffolds function as allosteric regulatory proteins, enhancing or inhibiting the activation of their interacting proteins; **C)** Moreover, they protect MAP kinases from phosphatases action, facilitating flux signal. **D)** Scaffolds serve as spatial regulators of ERK signals, as well as, **E)** ERK dimerization platform, which give them specific localization and striking specificity toward substrate activation.

Saccharomyces cerevisiae Ste5 was the first scaffold to be described. It functions as an assembly platform, forming, in response to mating pheromones, a macro-complex with the yeast three orthologs of the MAPK pathway: Fus3 (MAPK), Ste7 (MAPKK) and Ste11 (MAPKKK) (Chol et al., 1994). Soon after, the first mammalian scaffold was identified: KSR1 (Kinase Suppressor of Ras) (Therrien et al., 1996). KSR1 was described as a modulator of RAF, MEK and ERK proteins, enhancing their kinase activity. Now, it is known that scaffolds function not only as a simple hub assembling different kinases along the pathway, but also cooperate in order to fine-tune signals amplitude and duration (Casar and Crespo, 2016; Garbett and Bretscher, 2014). From the structural point of view, scaffold proteins increase the local concentration of the interacting molecules, as well as, placing them in the right orientation, thereby facilitating the phospho-transfer reactions (Levchenko et al., 2000). Moreover, Scaffolds can allosterically stimulate, or inhibit, their partners activity, therefore enhancing, or blocking, signal flux through the pathway (Fig 1.14 B). A clear example of these functions is given by KSR1. It is known that in resting cells, KSR1 is constitutively bound to MEK at the cytoplasm. In this state, KSR1 activity is blocked by the E3 ubiquitin ligase IMP. Upon stimulation, Ras-GTP induces IMP degradation, thereby releasing KSR and allowing its translocation to the plasma membrane, where it interacts with RAF (Shaul and Seger, 2007). There, RAF interaction with KSR in cis induce a conformational change on MEK which exposes its activation loop in order to be phosphorylated in trans by RAF (Rajakulendran et al., 2009).

Additionally, scaffold proteins serve as a molecular protection, shielding MAPKs from dephosphorylation (Fig 1.14 C). Therefore, scaffolds would protect kinases from cytoplasmic phosphatases action, increasing MAPKs signalling (Levchenko et al., 2000; Locasale et al., 2007).

Another essential scaffolds feature, which adds to the aforementioned functions, is their ability to serve as spatial regulators of ERK signals, acting in a sublocalization-specific fashion (Fig 1.14 D) (Casar and Crespo, 2016). All of the ERK scaffolds are extranuclear proteins, and it has been unveiled that scaffolds has a specific localization within the cytoplasm (Plotnikov et al., 2011).

Moreover, it has been established that depending from which cell compartment the Ras signal emanates, a specific scaffold determines ERK substrate specificity (Casar et al., 2009). Accordingly, KSR1 controls ERK signals generated in lipid raft domains (Matheny et al., 2004), MP1 specifically supports MEK1 and ERK1 signals at late endosome (Teis et al., 2002), Paxillin at focal adhesion (Ishibe et al., 2004) and Sef is the scaffold functioning at the Golgi complex (Torii et al., 2004). Additionally, scaffold proteins have the ability of serving as dimerization platform (Fig 1.14 E) (Casar et al., 2008). In this process, ERK dimers serve as connectors between scaffolds and ERK substrates. This feature would further increase ERK selectivity toward its substrates. In support of this idea, results from our lab have shown that ERKs cytoplasmic substrates like $cPLA_2$, EGFR, RSK1 and PDE4, specifically bind to ERK in dimeric form. Precisely, KSR1 is the scaffold involved in $cPLA_2$ activation, whereas IQGAP1 is the scaffold which mediates on EGFR phosphorylation. Intriguingly, when ERK is retained by a scaffold at the cytoplasm, ERK nuclear events are decreased in parallel. This evidence supports the notion that ERK nuclear activity is mainly carried out in monomeric form (Casar et al., 2009, 2008; Herrero et al., 2015).

Up to now, 15 mammalian scaffolds have been identified. The following list includes some scaffolds which stand up for their role in ERK regulation (Fig.1.15).

- **KSR 1/2** (Kinase Suppressor of Ras), due to its structural homology with RAF, it has ignited an unsolved debate about its role as a kinase (Hu et al., 2011; Nguyen et al., 2002). In resting cells, KSR is constitutively bound to MEK. Upon Ras activation it translocates to the plasma membrane, where it coordinates Ras/MEK/ERK association (Lavoie and Therrien, 2015; Therrien et al., 1996). KSR1 specifically mediates $cPLA_2$ activation when ERK is activated from lipid raft (Casar et al., 2009; Casar and Crespo, 2016).
- **IQGAP** (Ras GTPase-activating-like protein) family are composed by three isoforms, being IQGAP1 the best characterized (White et al., 2009). It is localized at the cytoplasm where it binds B-RAF, MEK and

ERK, promoting ERK activation by EGF (Roy et al., 2005). IQGAP1 mediates EGFR phosphorylation upon EGF stimulation (Casar et al., 2009). IQGAP also interacts with Cdc42 and Rac1 promoting cell proliferation, cell motility and invasion (White et al., 2009). IQGAP1 can also function as a PI3K pathway scaffold, interacting with AKT and PDK1. This interaction is mutually exclusive, thus the binding of ERKs excludes the binding of PI3K pathway members (Choi et al., 2016). This interaction could indicate an additional node of regulation existing among the two pathways, which is usually altered in multiple cancers (Pan et al., 2017).

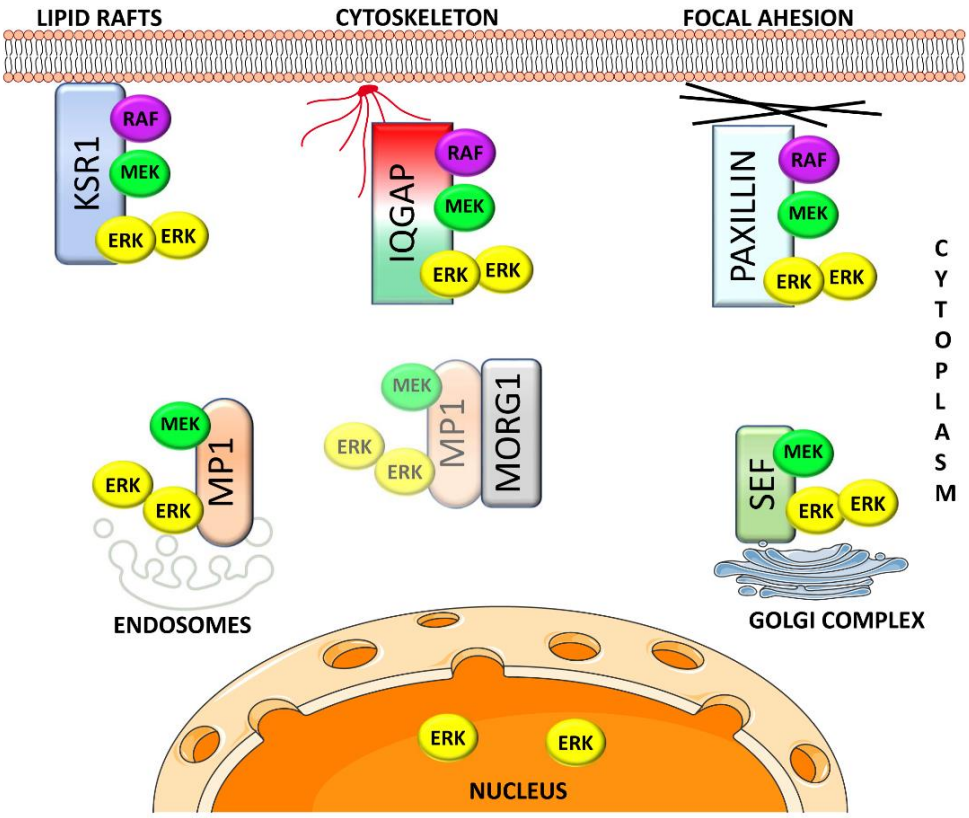

Figure 1.15. Representation of some Scaffolds proteins involved in the spatial regulation of Ras-ERK pathway. Depending from where cellular compartment Ras signals are emanated, different scaffolds determine ERK localization and specific substrate activation. Adapted from (Casar and Crespo, 2016).

- **Paxillin** is localized at focal adhesion where it orchestrates ERK signalling through other kinases such as Focal Adhesion Kinase (FAK) (Ishibe et al., 2004). Upon HGF (hepatocyte growth factor) stimulation, Paxillin-MEK-ERK complex regulates FAK and Rac activation, through which it promotes cellular spreading, plasticity, and metastasis (Deakin et al., 2012).
- **Sef** (similar expression to fgf genes) was originally described in zebrafish as an inhibitor of FGF-induced Ras-ERK pathway (Fürthauer et al., 2002). hSef is localized at the Golgi apparatus where it binds active MEK, it inhibits MEK-ERK complex dissociation, preventing ERK nuclear translocation (Torii et al., 2004). In PC12 cells, Sef-ERK cytoplasmic retention inhibits differentiation induced by NGF (Xiong et al., 2003).
- **MP1** (MEK Partner 1) specifically binds to MEK1 and ERK1, but not MEK2 or ERK2 (Schaeffer, 1998). MP1 interacts with p14, an adaptor protein associated with late endosomes (Teis et al., 2006, 2002), otherwise it is localized at the cytoplasm, where it is rapidly degraded (De Araújo et al., 2013). At late endosomes, MP1-p14 complex enhance ERK signalling (Teis et al., 2006). The MP1-p14 scaffold is also involved in MEK1 activation, mediated by PAK1. In such a way, this complex regulates cell adhesion and cell spreading on fibronectin. Moreover, MP1 is needed for the transient suppression of Rho and ROCK (Rho-associated protein kinase), which is a further requirement for cell adhesion and spreading (Pullikuth et al., 2005).
- **MORG1** is a cytoplasmic scaffold whose association with C-RAF, MEK and ERK facilitates ERK activation upon LPA (lysophosphatidic acid) or serum but not EGF stimulation. MORG1 also interacts with MP1 forming a macro-complex (Vomastek et al., 2004). This association among different scaffolds would confer an additional degree of complexity to the already extremely intricate regulation of signal flux through the RAS-ERK pathway.
- **RKIP** (RAF Kinase Inhibitor Protein) is bound to RAF in resting cells, forestalling MEK1 activation. Although RKIP features are quite different from a classic scaffold, its ability to regulate Ras-ERK pathway is well established, thus it can be included within the scaffold group

(Kolch, 2005). Upon mitogenic stimulation, RKIP releases RAF, allowing MEK and ERK activation. RKIP functions as tumour suppressor and its down-regulation is often associated with resistance of cancer cells to anti-neoplastic treatments (Casar and Crespo, 2016).

- **PEA15** (Phosphoprotein-Enriched in Astrocytes 15) binds to active cytoplasmic ERK1/2, blocking their cytoplasmic activity and nuclear translocation. In addition to this, PEA15-ERK binding also reduces ERK dephosphorylation, by that means providing a store of active ERK ready to act independently on its upstream activator (Mace et al., 2013; Zaballos et al., 2019). PEA15-ERK dissociation is mediated by the phosphorylation of two Serines: Ser106 by PKC and Ser104 by AKT (Mace et al., 2013). Interestingly, NGF-stimulated PC12 cells show a sustained AKT activation and a stronger dissociation of the complex PEA15-ERK, when compared to EGF stimulation. In such a way, PEA15 would mediate the crosstalk between AKT-ERK and ERK-PKC (Von Kriegsheim et al., 2009). Alterations in PEA15 expression have been associated with resistance in tumour cells (Zaballos et al., 2019).

1.3 RAS-ERK signalling in Cancer

The Ras-ERK pathway regulates a broad variety of physiological processes, thus is logical that alterations in this route trigger dramatic responses. Indeed, alterations in this pathway are closely linked to cancer, representing an arduous challenge for researcher all over the world.

1.3.1 RAS mutations

Ras oncogenes appear mutated in approximately one-third of all cancers. This percentage is still more dramatic when its prevalence is examined in specific types of cancers; being 90% in pancreas, 50% in colon and in thyroid, 30% in lung and 25% in melanoma. Among the three RAS isoforms, H-RAS, N-RAS and K-RAS, K-RAS is the most commonly mutated (Ryan and Corcoran, 2018).

Ras proteins normally switch between two states: inactive, where RAS is GDP bound, and active, where RAS is GTP bound. The oncogenic mutations make RAS insensitive to the GTPase activity of GAP proteins and, as a consequence, result in its constitutively activation. This leads to an aberrant activation of its downstream effectors, which promote cellular transformation and tumour progression.

Despite the fact of having been described more than 40 years ago and having been largely investigated, no effective RAS inhibitor has been developed so far, which has moved the researcher's attention to downstream targets, such as RAF or MEK.

1.3.2 RAF mutations

RAF genes are the most frequently mutated among constituents of the ERK pathway. Particularly, B-RAF is mutated in around 7-10 % of human cancers. As in the case of RAS, this percentage is dramatically higher in certain types of cancer, such as in melanoma, where it reaches 55% (García-Gómez et al., 2018; Yaeger and Corcoran, 2019). C-RAF was the first to be identified as a potential oncogene. However, due to its low mutational incidence in cancer, the attention shifted towards B-RAF (Samatar and Poulikakos, 2014). The most common B-RAF mutations found in cancer are point mutations, that enhance its

kinase activity, like the V600E substitution, but also fusions and in-frame deletions have been identified.

Depending on the reliance on Ras activity, B-RAF mutations have been classified into three classes:

I) Class I B-RAF mutants: that signal as monomers, RAS-independently. The B-RAF V600E mutation is found in around 50% of melanomas (Yaeger and Corcoran, 2019). Due to its particular composition of the phosphorylation domain, WT B-RAF contains two phosphomimetic aspartic aminoacids (SSDD motif), which confer a higher basal activity compared with the other two isoform (Lavoie and Therrien, 2015). In fact, A-RAF or C-RAF mutations are very rare in cancer. Therefore, when it acquires the mutation V600E, B-RAF activity is further enhanced, also being capable of signalling as a monomer. Thus, B-RAF V600 mutant strongly activates its downstream effectors, MEK and ERK, independently of Ras (Yaeger and Corcoran, 2019).

II) Class II B-RAF mutants: they signal as dimers, such as mutants K601E, L597Q and G469A. These mutants do not require RAS activity to dimerize, thereby they are constitutively active as dimers. These mutations generally appear as a result of acquired resistance to inhibitors (Yaeger and Corcoran, 2019). In-frame deletions and B-RAF fusions can be included in this class. Particularly, deletions normally affect the β3-αC region, close to the P-loop, rendering this region shorter, blocking the αC helix in the “in” position, thus constitutively active, thereby enhancing B-RAF kinase activity.

III) Class III B-RAF mutants, contrarily to the previous groups, this comprises impaired (D594G/N) or reduced activity (G466V/E) (Yao et al., 2017). Despite their null or low activity, these mutants increase ERK signalling, enhancing C-RAF activation through heterodimerization between mutant B-RAF and WT C-RAF. Moreover, this activity is RAS dependent. In fact, class III B-RAF mutants bind tightly to RAS. As a consequence, these mutations are normally associated with RAS activating mutations, RTK overactivation or NF1 downregulation (Heidorn et al., 2010; Yaeger and Corcoran, 2019; Yao et al., 2017).

1.3.2.1 RAF inhibitors

Hitherto, many compounds have been developed to counteract RAF overactivation (Fig.1.16). However, despite initial positive effects most of them wane their effectiveness, causing relapse withing a year. This is the case of the ATP-competitive inhibitor Vemurafenib (PLX4032), the first B-RAF V600E selective-inhibitor to be approved for clinical use by FDA (Bollag et al., 2010; Flaherty et al., 2010). Interestingly, Vemurafenib therapeutic efficacy corresponds with a reduction in ERK cytoplasmic but not nuclear phosphorylation (Bollag et al., 2010; García-Gómez et al., 2018). Dabrafenib (GSK2118436) is also effective for the treatment of metastatic melanoma harbouring B-RAF mutations. Unfortunately, these compounds are only effective in those tumours where B-RAF V600 signals as a monomer. Contrarily, not only they are unable to block RAF dimers signals, but binding to one protomer provokes the hyperactivation of the other protomer. This phenomenon has been defined as the “paradoxical activation of RAF” and leads to the re-activation of the pathway, causing ERKs overactivation. This provokes relapse and tumour progression. To overcome this issue, new compounds, named RAF dimer inhibitors, such as LXH225 or LY3009120, have been developed. Mechanistically, these inhibitors should inhibit tumours with mutant RAF dimers. Moreover, they should be effective also in those tumours harbouring other B-RAF mutations or RAS mutations (Yaeger and Corcoran, 2019). In addition, other compounds, named “paradox breakers” (PLX8394), are currently in phase I studies (Zhang et al., 2015). These compounds specifically disrupt B-RAF-containing dimers, such as B-RAF homo- or heterodimers. However, since they also inhibit signalling in normal cells, its therapeutic window is limited. In addition, PLX8394 is not able to inhibit C-RAF, which could eventually lead to its paradoxical activation. Thus, B-RAF-mutant tumours belonging to class II or III should be treated with downstream inhibitors, such as those for MEK or ERK (Liu et al., 2018; Yaeger and Corcoran, 2019).

1.3.3 MEK mutations

MEK mutations are uncommon in human cancer. They usually appear as an adaptive acquired resistance, provoked by sustained treatment with RAF or MEK inhibitors. As in RAF, MEK mutations have been classified into three classes. i) A class of RAF-independent MEK alterations have been identified in certain cancers, even though its frequency is quite low. These alterations affect MEK negative regulatory region (in-frame deletions comprising Δ98-104), which lead to its overactivation in a RAF-independent fashion (Gao et al., 2018; Yuan et al., 2018). Thus, these mutants act independently of its phosphorylation and are considered as strong ERK "activators" (Yaeger and Corcoran, 2019). ii) RAF-dependent mutants are another class of MEK alterations. This type of mutations normally coexists with RAS, RAF or NF1 alterations in tumours. Particularly, this class of MEK1 mutants coexist with B-RAF V600E in untreated melanomas (Gao et al., 2018). Iii) Finally, RAF-regulated MEK alterations display some basal level of activity which is further increased by RAF. Mutations like K57N or F53L have been identified in patients with B-RAF V600E colorectal cancer with acquired resistance to upstream inhibitors (Gao et al., 2018; Yaeger and Corcoran, 2019).

1.3.3.1 MEK inhibitors

U0126 was the first MEK inhibitor developed. However, despite its high specificity towards MEK, U0126 showed poor pharmacological properties and its use has been limited to the laboratory scope (Frémin and Meloche, 2010). To date, most MEK inhibitors having therapeutic application, like trametinib, cobimetinib and binimetinib (FDA-approved), are allosteric kinase inhibitors (Fig.1.16) (Yaeger and Corcoran, 2019).

The advantage of these compounds is that they are extremely specific. They bind to an allosteric pocket in MEK producing a conformational change, forcing MEK to acquire an inactive state. Moreover, trametinib also reduces the interaction between RAF and MEK, preventing MEK activation. However, these drugs present a big limitation, especially when upstream mutations increase MEK activation; as these compounds show more affinity toward inactive MEK, they do not distinguish between tumour and normal cells, thus, resulting in toxicity and limitation of its efficacy. To overcome these issues, new inhibitors have recently emerged. The ATP-competitive MAP855, binding to the catalytic site of MEK, is effective against all MEK alterations. Particularly, it has turned out to be especially effective in the case of RAF-independent MEK alterations, which are insensitive to previous MEK inhibitors (Gao et al., 2018).

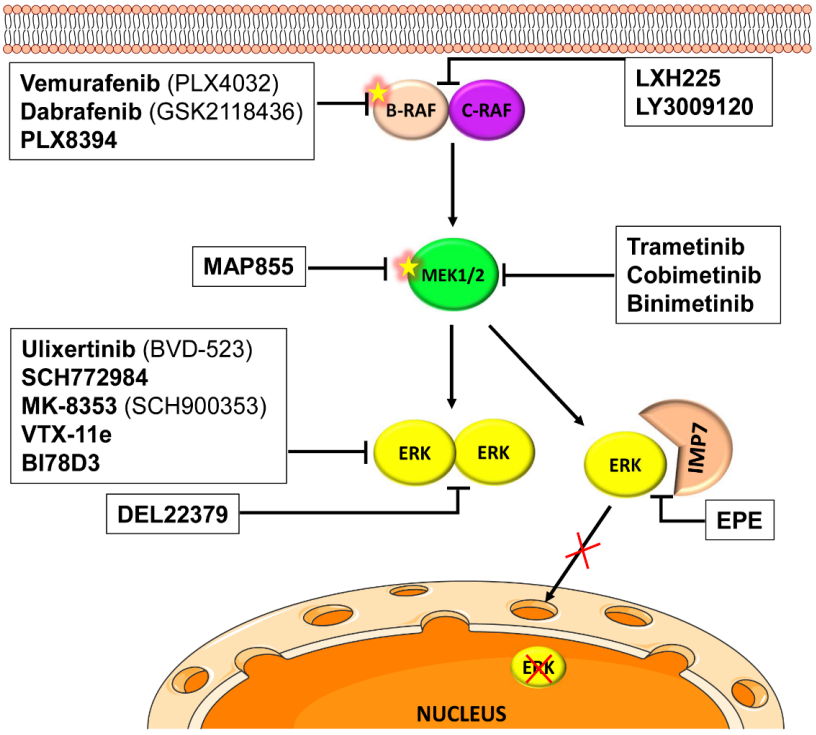

Figure 1.16. Representation of some RAS-ERK pathway inhibitors currently used to modulate aberrant pathway activation. The ATP-competitive Vemurafenib and Dabrafenib selectively inhibit BRAF V600 oncogene. The newer PLX8394 shows similar mechanism of action and prevents paradoxical activation. LXH225 and LY3009120 are RAF dimers breakers. Trametinib, cobimetinib and binimetinid are allosteric MEK inhibitors. The ATP-competitive MAP855 blocks MEK activation. Ulixertinib, SCH772984, MK-8353 and VTX-11e are ERK1/2 ATP-competitive inhibitors. The small molecule BI78D3 targets ERK DRS site. DEL22379 prevents ERK dimerization, while EPE peptide blocks ERK nuclear translocation inhibiting ERK-Importin7 binding. Stars positioned over B-RAF and MEK indicate activating mutations.

1.3.4 ERK mutations

ERKs mutations are very uncommon in cancer. Noticeably, the mutation rate decreases progressively moving downstream along the Ras-ERK pathway. Moreover, attempting to generate constitutive active ERK has failed, hinting that it is not as simple as introducing a phosphomimetic aminoacid in the activation lip, probably due to its tight regulation (Canagarajah et al., 1997). Very recently, from a bioinformatic-based evolutionary study has emerged that ancestor ERKs were active independently of its upstream activators. Thus, to obtain a constitutive active ERK it would be necessary the insertion of two residues, one in the region connecting the αC-helix and the β3 strand (ERK1 position 74), and the other in the gatekeeper residue (ERK1 Gln122) (Atias et al., 2020; Sang et al., 2019).

Furthermore, genetic screens in *D. Melanogaster* and *S. cerevisiae* revealed several ERK orthologs mutations having gain-of-function (GOF) in these species, which are evolutionary conserved and would render ERK constitutively active (Askari et al., 2006; Brunner et al., 1994). These studies, have led to the generation of an active ERK2 (Emrick et al., 2001). This required the incorporation of three point-mutations, namely the L75P+S153D+D321N. Although this mutant shows a MEK-independent activity *in vitro*, its activity is not much higher than MEK-phosphorylated ERK. The combination of the above cited mutations was also tested in Zebrafish, where injected fishes showed an increased phosphorylation of CDK1 and hyperphosphorylated RSK and CREB (Rian et al., 2013). Specifically, L75P mutation was found as a determinant mutation in a screening aiming to unveil mutations that could confer resistance to VRT-11e ERK inhibitor (Atias et al., 2020; Brenan et al., 2016). D321N mutation was first described as a ROLLED GOF mutation in *D. Melanogaster*. Due to its ability to activate the sev pathway was named “sevenmarker”. Moreover, this residue also appeared in the list of inhibitor-resistant ERK2 mutants (Brenan et al., 2016), and in cancer patients (Atias et al., 2020). Next to the sevenmarker, E322K appeared in a few patients affected by cervical and head and neck carcinoma. These mutations, neighbouring ERK CD domain, increase ERK activity, by decreasing its dephosphorylation, as a consequence of reduced affinity to DUSP (Taylor et al., 2019).

On the other hand, R84S (ERK1) is the only single mutation capable of generating an intrinsically active ERK (Smorodinsky-Atias et al., 2016). ERK1 R84S shows a prompt ability to transform NIH3T3 cells, thus acting as an oncoprotein. The mutant R84S, the serine being smaller than arginine, shows enhanced activation lip flexibility due to the loss of interaction between R84 and the DGF motif. This lack of interaction seems to be the determinant for its autophosphorylation propensity (Atias et al., 2020).

Noticeably, R84S and R67S (ERK2) were found in only 2 cancer patients, and also in a screening for mutants resistant to trametinib and dabrafenib, highlighting again that activating ERK mutation are rarely found in cancer (Atias et al., 2020; Goetz et al., 2014).

Indeed, the majority of ERK mutations have been discovered in laboratory screenings. Although ERK mutations are distributed along the protein, from these analyses emerge that ERK2 mutations mostly occurs close to the ATP/drug binding pocket, thus might interfere with inhibitors. Contrarily, ERK1 mutations are clustered in domains important for catalysis that could provide autoactivation property. Generally, mutation at the CD site alter protein-protein interaction and seem to be more prominent in ERK2. By contrast, mutation in the gatekeeper, in the proximity of the αC-helix, increase ERK1 intrinsic kinase activity. This could indicate that there are specific isoform mutations which may affect differently ERK1/2 activity (Atias et al., 2020; Brenan et al., 2016; Goetz et al., 2014; Jaiswal et al., 2018).

1.3.4.1 ERK inhibitors

Knowing that mutations occurring along the RAS-ERK pathway ultimately drive ERKs overactivation and considering all the difficulties faced by RAF and MEK inhibitors, ERK becomes an attractive target as an effective anti-cancer approach.

ERK inhibitors are classified into five categories. Type I and II are inhibitors which bind the ATP-binding pocket in the active or inactive conformation, respectively (Lechtenberg et al., 2017). Two compounds of these categories are currently in clinical trial, namely the BVD-523, also known as Ulixertinib

(Germann et al., 2017) and SCH772984 (Morris et al., 2013) (Fig. 1.16). Both are potent ATP-competitive inhibitors showing antiproliferative effects in cell lines harbouring B-RAF or K-RAS mutation. BVD-523 efficacy was also tested in patient-derived xenografts resistant to vemurafenib. Moreover, it is currently in phase I/II of clinical trials for solid tumours and melanoma resistant to RAF-MEK inhibitors. In the case of SCH-772984, it prevents ERK kinase activity as well as MEK-mediated ERK phosphorylation (Liu et al., 2018). MK-8353 is an orally bioavailable successor of SCH-772984, showing improved pharmacokinetic properties. It entered phase I trial in patients with advanced solid tumours (Moschos et al., 2018).

Another compound with a similar mechanism of action is VTX-11e. X-ray co-crystallography studies of VTX-11e-ERK interaction reveals the ability of this compound to shift the activation loop towards a released position, more susceptible to phosphatases action (Pegram et al., 2019). However, despite this promising result, it has not passed into clinical trial yet (García-Gómez et al., 2018).

Type III and IV are allosteric inhibitors which bind close or far from the ATP binding pocket, respectively. However, none of these inhibitors have found application out of the laboratories.

A newer approach to block ERK activity is targeting protein-protein interactions using small molecules. The interest towards these compounds arise from recent evidence of ERK mutations (e.g. G186D ERK1) induced by long-term exposure to SCH-772984 (Jha et al., 2016), therefore newer inhibitors are essential to overcome incoming resistance issues. This type of inhibitors target two ERK regions, normally the ATP-binding pocket and the DRS, the D-site substrate recruitment of ERK. Structure-guided analysis lead to the development of SBP3, which is a combination of the FR180204 ATP-competitive inhibitor and a DRS-targeting peptide, derived from RSK1 structure, both chemically linked. However, despite encouraging initial results, efficacy and selectivity of this compound require further adjustment. (Lechtenberg et al., 2017). In the same line goes another compound which targets the ERK-DRS. BI78D3, which is able to form a covalent bound with a conserved cysteine (C159) residue, located in

the core of the DRS, preventing ERK signalling *in vivo*. Although it is still in an early stage, this compound blocked cell cycle progression, inducing apoptosis both in B-RAF naïve and B-RAF resistant cell lines (Kaoud et al., 2019).

Another strategy proposed by Seger lab is the inhibition of ERK nuclear translocation. Since most of resistance phenomena are associated with inhibition of ERK-mediated negative feedback loops, which are mainly cytoplasmic signals, inhibiting ERK entrance to the nucleus would prevent cell proliferation without affecting cytoplasmic ERK activity. As already mentioned, ERK-SPS phosphorylation is essential for the binding with Importin7, which allows ERK translocation to the nucleus. Thus, these researchers have synthesized a peptide, that mimics the ERK-NTS sequence and competes with importin7 binding. Thereby, blocking ERK nuclear shuttling. This peptide induces apoptosis in B-RAF melanoma cells resistant to MEK or B-RAF inhibitors (Flores et al., 2019; García-Gómez et al., 2018; Plotnikov et al., 2015). Contrarily, in our lab we have described the efficacy of another small molecule, DEL22379, which prevents cytoplasmic signals by blocking ERK dimerization. Thereby, DEL22379 reduces tumour progression both in cells and in xenograft harbouring B-RAF mutations. Interestingly, DEL22379 shows mild adverse effects and it is not affected by resistance mechanism. Thus, the advent of these compounds might represent a novel opportunity to treat tumours, evading resistance mechanisms mutation-associated (Herrero et al., 2015), and also being a valid alternative in circumstances where other inhibitors fails (Brenan et al., 2016; Goetz et al., 2014)

2. OBJECTIVES

Signals conveyed through ERK1/2 Mitogen-Activated Protein Kinases are well-known to play a critical role in cancer initiation, progression and therapy resistance. It has been demonstrated that the balance between ERK monomer and dimers and cytoplasmic and nuclear sub-signals are critical for the biological outcomes resulting from ERK activation subcellular distribution. During the course of our experiments leading to the discovery of DEL-22379, a new compound that blocks ERK dimerization, we made the startling observation that ERK dimers were absent in fish, birds or amphibians, ERK dimerization being restricted to mammalians. A comparison of the ERK2 sequence through the evolutionary scale unveiled that Serine284 (H.sapiens) was conserved in those species in which ERK2 dimerized.

In light of the previous literature and of the aforementioned preliminary data, the aims of this thesis are:

1. To unravel the mechanistic details of the role played by serine 284 phosphorylation on ERK dimerization and subcellular distribution.
2. To elucidate the functional consequences of S284 phosphorylation on the biochemical nature of ERK2 signals and on the biological outputs governed by them.
3. To establish the relevance of ERK2 S284 phosphorylation for carcinogenic processes and its potential use as a prognostic marker in melanoma.

3. MATERIALS AND METHODS

3.1 DNA MANIPULATION AND ANALYSIS

3.1.1 Plasmidic DNA purification

Plasmid DNA purification was carried out from bacterial cultures derived from bacterial competent cells DH5α (Invitrogen), an Escherichia coli strain modified to maximize transformation efficiency. Transformed bacteria were inoculated in 250 mL (maxiprep) or 5 mL (miniprep) of Luria-Bertani Broth (LB) culture medium with their specific resistance antibiotic provided by the plasmid, usually ampicillin or kanamycin at the concentration of 50 µg/mL. After being incubated overnight (O/N), bacterial were centrifuged at 6000 rpm for 15 min (maxiprep) or at 4000 rpm for 10 min (miniprep). For maxiprep, the Qiagen Plasmid Maxi Kit was used. Pellet was resuspended in 10 mL of resuspension buffer (50mM Tris/HCl pH 8, 10Mm EDTA, 10 µg/mL RNaseA). Cells were lysed with 10 mL of lysis buffer (200mM NaOH, 1% SDS), mixed by inverting 6 times and incubated for 5 min at room temperature. A neutralization solution (3M CH_3COOH pH 5,5) was added and incubated for 5 min. Then, the mix was centrifuged at 12000 rpm for 5 min to eliminate the precipitated material containing genomic DNA, proteins and cellular debris. The supernatant, containing the plasmid DNA, was filtrated in a properly equilibrated anion-exchange Qiagen column by gravity flow. After two washes, the DNA was eluted with 5 mL of elution buffer and 10 mL of cold isopropanol were added to precipitate the DNA. After 5 min, this mix was centrifuged at 10000 rpm 30 min at 4ºC, and then washed with 1 mL of ethanol 70%. Once dried, DNA was resuspended in 300 µL of distilled deionized water (ddw).

In the case of bacterial cultures of lower scale (5 mL of volume), the bacterial culture was processed by GeneJET Plasmid Miniprep Kit (Thermo Fisher) according to the manufacturer's instructions. The purified DNA was eluted in 40 µL of Elution Buffer (10 mM Tris, 1 mM EDTA).

The plasmid DNA was quantified using Nanodrop (Thermo scientific). 1 µL of DNA was used for the quantification. To further analyze the quality and any RNA contamination, 2 µL of DNA was loaded in a 0,8% agarose gel electrophoresis, run at 80 V in TAE buffer (0.09 M Tris-acetate, 2 mM EDTA)

and stained with SYBER safe (Invitrogen). A loading buffer with bromophenol blue to monitor the progress of the electrophoresis was added to the DNA sample.

3.1.2 Plasmid description

All the plasmid used in this thesis are listed in the following table.

Table 3.1 Description of the plasmids used in this Thesis

PLASMID	DESCRIPTION
pCEFL	Mammal expression vector. EF-1α Promoter/ bGH poly-A. Empty vector used as a control to normalize the amount of DNA to transfect.
pCEFL HA ERK 2 WT	Mammal expression vector. EF-1α Promoter/ bGH poly-A. Encodes the isoform ERK2 fused to HA epitope. Source: Dr. D. Engelberg
pCEFL FLAG ERK2 WT	Encodes the isoform ERK2 fused to FLAG epitope. Source: GeneArt Gene Synthesis, Thermo Fisher Scientific
pCEFL FLAG ERK2 S284P	Encodes the ERK2 mutant unable to dimerize fused to FLAG epitope. Source: GeneArt Gene Synthesis, Thermo Fisher Scientific
pCEFL FLAG ERK2 S284E	Encodes the ERK2 phospho-mimetic mutant fused to FLAG epitope Source: GeneArt Gene Synthesis, Thermo Fisher Scientific
pCEFL FLAG ERK2 Dr WT	Encodes the zebrafish (*Danio Rerio*) ERK2 isoform wild type FLAG-tagged. Source: Dr. L. Agudo
pCEFL FLAG ERK2 Dr P292S	Encodes the zebrafish (*Danio Rerio*) ERK2 isoform mutant P292S fused to FLAG epitope. Source: Dr. L. Agudo
pECE myr-HA AKT Δ4-129	Constitutively activated AKT isoform. N-terminal myristoylation sequence. HA tagged at C-terminus. Pleckstrin homology domain deleted (Δ4-129 PH). SV40 promoter/SV40 poly-A. Source: Dr. I. Arozarena
pCMV FLAG AKT1	Encodes the AKT1 FLAG-tagged. Source: Dr. A. Cuadrado
pCAGGS FLAG ERK2 WT	Mammal high levels of gene expression vector. CAG promoter/β-globin poly-A. Encodes the mouse ERK2 isoform fused to FLAG epitope at C-terminus. Source: Dr. K. Aoki
pCAGGS FLAG ERK2 S282P	Encodes the mouse ERK2 mutant unable to dimerize fused to FLAG epitope (C-terminus). Source: Dr. K. Aoki

pCAGGS FLAG ERK2 S282E	Encodes the mouse ERK2 phospho-mimetic mutant. FLAG epitope at C-terminus. Source: Dr. K. Aoki
pCAGGS FLAG ERK2 WT mCFP	Encodes CFP at N-terminus and mouse ERK2 isoform FLAG-tagged. Source: Dr. K. Aoki
pCAGGS FLAG ERK2 S282P mCFP	Encodes CFP at N-terminus and mouse ERK2 isoform S282P mutant FLAG-tagged. Source: Dr. K. Aoki
pCAGGS FLAG ERK2 S282E mCFP	Encodes CFP at N-terminus and mouse ERK2 phospho-mimetic mutant FLAG-tagged. Source: Dr. K. Aoki
pBabe puro	Mammalian and retroviral expression vector used to generate virus particles carrying the gene of interest. Puromycin resistance for mammalian selection. SV40 promoter.
pBabe puro FLAG ERK2 WT	Encodes the ERK2 WT, FLAG-tagged and puromycin resistance to establish stable cell expression. Source: Generated for this thesis
pBabe FLAG ERK2 S284P	Encodes the ERK2 S284P mutant FLAG-tagged. Source: Generated for this thesis
pBabe FLAG ERK2 S284E	Encodes the ERK2 S284E mutant FLAG-tagged. Source: Generated for this thesis
pCMV HA MEK1	Mammal expression vector. Cytomegalovirus (CMV) promoter/ SV40 polyA. Encodes MEK1 isoform HA-tagged. Source: Dr. M. Weber
pCEFL GST MEK1	Encodes MEK1 isoform GST-tagged. Source Dr. V.Sanz
pET HIS ERK2 WT	E. Coli expression vector. T7 promoter. Encodes HIS-tagged ERK2 isoform at N-terminus. Source Dr. M. Cobb
pET HIS ERK2 H176L4A	Encodes HIS-tagged ERK2 HL mutant. Source Dr. M. Cobb
pET HIS ERK2 S284P	Encodes HIS-tagged ERK2 S284P mutant. Source: Generated for this thesis
pET HIS ERK2 DK	Encodes HIS-tagged ERK2 Dead kinase mutant. Source: Generated for this thesis
pGEX GST MEK1EE	E. Coli expression vector. T7 promoter. Encodes MEK1EE mutant, GST-tagged. Source: Dr. C. Marshall
pCMV HA IMP7	Encodes IMP7 N-terminal HA-tagged.

3.1.3 Plasmid cloning

For subcloning protocol, the gene of interest was cut with specific restriction enzyme endonuclease and inserted in a new vector by ligation. Alternatively, the restriction sequences were introduced amplifying the gene of interest by PCR using primers targeting the 5’ and 3’ of the gene.

Digestion of plasmids was carried out following the manufacturer's instruction provided (ThermoFisher). DNA fragments were separated by agarose gel electrophoresis at 0.8% w/v. Agarose gels were prepared by dissolving agarose (% w/v) in 1X Tris-acetate-EDTA (TAE) buffer. SYBR safe (Invitrogen) was added to allow visualization of DNA under UV lights. DNA samples were mixed with DNA loading buffer (0.005% (w/v) bromophenol blue (Sigma) and 30% of glycerol (Sigma) and run at 80-100 V. 1Kb DNA ladder was used as molecular weight marker. DNA band, corresponding to the desired fragment, was excised and purified from agarose gel using JETquick column, according to the manufacturer's instructions. Once vector and DNA fragment were purified, ligation mediated by T4 DNA ligase (Promega) was performed. Ligation reaction was carried out O/N at 21 ºC, in a final volume of 20 µL using ligation buffer (300 mM Tris-HCl, pH 7.8, 100 mM $MgCl_2$, 10 mM ATP, 100 mM DTT). Finally, 4-6 µL of ligation mix were transformed into DH5α Escherichia coli competent and incubated during 1 hour at 37ºC in SOC medium antibiotic-free, to allow the expression of the resistance antibiotic gene. Transformed bacterial were then seeded in LB-agar plates made dissolving 1.5% of agar and 50 µg/mL of ampicillin or kanamycin for selection.

For PCR amplification of DNA fragments Phusion High-Fidelity DNA Polymerase (2 U/µL, ThermoFisher) was used. The primers used for the PCR were:

BAmHI ERK2 5´ATTCATAGTGGATCCTATGGCGGCGGCGGCGGCGGC3'

NotI ERK2 5'ATTACTAGCGGCCGCTCAGCTTCTGTAGCCGGGCTGGAAT3'.

PCR conditions are reported in the table 3.2. PCR product was finally cut, purified and ligated to the new vector following the same protocol previously described.

Table 3.2. PCR condition for gene amplification

Step	Cycles	Temperature	Time
Denaturing	1 X	95ºC	1 min
Denaturing	35 X	95 ºC	30 seconds
Primers Annealing		56 ºC	20 seconds
Extending		72 ºC	30 seconds
Elongation	1 X	72 ºC	10 min
Hold	1 X	4ºC	∞

3.2 TISSUE CULTURE

3.2.1 Cell lines

Cells were grown in DMEM (ThermoFisher) supplemented with FBS (Gibco) and 1% of Penicillin-Streptomycin antibiotics mix (10000U/mL) (Thermo Fisher). Unless specified otherwise in this thesis, all cells were grown at a 37ºC and 5% CO_2.

Table 3.3 Provides a list of cell lines used in this study

CELL LINE	CULTURE MEDIA	DESCRIPTION
8505C	DMEM + 10% FBS	Thyroid gland undifferentiated carcinoma cells. B-RAF mutant
A375P	DMEM + 10% FBS	Epithelial human metastatic melanoma cells. B-RAF mutant.
HEK 293T	DMEM + 10% FBS	Epithelial cells derived from Human Embryo Kidney. Immortalized with SV40 T-antigen
HEK 293T *phoenix*	DMEM + 10% FBS	Modified Human Embryonic kidney cell. Second-generation retrovirus producer lines for the generation of helper free ecotropic and amphotropic retroviruses. Transformed with adenovirus E1a and carrying a temperature sensitive T antigen co-selected with neomycin.
HeLa	DMEM + 10% FBS	Epithelial cells derived from human cervical carcinoma.
M249	DMEM + 10% FBS	Epithelial human metastatic melanoma cells. B-RAF mutant.
MEFs	DMEM + 10% FBS	Mice Embryonic fibroblasts cells.
MEFs ERKless (ERK1 $^{-/-}$,	DMEM + 10% FBS	Mice Embryonic fibroblasts cells. ERK1 null ($ERK1^{-/-}$) and ERK2 floxed ($ERK2^{fl/fl}$).

ERK2 $^{lox/lox}$)		
MEFs KSR1 -/-	DMEM + 10% FBS	Mice Embryonic fibroblasts. KSR1 knock down.
MELJUSO	DMEM + 10% FBS	Epithelial human melanoma cells. N-RAF mutant.
PAC 2	L-15 Medium (Leibovitz) +15% FBS 28ºC, CO_2 free.	Fish embryonic fibroblasts cells.
SKMEL2	DMEM + 10% FBS	Epithelial human metastatic melanoma cells. N-RAF mutant.
SKMEL28	DMEM + 10% FBS	Epithelial human melanoma cells. B-RAF mutant
WM35	DMEM + 10% FBS	Epithelial human melanoma cells. B-RAF mutant

Basal medium: DMEM culture media without Fetal Bovine Serum.

Throughout this thesis EGF (Epidermal Growth Factor, SIGMA) has been used to stimulate cells at 50 ng/mL final concentration for 5 min or indicated time.

DEL-22379 (Vichem Chemie), an ERK2 dimerization inhibitor described previously by our laboratory (Herrero et al., 2015), was used at 10 µM for 30 min.

U0126, a MEK inhibitor (ROCHE Diagnostics) was used at 10 µM for 30 min.

MK2206, an AKT1 inhibitor (Selleckchem) was used at 5 µM for 2h.

The B-RAF inhibitor Vemurafenib (PLX4032, Selleck Chemicals) was used in melanoma cells at 10 µM for 2 hours.

3.2.2 Cell transfection

Polyethylenimine (PEI)

HEK293T cells were transfected using Polyethylenimine (PEI). PEI condenses DNA into positively charged particles that bind to anionic cell surfaces. In this way, the DNA-PEI complex is endocytosed by the cells and the DNA released into the cytoplasm (Longo et al., 2013).

HEK293T were split into p60 plates in order to reach a final confluency of around 60-70% at the time of the transfection. In this way, all of cell surface is completely exposed and it makes DNA entrance easier into the cell and subsequently into the nucleus. PEI (1 mg/mL) (Polysciences, Inc.) was used in a ratio of 1:3 w/w (DNA:PEI). 3 µL of PEI were diluted in 200 µL of Opti-MEM medium (Gibco) and 1 µg of DNA was diluted in another tube. After 5 min of incubation, the two tubes were mixed, vortexed and incubated again for a further 20 min at room temperature. Finally, the mix was added to the cells, reaching a final volume of 2.5 mL in the plate. For optimal expression, the cells were harvested at least 48 h post-transfection.

Lipofectamine LTX

Lipofectamine contains lipids that can form liposomes in an aqueous environment which catches the DNA plasmids. The cationic liposomes form a complex with negatively charged DNA to overcome the electrostatic repulsion of the cell membrane.

HeLa and HEK293T cells were transfected using Lipofectamine LTX (Invitrogen, Thermo Fisher). Cells were split 24 h before transfection to reach 60-70% of confluence at transfection. 8 µL of LTX was diluted in 250 µL Opti-MEM medium (Gibco, Thermo Fisher). 1 µg of DNA was diluted in another Eppendorf tube containing 250 µL Opti-MEM medium and 4 µL of PLUS Reagent. After 5 min of incubation at room temperature, the content of the DNA tube was added to the Lipofectamine LTX Reagent tube. After 10 min of incubation at room temperature, the mix DNA-lipid complex was added to the cells.

Lipofectamine 3000

Pac-2 cells were transfected with Lipofectamine 3000 (Invitrogen, Thermo Fisher). 1 µg of DNA plus 14 µL of P3000 reagent were diluted in 250 µL of Opti-MEM medium and 7 µL of Lipofectamine 3000 reagent were added to another tube with 250 µL of Opti-MEM medium. They were incubated separately for 5 min at room temperature and then, the content of the DNA tube

was added to the one with Lipofectamine. They were incubated for 10 min and finally added to the cells.

Lipofectamine RNAiMAX

The small interfering RNA (siRNA) against the serine/threonine kinases of human kinome were transfected in HEK293T cells using Lipofectamine RNAiMAX (Invitrogen, Thermo Fisher). Following the manufacturer protocol, 2 µL of 5 µM siRNA were diluted in 50 µL of Opti-MEM medium. In another tube 1,5 µL of Lipofectamine RNAiMAX were diluted in 50 µL of Opti-MEM medium. After 5 min at room temperature, the 2 tubes were mixed, vortexed and incubated for 10 min. After this incubation, the mix was added to the cells laid in 96-well plates.

For an optimal knocking down, cells were harvested 72 h post-transfection.

Retrovirus infection

To analyze the dependence of mammalian cellular viability on S284 phosphorylation, MEFs ERK-less cells were infected with retroviral particles, carrying the different ERK2 constructs.

To generate retroviral particles, HEK293T phoenix cells were transfected with PEI. 50 µg of DNA of interest was diluted in 500 µL of DMEM FBS-free medium. In another tube, 125 µL of PEI was diluted in 375 µL of DMEM FBS-free (PEI:DNA ratio 2.5:1). The two tubes were mixed, vortexed and incubated for 10 min at room temperature. Finally, the mix was added to a P150 plate where cells were in a 70-80 % of confluency.12 h post-transfection, medium was refreshed, and retroviral particles were collected in two rounds (48- and 72-h post-transfection). After clarifying supernatant by centrifugation (1500 rpm for 10 min) and by filtration (0.45 µm filters), retrovirus particles are concentrated using PEG8000 (15% final concentration). Mixture was homogenized by inversion and stored at 4 ºC for at least 6 h. Finally, mixture was centrifuged at 1500xg for 30 min at 4 ºC. Viral particles were resuspended in 500 µL of DMEM FBS-free and stored at -80ºC ready to use for MEFs infection.

For the infection, cells were previously rinsed with PBS 1X buffer, trypsinazed and resuspended in 500 µL of DMEM FBS-free. To increase the infection efficiency, the same volume of mix, containing virus particles, was mixed with resuspended cells and centrifugated at 1500g for 1 hour. Cells were finally seeded and incubated at 37ºC O/N in a small volume of medium. Next morning, plate was filled with fresh medium 10 mL/P100. After 2 days of incubation, medium was re-freshed and antibiotic was added in order to select those cells carrying a stable expression of the gene.

3.2.3 Cell proliferation assay

This assay was used to determine the effect of a non-dimerizing ERK2 on mammalian cells proliferation. To this aim, we generated stable expression cells of the different ERK2 mutant in Ser284, and repressed endogenous ERK2 by treatment with 4-hydroxytamoxifen (600nM) for 5 days. Cells were counted by Neubauer chamber or Nucleocounter (method based on propidium iodide staining). 2000 cells were plated per well in 96-well plates, one for each time point (24, 48 and 72 h) and three replicates per condition. At the estimated time, 10 µL of PrestoBlue™ (Invitrogene) was added and incubated in the dark at 37ºC and the absorbance was read every 30 min.

(PrestoBlue™ Cell Viability Reagent Invitrogen), used to perform proliferation assays, has as active component a non-toxic, cell-permeable non-fluorescent blue compound called Resazurin. This compound can be reduced by aerobic respiration of metabolically active cells to a red highly fluorescent compound named Resorufin. The change of color can be measured, using absorbance-based place readers at 600 nm as a reference wavelength and monitoring reagent absorbance at 570 nm. This indicates cells viability, metabolic activity and, indirectly, number of cells.

3.2.4 Determination of IC50 values

Tumor cells were plated in 96 well plates at 3000 cells per well and incubated overnight at 37°C at 5% CO_2. Drugs were added at different concentrations and plates incubated for 24 hours at 37°C at 5% CO_2. IC50 cell viability was estimated using a colorimetric (PrestoBlue™ Cell Viability Reagent Invitrogen) assay. Briefly, on the day of the assay the medium was changed to medium containing 10% Prestoblue stock solution. Plates were incubated at 37°C for 2-4 hours, depending on the cells, and absorbance was measured at 480 and 620 nm using a microplate reader (Tecan infinite M200 Pro). The half-maximal inhibitory concentration (IC50 value) was calculated using GraphPad Prism software (USA).

3.3 PROTEIN ANALYSIS

3.3.1 Immunoblotting analysis

This technique was used to analyse protein expression, protein-protein interaction and state of the protein. For protein extraction cell plates were laid on ice, rinsed with cold PBS 1x and harvested using 250 or 500 µL of lysing buffer depending on the plates size.

SDS-PAGE gel electrophoresis

To analyse protein expression or protein-protein interaction cells were harvested using a specific lysis buffer depending on the assay. After clarifying the lysate at 13000 rpm for 15 min at 4ºC, supernatant was collected, and protein concentration was determined using Bradford method reading the absorbance at 620nm wavelength (Protein assay reagent – Bio-Rad). Laemmli loading buffer 5X was added to around 30 µg of protein and the mix was boiled at 95ºC for 5 min. Proteins were resolved for separation by size in sodium dodecyl sulfate (SDS)- polyacrylamide gel electrophoresis (PAGE). SDS-GEL was composed of a stacking part and a resolving part ranging from 8 to12 % of polyacrylamide. The vertical electrophoresis separation was performed in Mini-protean Bio-Rad device with running buffer during approximately 2h at 120V or

until the dye front run off the bottom of the gel. Then, proteins were transferred to nitrocellulose membranes (Thermo Fisher) at 400 mA constant amperage (1 minute for each kDa of the protein) at 4ºC in transfer solution. Membranes were blocked in Tris Buffered Saline-Tween (TBS-T) containing 4% BSA (blocking solution) for 1 hour shaking at room temperature. Blots were incubated from 1 hour at room temperature to ON at 4ºC (depending on the antibody affinity) with the different antibodies (table 3.4) prepared in blocking solution. The blots were washed 3 times for 5 min with TBS-T and incubated for 1 hour shaking at room temperature with anti-rabbit Immunoglobulin (Ig) (Bio-Rad) or anti-mouse Ig (Bio-Rad) secondary antibodies conjugated with peroxidase (1:10000) in 2% milk (GE Healthcare) in TBS-T. Then, membranes were washed (3 x 5') with TBS-T and the proteins were detected by chemiluminescence with an enhanced chemiluminescent system (ECL) and an autoradiography with Konica films was performed to develop the blots.

Buffer lysis: 20 mM HEPES pH 7.5, 10 mM EGTA, 40 mM β-Glycerophosphate, 1% NP40, 2.5 mM $MgCl_2$, 1 mM $NaVO_4$, 1 mM DTT and protease inhibitors added just before lysing: 10 µg/mL of aprotinin and 10 µg/mL of leupeptin.
5X Laemmli loading buffer: 100 mM Tris pH 6.8, 4% SDS, 20% glycerol, 20 mM DTT and 0.005% bromophenol blue.

Poliacrylamide gels:

-**Stacking gel**: 4% acrylamide, 125 mM Tris-HCl pH 6.8, 0.4% SDS, 0.1% Ammonium Persulfate (APS) and 0.1% Tetramethylethylenediamine (TEMED) in H_20.
-**Resolving gel**: acrylamide (the percentage range from 8% to 12%, depending on the molecular weight of the protein), 375 mM Tris-HCl pH 8.8, 0.4% SDS, 0.1% APS and 0.1% TEMED in H_20.

Running buffer: 25 mM Trizma base, 192 mM Glycine, 0,1% SDS.
Transfer buffer: 25 mM Trizma base and 192 mM Glycine.
Tris Buffered Saline-Tween (TBS-T): 20 mM Tris, pH 7.4, 137 mM NaCl and 0.05% tween.
Enhanced chemiluminescent system (ECL)

Solution 1: 1M Tris HCl pH 8.5, 90 mM Coumaric Acid, 250 mM Luminol.
Solution 2: 1M Tris HCl pH 8.5, 30% Hydrogen Peroxide.

Table 3.4 Primary and secondary antibodies used in this work

Name	Source	Dilution	Supplier
Primary antibodies			
α-Tubulin	Mouse monoclonal	1:5000	T5168, Sigma
ERK2	Mouse monoclonal	1:1000	sc-1647, Santa Cruz
FLAG	Mouse monoclonal	WB: 1:4000 IP: 0.8 µg	F1804, Sigma
HA	Mouse monoclonal	WB: 1:1000 IP: 1 µg	probe F-7, sc-7392, Santa Cruz
HIS	Mouse monoclonal	WB: 1:2000	Sc-8036, Santa Cruz
KSR1	Rabbit polyclonal	1:1000	(EPR2421Y) ab68483, Abcam
MEK	Rabbit polyclonal	1:500	8727S, Cell Signaling
p-ERK1/2 (Tyr 204)	Mouse monoclonal	1:1000	sc-7383, Santa Cruz
p-MEK	Mouse monoclonal	1:500	sc-136542, Santa Cruz
p-RSK1	Rabbit polyclonal	WB: 1:1000	9344S, Cell Signaling
RSK-1	Rabbit polyclonal	WB: 1:1000	sc-231, Santa Cruz
p-Ser284	Rabbit polyclonal	WB: 1:800 IF: 1:100	Genscript
p-AKT1 (Thr308)	Rabbit polyclonal	WB: 1:1000	9275S, Cell Signaling
AKT	Rabbit polyclonal	WB: 1.500	Sc-8312, Santa Cruz
Rho GDI	Mouse monoclonal	WB: 1:1000	sc-365190, Santa Cruz
LaminA	Rabbit monoclonal	WB: 1:1000	sc-10680, Santa Cruz
Sin3b	Mouse monoclonal	WB: 1:1000	Sc-13145, Santa Cruz

HRP-conjugated secondary antibody			
Anti-Mouse-HRP (Mouse IgG)	Goat	1:10000	170-5047, Bio-Rad
Anti-Rabbit-HRP (Rabbit IgG)	Goat	1:10000	170-5046, Bio-Rad
FITC (mouse IgG)	Goat	1:300	31569 Invitrogen, Thermo Fisher
Alexa 594 (Rabbit IgG)	Goat	1:800	A32740 Invitrogen, Thermo Fisher

3.3.2 ERK MONOMER/DIMER SEPARATION

To separate ERK monomers from its dimeric form two methods were used: the first one, described by Philipova (Philipova and Whitaker, 2005), separation occurs in a semi-denaturation condition, whereas the second one, described in our lab (Casar et al., 2008), is based on a native gel electrophoresis.

PHILIPOVA AND WHITAKER METHOD

For this method, we used a specific lysis buffer P.W to harvest the cells. Once lysate was clarified, 50 μg of protein extract was mixed with the loading buffer P.W. Samples were incubated for 20 min at room temperature with loading buffer and boiled for 30 seconds at 95ºC. Next, the samples were loaded in a 10% SDS- acrylamide gel and run for 2 h at 100 V constant voltage using SDS- free running buffer. The following steps were similar to the SDS-PAGE protocol described above. Dimers and monomers were separated by size in such a way that the monomer runs at 42-44 kDa and the dimer around 80 kDa.

Lysing buffer P.W.: 50 mM Tris-HCl pH 7.5, 1% triton X-100, 10 mM EDTA pH 8, 0.5 M NaCl, 10% glycerol, 10 μg/mL Aprotinin and Leupeptin).
Loading buffer P.W.: 100 mM Tris pH 6.8, 2% SDS, 20% glycerol, 0.05% β-mercaptoethanol and 0.005% bromophenol blue).

NATIVE GEL ELECTROPHORESIS

In this method, cells were harvested using the kinase assay lysis buffer. 30 μg of protein was mixed in a 1:1 volume ratio with the 2x loading buffer. Samples were run in an 8% acrylamide gel without SDS at 80 V constant voltage during 2 h with SDS- free running buffer. The following steps are those of the SDS-PAGE protocol described above. In this case, proteins must be transferred into a Nitrocellulose membrane at 400mA constant amperage for 80 min. ERK dimers will run faster than the monomer because the separation depends on the protein charge and this, in turn, depends on the conformation.

2X loading buffer: (0.126 M Tris HCl pH 6.8, 20% Glycerol, 0.1% (w/v) Bromophenol blue).

3.3.3 COOMASSIE BLUE STAINING

Coomassie Blue was used to stain protein, extracted from BL21-DE3 strain of E. Coli, in polyacrylamide gels. After running the protein in a SDS-PAGE gel, coomassie blue solution was added to the thin polyacrylamide gel and incubated for 30 min at room temperature. Next, gel was de-staining until the protein bands were well-defined. A Bovine Serum Albumin (BSA) was used to calibrate unknown concentrations.

Comassie blue solution: 0.1g brilliant blue, 10 mL acetic acid, 50 mL methanol, water up to 100 mL.

De-staining solution: 30% Methanol, 10% Acetic Acid, 60% water

3.3.4 CO-IMMUNOPRECIPITATION ASSAY

To detect protein-protein interaction, co-immunoprecipitation assay was performed. The purpose of this method is immunoprecipitated the protein of interest using a specific antibody anti-epitope and pulls down its interacting partners.

After clarifying the lysate, 30 µg of protein from the total lysate were separated and loaded with Laemmli 5x buffer. The rest of lysate was incubated rocking at 4ºC for 3 h with 1 µg of the specific antibody for immunoprecipitation. After this time, 5 µL of magnetic beads protein G (Dynabeads™ Protein G Immunoprecipitation Kit – Invitrogen) was added. The protein G bind the immunoglobulins of the primary antibody which allows to precipitate the immunocomplexes (protein-antibody) using a magnetic retainer. The next step was washing the beads three times with lysis buffer. Finally, the beads were resuspended in 20 µL of loading buffer Laemmli 2.5 X and boiled 5 min at 95ºC. Protein-protein interaction was analysed by SDS-PAGE as previously described.

3.3.5 IMMUNOFLUORESCENCE

For this analysis HeLa cells were used. Transfected HeLa were grown to sub-confluence in a glass of 10 mm of diameter. Cells were washed with 1X PBS and were fixed with 4% paraformaldehyde (PFA) during 10 min at room temperature. Cells were subsequently washed twice with 1X PBS for 5 min, followed by one wash with 0.1 M glycine and two with 1X PBS. Subsequently, cells were permeabilized during 10 min with a permeabilization solution and washed again with 1X PBS for 5 min. Then, cells were blocked during 15 min by incubation with blocking solution. The primary antibody was prepared in blocking solution in a dilution ranging from 1:75 to 1:200 depending on the antibody specificity. Diluted primary antibody was added as a drop over the glass and incubated for 1 hour in a humidity chamber to prevent drying. After the primary antibody incubation, cells were washed twice for 5 min with PBS 1X. Subsequently, glasses were washed with 0.05% Tween^{TM}20 (Thermofisher) PBS 1X solution in order to reduce surface tension. A secondary antibody (conjugated with a fluorophore), specific for the primary antibody, was added for 1 hour in the humidity chamber and then removed washing twice with 1X PBS. Finally, the glasses were set over a slide in mounting media with DAPI and sealed with clear nail polish. The cells were examined by fluorescence microscopy (photomicroscope Axiophot, Carl Zeiss). The images were processed using Image J software.

Permeabilization solution: 0.1 M glycine, 0.5% Triton X-100 in PBS 1X
Blocking solution: 3% BSA, 0.01% Triton X-100 in 1X PBS

3.3.6 NUCLEAR-CYTOPLASMATIC FRACTIONATION

To study ERK2 distribution in nucleus and cytoplasm compartments, either in basal condition or upon EGF stimulation, nuclear-cytoplasmatic fractionation was performed.

Cells were washed with PBS 1X and after adding 400 µL of Buffer 1 per P100, cells were scraped carefully. Lysate were incubated for 1 hour at 4 ºC rocking to allow cytosolic membrane break. After centrifugation at 1500rpm for 5 min, cytoplasmatic fraction was collected and stored at -80 ºC. Next, to avoid any

kind of cytoplasm contamination of the nucleus, the pellet was washed again with PBS 1X. Once centrifugated, 100 µL of buffer 2 were added to the pellet, pipetting vigorously to facilitate nucleus disintegration. Next step was centrifugation for 20 min at maximum speed and store the supernatant at -80ºC. Protein localization was analysed by SDS-PAGE as previously described. RhoGDI antibody was used as cytoplasm marker whereas Sin3b as nuclear marker.

Buffer 1: 10mM HEPES pH=7, 10mM KCl, 0.25mM EDTA pH= 8, 0.125 mM EGTA pH=8, 0.1% IGEPAL, 1mM DTT, proteases and phosphatases inhibitors.
Buffer 2: 20mM HEPES pH=7, 400mM NaCl, 0.25mM EDTA pH= 8, 1.5 mM $MgCl_2$, 0.5 mM DTT, proteases and phosphatases inhibitors.

3.3.7 Label Free Quantification (LFQ) Proteomics

To identify proteins interacting with ERK2 S>P mutant a mass spectrometry analysis was performed.

HEK293T cells were transiently transfected with FLAG-tagged ERK2 constructs. After 48 hours post-transfection, they were either starved O/N or EGF- stimulated for 5 min. Cells were lysed using lysis buffer and proteins were immuno-precipitated using 6 µL of Flag-M2 agarose beads (Sigma-Aldrich) for 2 hours at 4ºC. The FLAG-ERKs immunoprecipitated were washed 4 times using a proteomic washing buffer (20mM HEPES pH7.5, 150mM NaCl) to remove detergent contamination.

Then, immunoprecipitates were digested with trypsin, reduced, and alkylated as described by (Turriziani et al., 2014). Tryptic peptides were analysed on a Thermo Scientific Q-Exactive Mass Spectrometer connected to an Ultimate Ultra3000 chromatography system incorporating an autosampler. Data were acquired with the MS operating in automatic data-dependent switching mode, selecting the 12 most intense ions prior to tandem MS analysis. MS raw data were analysed by the MaxQuant software (Cox and Mann, 2008). Specifically, tandem MS spectra were searched against the human Uniprot database with a mass accuracy of 4.5 ppm and 20 ppm (for MS and MS/MS). Carbamylation was selected as fixed modification. Variable modifications were N-terminal

acetylation (protein) and oxidation (M). LFQ and peak matching was selected and was limited to within a 30 s elution window with a mass accuracy of 4.5 ppm. The results are based on 3 independent biological replicates.

3.4 RECOMBINANT PROTEIN PURIFICATION

To perform *in vitro* kinase assay, some of the proteins used were obtained from bacterial culture of BL21 DE3 strain of E.Coli. For this purpose, the gene of interest was subcloned into a pHis parallel vector in order to obtain recombinant protein 6x histidine-tagged at their N-terminus. Transformed bacterial cells were inoculated in a small volume of LB culture medium, supplied with the specific antibiotic, and incubated O/N at 37ºC shaking. The day after, bacterial culture was diluted in 500 mL of LB and re-incubated until 0.6-0.8 OD (optical density) was reached. Protein expression was induced by the addition of 1mM IPTG (isopropyl-β-d-thiogalactopyranoside). IPTG blocks the lac repressor activity; thus, when IPTG is added the T7 promoter is released allowing the T7 RNA polymerase to transcribe the protein of interest.

After 4 h of IPTG induction at 37ºC, cells were harvested by centrifugation and suspended in 7 mL of buffer A for being lysed mechanically. After 20 min of incubation, 7 mL of buffer B was added. Bacterial cells were pipetted vigorously until a gelatinous suspension was obtained. Lysates were collected by centrifugation at 40k rpm for 40 min at 4ºC. Supernatant, containing the protein of interest histidine-tagged, was divided into Eppendorf tubes of 1.5 mL and subsequently incubated with 50 µL of magnetic dynabeads His-Tag isolation (Life Technologies), rocking for 15 min at 4 ºC. Protein were pull down thanks to a magnetic retainer and washed four times using washing buffer to eliminate impurities that might bind unspecifically. Finally, proteins were eluted in 75 µL of elution buffer and stored at 4ºC for short period of time. Proteins extraction yield was checked running a small amount of the eluted protein in a SDS-PAGE, stained with Coomassie blue as described above.

Buffer A: 50mM Tris-base pH 7.4, 10% sucrose, 50 mg lysozyme, 0.001% PMSF, 50 mg A/L and 2,5 mM Benzamidine.

Buffer B: 50mM Tris-base pH 7.4, 1M NaCl, 0.6% Triton™ X-100, 0.001% PMSF, 50 mg A/L.
Washing buffer: 50 mM Na_2HPO_4, 300 mM NaCl, 0.01% Tween20.
His elution buffer: 300 mM imidazole, 80 mM Na_2HPO_4, 300 mM, 300 mM NaCl, 0.01%Tween20.

3.5 *IN VITRO* KINASE ASSAY

3.5.1 MBP PHOSPHORYLATION MEDIATED BY ERK

To elucidate ERK2 S>P mutant ability to phosphorylate its substrate an *in vitro* kinase assay was performed, using myelin basic protein (MBP) as ERK2 substrate.

First, transfected cells with ERK2 WT and S>P constructs, HA and FLAG tagged respectively, were stimulated with EGF at the indicated time and the exogenous proteins were immunoprecipitated as described previously. ERK2 proteins were then washed once with LiCl buffer and subsequently with kinase reaction buffer.

LiCl buffer: 0.5 M LiCl, 100 mM Tris pH 7.5.
kinase reaction buffer: 12.5 mM MOPS pH 7.5, 12.5 β-Glycerolphosphate, 7.5 mM $MgCl_2$, 0.5 mM EGTA, 0.5 mM Sodium fluoride, 0.5 mM Vanadate, 1 mM DTT.

To perform kinase assay, each sample was incubated with: 25µL of kinase reaction buffer, 1.5 µL of cold ATP (20 µM), 1.5 µL of MBP (stock 10 mg/mL Sigma cat. M-1891) and 0.1 µL (1 µCi) of ATP (γ-32P). The mix was then incubated at 30ºC for 30 min. The reaction was stopped by adding 5 µL of Laemmli loading buffer 5X. Samples were boiled at 95 ºC for 5 min and run in 12% SDS-PAGE gel. The gel was finally dried, using a gel dryer device for 2 h (Bio-Rad), and phosphorylated MBP was detected by autoradiography using Konica films. The MBP phosphorylation was then quantified using ImageJ and normalized to not stimulated ERK2 WT. The results were plotted using GraphPad.

3.5.2 ERK2 PHOSPHORYLATION MEDIATED BY MEK and AKT

To test MEK and AKT ability to phosphorylate ERK2 at Ser284 residue an *in vitro* kinase assay was performed. ERK2 phosphorylation was detected either by autography using labelled ATP (γ-32P) or by immunoblotting using anti p-Ser284 antibody and non-labelled ATP. ERK2 proteins (WT and its mutants) and MEK EE (a constitutively active mutant of MEK) were obtained by overexpression in bacterial BL21 strain as described in the protein purification section. When specified, MEK and AKT proteins were obtained by IP of transfected cells, upon EGF stimulation.

To carry out the kinase assay, proteins were incubated in a different kinase reaction buffer, especially prepared for testing MEK activity. GST-MEK or FLAG AKT, (0.2 µg) were resuspended in 25 µL of MEK kinase buffer and incubated with 5 µL of ERK2 purified protein (1 µg), 1.5 µL of cold ATP and 0.1 µL ATP (γ-32P). The subsequent steps were the same as described in the previous section.

MEK kinase buffer: 25 mM β-Glycerolphosphate, 10 mM $MgCl_2$, 1.25 mM EGTA, 0.05 mM Vanadate, 1.5 mM DTT, 0.8 mg/mL BSA.

3.6 KINOME-WIDE siRNA SCREENING

To uncover which kinases are phosphorylating ERK2 at Ser284 siRNA targeting human kinome (Silencer™ Select Human Kinase siRNA Library, life technologies) was used.

$2x10^4$ HeLa cells, seeded in T96-well plates, were transfected with small interfering RNA (siRNA) of human kinome using Lipofectamine RNAiMAX (Invitrogen. Thermo Fisher). 2 µL of each siRNA (final concentration of 5 pM) were diluted in 50 µL of Opti-MEM medium. In another tube, 1,5 µL of Lipofectamine RNAiMAX were diluited in 50 µL of Opti-MEM medium. After 5 min at room temperature, the 2 tubes were mixed, vortexed and incubated for 10 min at room temperature. After this incubation, the mix was added to the cells. After 48h cells were starved using basal medium. 72 h after transfection,

cells were EGF-stimulated for 5 min and lysed using 50 µL of lysis buffer. Lysates were then stored at -20 ºC for being subsequently analyzed by double-sandwich immune Elisa assay.

3.7 ELISA ASSAY

A Double-Sandwich ELISA was performed to detect which siRNA diminish the phosphorylation of ERK2 at Ser 284 residue.

Anti ERK2 mouse monoclonal antibody was diluted 1:1000 into BBS coating buffer and incubated O/N at 4ºC for coating PVC microtiter wells. After 2 washes using washing buffer (PBS 1X and 0.2% Tween20) to eliminate unspecific protein-binding sites, blocking buffer (PBS 1X, 2% Tween20, 5% BSA) was added and incubated at 4ºC for 2 h. Then, 25 µL of diluted samples were added to each well (triplicates of each condition) and incubated for 2 h at 37°C. Starved cells lysates, EGF-stimulated cells and cells treated with specific inhibitors of RAS/ERK pathway (U0126) were used as standards. To remove the unbound proteins, plates were washed twice with washing buffer, and secondary antibody (p-Ser284 1:2000) was added and incubated O/N at 4 ºC. Finally, plates were washed twice and incubated at room temperature for 1 h with goat anti-rabbit alkaline phosphatase conjugate antibody (1:10000). To remove the excess of secondary antibody, plates were washed twice and the peroxidase enzyme substrate 1-step PNPP (thermo scientific) (*p*-nitrophenyl phosphate disodium salt) was added. After 15-20 min of incubation at room temperature, the reaction was stopped adding 50 µL of NaOH 2N and absorbance was measured at 405nm.

BBS coating buffer: Boric acid 6.28 g, Sodium chloride 4.38 g, Borax 9.54, Water up to 1L. (pH=8,4).
Washing buffer: PBS 1X and 0.2% Tween20.
Blocking buffer: PBS 1X, 2% Tween20, 5% BSA.

3.8 Immunohistochemistry of Human melanoma samples

Once embedded in paraffin, 5µm sections were cut at the microtome and placed on Poly-lysine treated microscopes slides. Previous any staining, slides were deparaffinize and tissue was rehydrated. Firstly, slides were dried for 1 hour at 60ºC or O/N at 37ºC.

Table 3.5 Standard procedure to rehydrate histological sections.

Solution	Time
Xylene	3 x 5´
Tap water	5´
100% Ethanol	5´
90% Ethanol	5´
80% Ethanol	5´
70% Ethanol	5´
Tap water	5´

In order to allow the antibody to enter more easily to each cell, a permeabilization step was done, incubating specimens for 10 minutes with 0,1% IGEPAL (Sigma) in 1x Tris Buffered Saline (TBS). Then, slides were washed twice for 5 minutes with 1x TBS, and non-specific bindings were eliminated using a serum free blocking reagent, background punisher (BIOCARE Medical) for 8 minutes. After that, a 1% Bovine Serum Albumin (BSA) 0.05% IGEPAL in 1x TBS solution containing a mouse anti-rabbit p-Ser antibody (1:100) (Gene Script) or not (negative control), was incubated O/N at 4ºC in a humid chamber (to avoid evaporation). Next day, slides were washed in 1x TBS (3 x 10´) and endogenous peroxidase was quenched using 3x Hydrogen Peroxide (H2O2) in 1x TBS for 20 minutes. Then, specimens were washed in 1x TBS (3 x 10´) and incubated with an anti-mouse biotinylated secondary antibody (Vector Labs) diluted in 1% BSA 0.05% IGEPAL in 1x TBS (1:400) for 1 hour in a humid chamber. After that, slices were washed, as before, and specimens were incubated with Horseradish Peroxidase (HRP) Avidin D diluted in 1x TBS (1:500) for 30 minutes in a humid chamber. Slices were washed again and incubated with the substrate diaminobenzidine (DAB) (Gibco) for 5 minutes or

until brownish color started to appear. Chromogenic reaction was stopped with H2O. To finish specimens were stained with Hematoxylin (Sigma), dehydrated, cleared and mounted with DPX. Images were taken at a Zeiss Axio Scope A1 microscope using 10x, 20x or 40x objectives.

3.8 CRISPR-CAS9-MEDIATED KNOCK-IN IN ZEBRAFISH

To study what biological consequence might have ERK2 dimerization in a specie where ERK2 does not dimerize, we edited zebrafish ERK2 gene using the Crispr-Cas9 technology.

3.8.1 sgRNA DESIGN

CRISPR target site was identified using the program Chopchop (https://chopchop.rc.fas.harvard.edu) and sgRNA was designed to target the sixth exon of ERK2 zebrafish gene (https://www.ensembl.org/Danio_rerio/Gene/Summary?db=core;g=ENSDARG00000027552;r=5:13104851-13167120). sgRNA was purchased by Sigma-Aldrich and was resuspended in RNase-free water to a final concentration of 1µg/µL, aliquoted and stored at -80 ºC. sgRNA: CTGACCTTT**AGG**GTCTGCGT.

3.8.2 REPAIR-TEMPLATE DESIGN

To replace the proline aminoacid with a serine, 120 base-pair (bp) repair-template (ssODN) contained symmetrical homology arms, flanking the theoretical Cas9 cut site (located 3 base pairs upstream of the PAM), was purchased by IDT company and resuspended in DNase-free water to 150ng/µL.

In order to avoid continuing cutting by Cas 9, the sequence corresponding to the PAM (shown in green) was masked by replacing a guanine with another nucleotide, encoding for the same aminoacid.

ssODN:
5’AGCGTGTGGAGCTGAACTCTGACCTTT**CGA**GTCTGCGTT**CG**GAAACAGG
CGGTTCCAGGGCACTTTGCTGCGGAGAGGAAGGGACAGCAGGTAAT 3’

3.9.3 ZEBRAFISH HUSBANDRY

Zebrafish (Danio rerio) were housed at the Biological Services Unit (BSU) of Manchester University and maintained at 28.5°C under a 14 h light/10 h dark cycle. Embryos were collected and raised in egg water (Instant Ocean salt 60 µg/ mL) at 28.5°C up to 5 day post-fertilization (dpf) and then transferred to the main aquarium system. Fishes were maintained according to standard conditions as described in (Westerfield, M. 2000). Younger fish was fed powder food and rotifers, while older fish and adults were fed powder food and brine shrimp. All food was supplied by ZM fish food.

3.9.4 ZEBRAFISH BREEDING AND EMBRYO COLLECTION

Zebrafish adult males and females (ratio 1:2) were set up in breeding boxes (Thoren, Aquatics Inc.), separated by a plastic divider, the afternoon before injections. The next morning, soon after the beginning of the light cycle, the divider was removed, and the fish were allowed to breed. Embryos were collected within 10-15 min of being laid.

3.9.5 ZEBRAFISH INJECTIONS

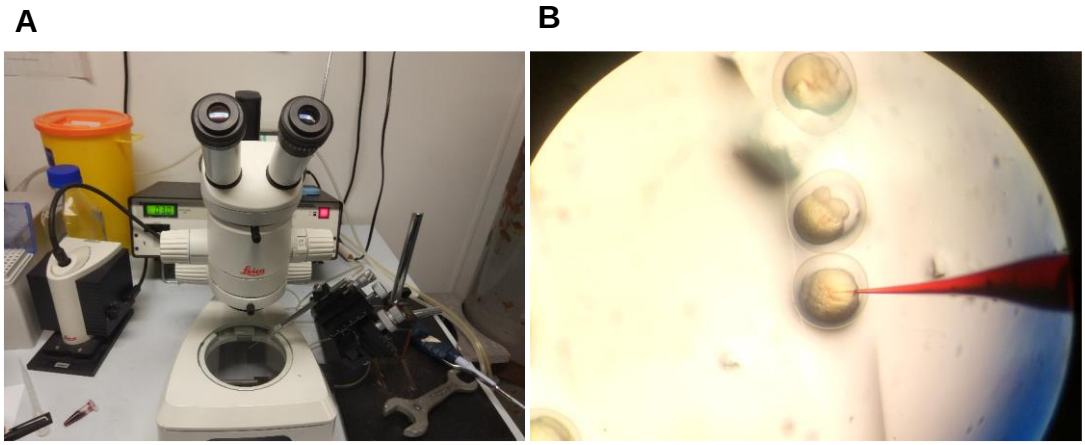

Figure 3.2 A) PLI-90 Pico- Injector microinjection station. **B)** One-cell zebrafish embryo injection.

Fertilized eggs were placed into the grooves made by a mold in agarose 2% in order to align embryos for the injection.

The injections were performed using a PLI-90 Pico-Injector micro-injection station in the yolk-sac margin of zebrafish embryos at the one-cell stage. All injection solutions were assembled on ice just before the injection procedure. Injection needles were calibrated to deliver a final volume of 1-2 nL of the injection solution (Fig 3.2).

3.9.6 CRISPR INJECTION MIX

Injection solution (table 3.5) was prepared by mixing the Cas9 protein and the sgRNA first. After 5 min of incubation at RT, the rest of the components were added, and the mix was stored on ice before the injection.

Table 3.5 Injection mix component

Injection MIX	
EnGen® Spy Cas9 NLS	1 µL
sgRNA 1µg/uL	2 µL
ssODN 150 ng/µL	1 µL
Buffer 3.1	0,6 µL
Phenol red 0.05% (v/v)	0.4 µL
H2B-mCerulan3	1 µL

Phenol red was added to allow visualization of the injected drop. Embryos were injected at one-cell stage and then incubated at 28.5°C. Embryos were screened for fluorescence at 24 h post-fertilization (hpf) to identify positively injected fish and some of them were collected to perform genomic DNA extraction and PCR screening to test the efficiency of the sgRNA. The remaining embryos were maintained in the incubator at 28.5°C up to 5 days and then raised to the adulthood for fin clipping and subsequent crossing.

1X NEBuffer™ 3.1: 100 mM NaCl, 50 mM Tris-HCl,10 mM $MgCl_2$,100 µg/mL BSA (pH 7.9 at 25°C).

3.9.7 HOTSHOT GENOMIC DNA EXTRACTION

To extract genomic DNA, embryos and fins were collected and placed in a 1.5mL tube. 50µL (embryos) or 100µL (fins) of NaOH was added in each tube and incubated at 95°C for 20 min. Samples were then neutralized by adding 40µL (embryos) or 60µL (fins) of Tris-HCl buffer (pH 8.5) and 2µL of each sample were used for PCR.

3.9.8 PCR AMPLIFICATION OF CRISPR-INJECTED FISH

To test CRISPR activity, specific primers to amplify the locus around the targeted region (173 bp) were designed, following the PCR condition indicated in the table 3.6.

ERK2P_S F: 5'-CCTGAACTGCATCATCAACATT-3'

ERK2P_S R: 5'-AAGGTGGCTTGATCTCCAAATA3'

To genotype adult fish, two different couple of primers were used, one for detecting the wild-type (WT) allele and the other for the mutant (MUT) allele, obtaining a 94 bp product.

WTERK2AMP F: 5'-CTGTTTCCCAACGCAGACC-3'

MUTERK2AMP R: 5'-GTTTCCGAACGCAGACTCG-3'

Table 3.6 PCR condition for injected embryos

Step	Cycles	Temperature	Time
Denaturing	1	95ºC	1 min
Denaturing	32	95 ºC	15 seconds
Primers annealing		60 ºC	15 seconds
Extending		72 ºC	30 seconds
Elongation	1	72 ºC	5 min
Hold	1	4ºC	∞

To test primers specificity and to set up the optimal PCR conditions a mutant amplicon string was purchase from IDT company and resuspended in DNase-free water to a final concentration of 25 ng/µL. This amplicon, diluted to a concentration of 250 fg/µL, was spiked into the genomic DNA in order to be used as positive control.

3.9.9 ZEBRAFISH FIN CLIPPING

Adult fishes were anaesthetized and transferred to a petri dish. Using a stainless-steel surgical blade (Swann Morton, Scientific Laboratory Supplies Ltd) a small amount of tissue was clipped from the end of the caudal fin. The sample was transferred into a microcentrifuge tube and genomic DNA extraction was performed. Fishes were transferred to individual on-system holding tanks with fresh water and monitored until they recovered. After 48 h, fishes were transferred back to main tanks.

3.9.10 ZEBRAFISH ANAESTHESIA AND EUTHANASIA

Anaesthesia was induced by placing embryos and adults in a 4% dilution of ethyl 3-aminobenzoate methanesulfonate (MS222) stock solution in chorion water. When fishes were no longer responsive, they were taken for fin clipping. Following completion of the procedure, fishes were recovered in fresh system water. Fishes were sacrificed with an overdose of MS222 (800 mg/L).

3.10 Bioinformatic analyses

Statistical analysis: Data was processed and analyzed using the **GraphPad Prism 7** Software (GraphPad Software, Inc., San Diego, CA).

In bar graphs data is given as Mean ± SD and Two tailed unpaired Student's t-test was used to determine differences between data sets and significance (*p<0.05, **p<0.01, ***p<0.001 and ****p<0.0001).

The western blot analyses and confocal images/videos processing were carried out and analyzed using **Fiji-Image-J Software**.

The bibliography was sorted by **Mendeley** reference management Software.

4. RESULTS

4.1 Ser284 role in ERK dimerization and subcellular distribution

4.1.1 Ser284, a novel phosphorylation site that regulates ERK dimerization

During the course of our experiments leading to the discovery of DEL-22379, we made the startling observation that ERK dimers were absent in fish, birds and amphibians, ERK dimerization being restricted to mammalians (Herrero et al., 2015). We also observed that ERK ability to dimerize was not dependent on the cellular context, since human ERK2 dimerized when transfected in zebrafish cells, while zebrafish ERK2 did not dimerize if transfected in human cells (Herrero et al., 2015). These results indicated that the capacity for dimerization resided on the ERK amino acid sequence. A comparison of the ERK2 sequence through the evolutionary scale unveiled that serine 284 (*H.Sapiens* numeration) was conserved in those species in which ERK2 dimerized, mammalians in all cases (Fig. 4.1). Interestingly, the corresponding residue in those species in which ERK2 did not dimerize was either a proline or an alanine (Fig.4.1). The same occurred for ERK1, in which this region is highly conserved. This data was suggestive of S284 playing some role in ERK dimerization.

Figure 4.1 Alignment of ERK2 sequences from different species retrieved from Uniprot. Canonical phosphorylation sites (TEY) are depicted in pink. Serine 284 (*H. Sapiens*) is depicted in yellow. This serine residue is conserved in mammalians, those species in which ERK2 dimerizes.

To investigate this point, we made a human ERK2 S284P mutant and also introduced a serine substitution in the corresponding residue in zebrafish (Dr)

ERK2, P293S. We performed native gel electrophoresis, in which the faster and slower migrating bands corresponded to ERK dimers and monomers, respectively (Casar et al., 2008; Herrero et al., 2015). We found that the S>P substitution completely prevented Hs ERK2 dimerization upon EGF stimulation, whereas the P>S mutation endowed the ability to dimerize to Dr ERK2 (Fig. 4.2 A).

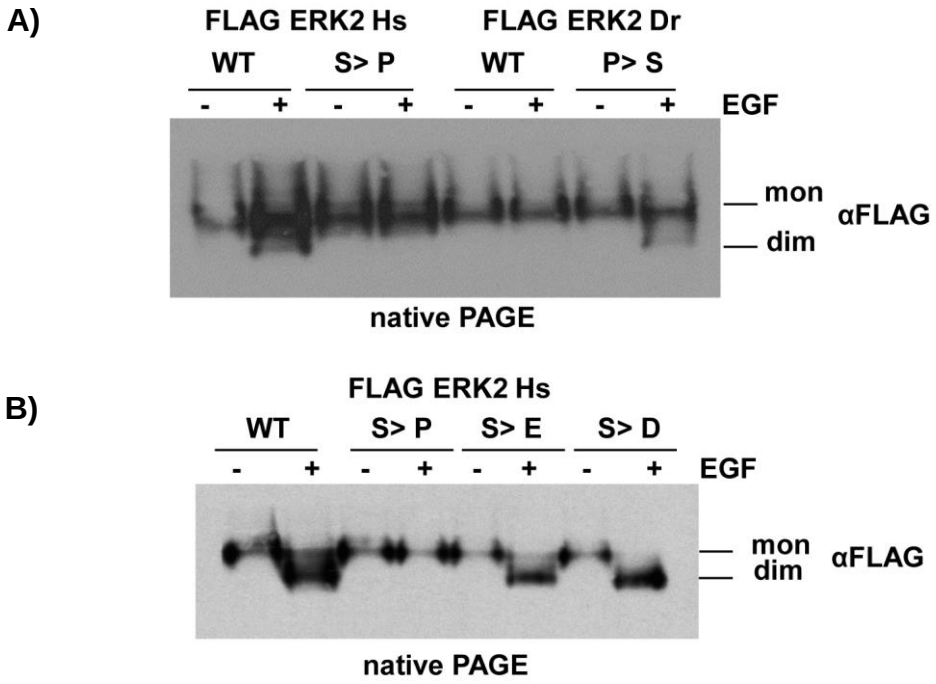

Figure 4.2. S284 is critical for ERK2 dimerization. A) FLAG-tagged human (Hs) and zebrafish (Dr) (wild types and S284P and P293S respectively) were transfected (1µg each) in 293T cells and dimerization upon EGF stimulation was analysed by native PAGE. B) Comparison dimerization analysis of FLAG-tagged Hs ERK2 phosphomimetic mutants (S>E and S>D) with ERK2 WT and non-dimerizing ERK2 S>P mutant by native PAGE.

Similarly, with the intention of generating a constitutively dimerizing ERK2, we made ERK2 phosphomimetic mutants, by replacement of Ser284 with a glutamic (E) or an aspartic (D) aminoacid, obtaining the S>E and the S>D ERK2 mutants, respectively. As shown in Fig. 4.2 B, these mutants could dimerize but only upon EGF stimulation, indicating that canonical TEY-ERK phosphorylation is also required for ERK dimerization, as previously demonstrated (Robinson et al., 1998); and that Ser284 phosphorylation is necessary but not sufficient for dimerization.

4.1.2 Active ERK2 is phosphorylated at Ser284.

Having established that S284 is critical for ERK dimerization, we searched for further information about this residue in the literature. Interestingly, S284 has emerged as an ERK2 phosphorylated residue in massive phosphoproteomic screenings (Fig.4.3 A) (Oppermann et al., 2009).

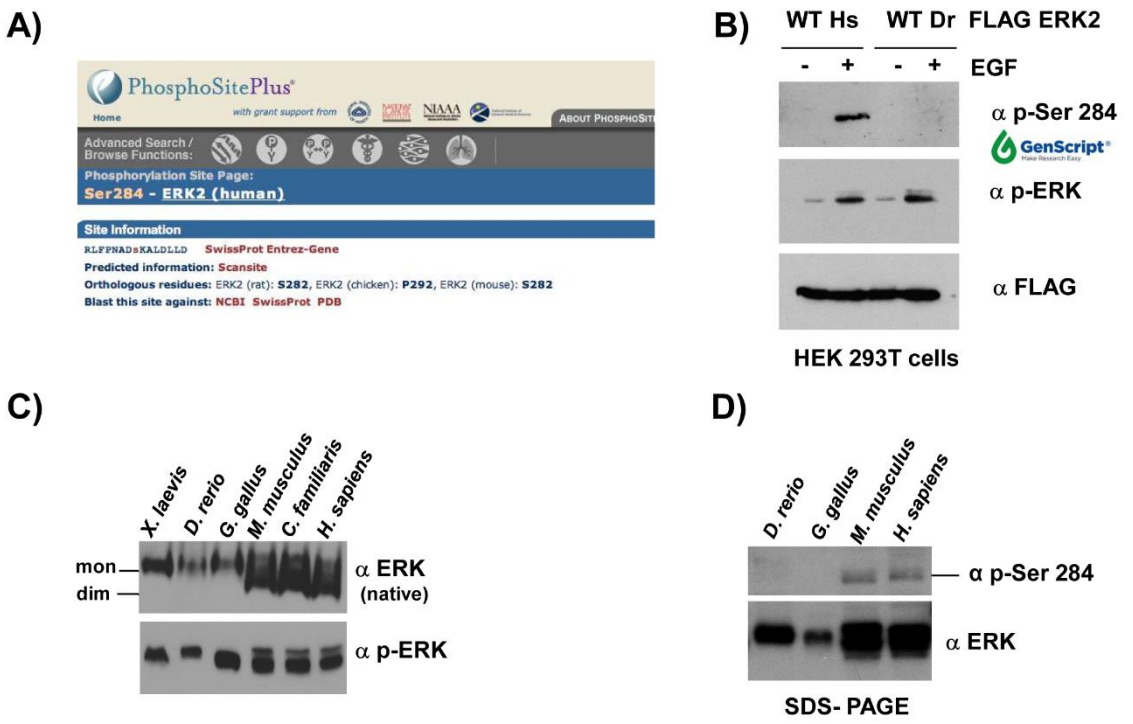

Figure 4.3. Identification and pattern phosphorylation of Ser284 residue. A) Information retrieved from phosphositeplus.org indicates that Ser284 is a phosphorylatable ERK2 residue B) 293T cells were transfected with Hs and Dr ERK2 WT (1 µg each) to analyse p-Ser284 antibody specificity SDS-PAGE. C) Comparative analysis of ERK dimerization, by Native-PAGE. D) Analysis of phospho-Ser284 by SDS-PAGE in the indicated species.

Thus, we generated a phospho-specific antibody for this residue and analysed the pattern of S284 phosphorylation in ERK2 under basal and stimulated conditions. HEK293T cells were transfected with Hs and Dr ERK2 WT and it was found that solely Hs ERK2 was phosphorylated in S284 upon EGF stimulation (Fig.4.3 B). Nevertheless, both ERK2 were phosphorylated at their activation lip (TEY motif). In light of the results obtained in our previous work (Herrero et al., 2015) (Fig. 4.3 C), we tested the antibody on cell lysates from different species in order to analyse the pattern of Ser284 phosphorylation and if it correlated with dimerization in these species. We found that only mammals

exhibited phosphorylated ERK2 Ser284 and this phosphorylation did correlate with ERK dimerization. Moreover, it further indicates that the phospho-Ser284 (p-Ser284) antibody is specific and only recognizes p-Ser284 (Fig. 4.3 D).

Next, we wanted to ascertain the relationship between ERK dimerization and Ser284 phosphorylation. For this purpose, we analysed ERK2 dimerization, performing a native gel analysis. Our results indicate that phosphorylation at Ser284 occurs exclusively when ERK2 is in dimeric form. Such phosphorylation was not detected in ERK2 monomers (Fig.4.4 A).

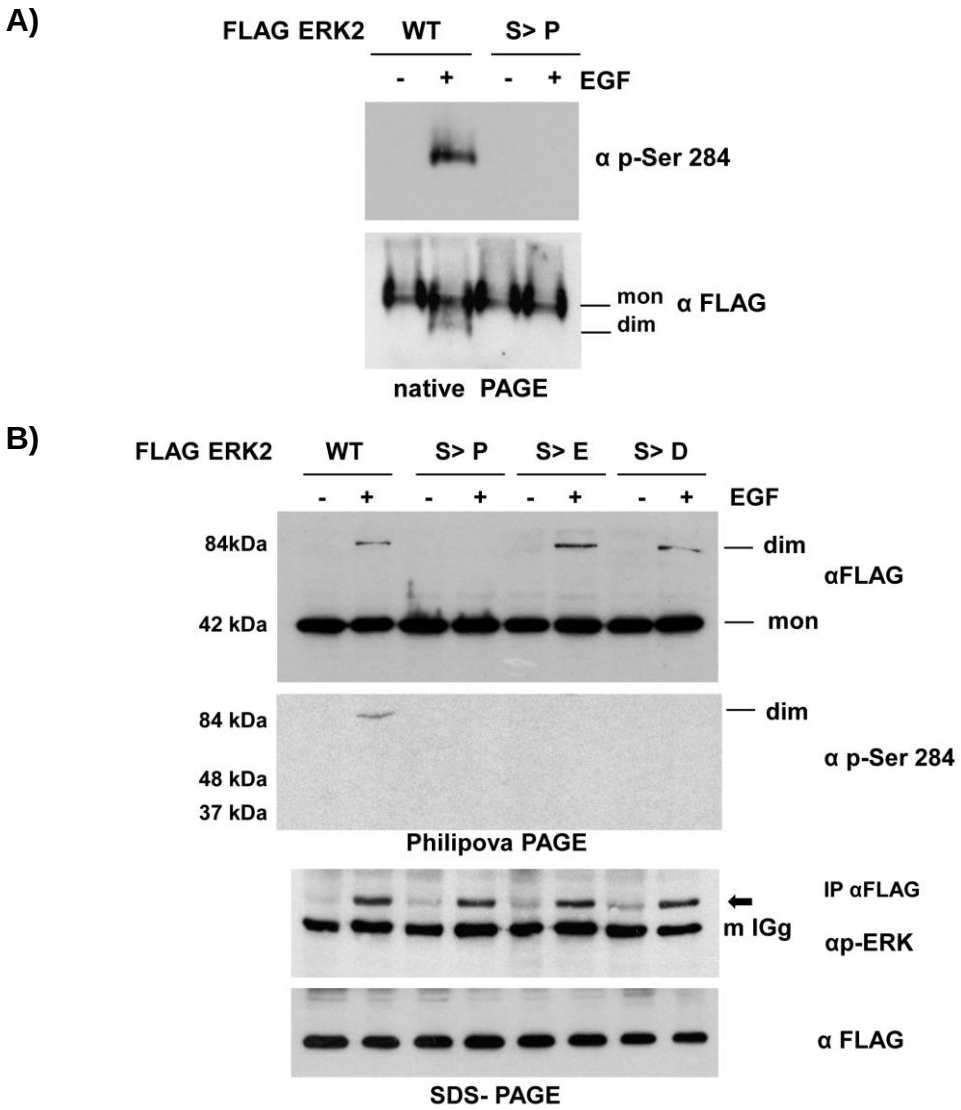

Figure 4.4. Only ERK2 dimers are phosphorylated at Ser284. A) ERK2 dimerization analysis of HEK293T cells transfected with FLAG Hs ERK2 WT and S>P (1µg each) by native PAGE. B) FLAG-tagged human ERK2 wild-type, S284P, S284D and S284E were transfected in 293T cells and dimerization upon EGF stimulation was analysed by semi-denaturing “Philipova” PAGE, in which dimers and monomers run at their real size (upper panel). Analysis of canonical phosphorylation residues of transfected FLAG-tagged human ERK2, previously immunoprecipitated and run by SDS PAGE (lower panel).

In fact, upon EGF stimulation ERK2 WT dimerizes and it is phosphorylated at Ser284, as the band of the p-Ser284 correspond with the ERK2 dimer band. To further elucidate this point, we performed a Philipova PAGE. This technique was first used to establish the correlation between active ERK1 and its dimerization capability *in vivo* (Philipova and Whitaker, 2005). Contrarily to native PAGE, in this case proteins run according to their molecular weight, in the case of ERK2 dimers being detected at around 84 kDa. Thus, we confirm that, except for ERK2 S>P, all of the rest of ERK2 proteins dimerize upon EGF stimulation (Fig.4.4 B). Notably, although all proteins show phosphorylated TEY motif upon EGF stimulation, only ERK2 WT is phosphorylated at Ser284, corresponding with its dimeric state. Therefore, these results indicate that S284 phosphorylation is critically involved in the dimerization process.

4.1.3 Identification of the kinases responsible for phosphorylating Ser284.

It was of interest to identify the kinase/s responsible for ERK phosphorylation at Ser284. For this purpose, we performed a whole kinome siRNA screen against all Ser/Thr kinases to detect the kinase/s whose depletion would prevent S284 phosphorylation upon EGF stimulation, as detected by our phospho-specific antibody by ELISA (Fig 4.5). All the kinases in the EGFr-ERK pathway emerged, which validated our assay. Interestingly, AKT1 and some other kinases like MLK1 and DAPK, with a lesser effect, also appeared in the screen.

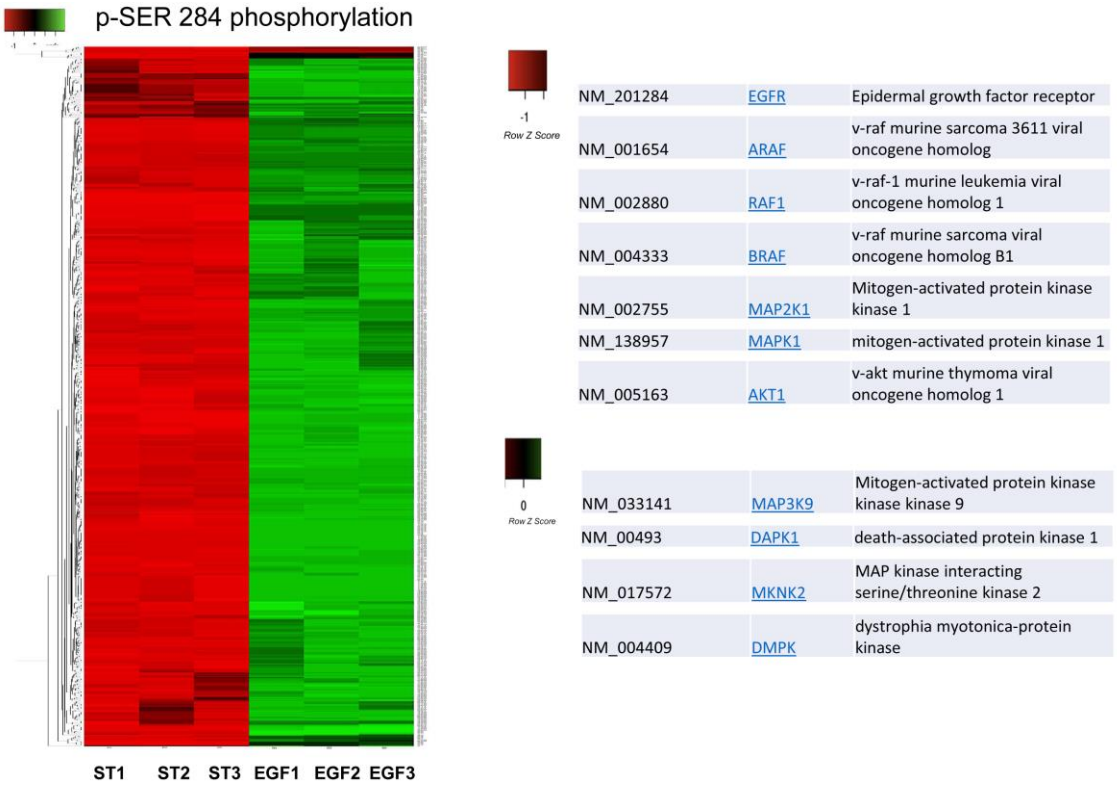

Figure 4.5. Whole kinome siRNA screen to determine possible kinases involved in ERK S284 phosphorylation. HEK293T cells were transfected with the corresponding siRNA (5 pM) and after 48h cells were starved overnight. Cells were EGF-stimulated for 5' before being harvested. P-Ser284 was analysed by ELISA double sandwich. ERK2 proteins were first blocked using anti-ERK2 monoclonal antibody coated plates and p-Ser284 was revealed by using p-nitrophenyl phosphate disodium as a colorimetric, soluble substrate of alkaline phosphatase. Row Z score data for all the kinases, run for triplicate in each condition (Starved and under EGF stimulation), are displayed as colours according to the legend.

To validate the kinases responsible for S284 phosphorylation and to ascertain which of these kinases directly phosphorylates ERK on S284, we performed an *in vitro* kinase assay. For this, we used bacterially-purified constitutively-active MEK1 and purified dead-kinase ERK2 K52R, to rule out autophosphorylation,

and ERK2 H176L (HL) dimerization impaired mutant, as substrates (Fig. 4.6 A). We checked total ERK phosphorylation using radiolabelled γ^{32}P-ATP and p-Ser284 by immunoblotting. Interestingly, MEK1 is one of the kinase capable of directly phosphorylating ERK at Ser284. Noticeably, we did not find p-Ser284 in the mutant unable to dimerize, which could indicate that ERK2 HL mutation affects ERK normal folding in a way that prevents its phosphorylation at Ser284.

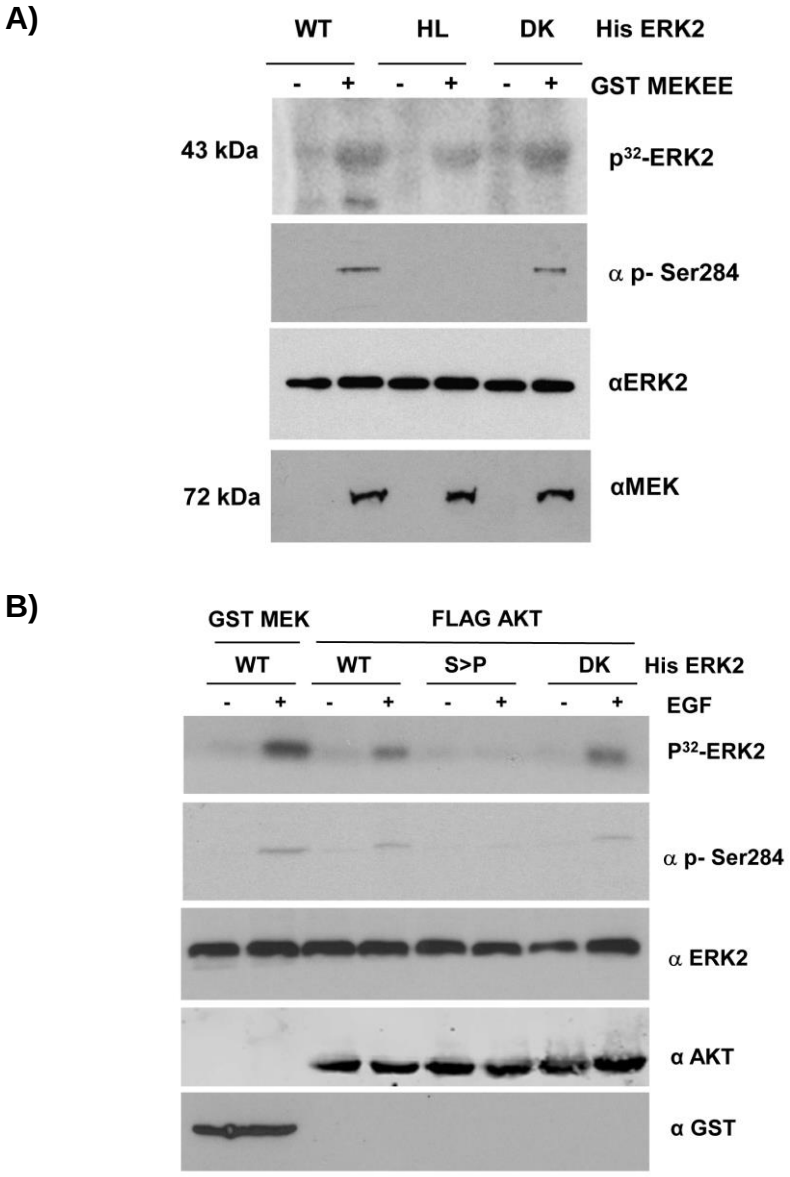

Figure 4.6. MEK1 and AKT1 phosphorylate Ser284 *in vitro*. A) *In vitro* kinase assay of Bacterially-purified human His-tagged ERK2 WT, HL and DK incubated with GST-MEK EE (+) constitutively active mutant, to activate ERK2. Total ERK phosphorylation was detected by autoradiography after ^{32}P-ATP incorporation. Ser284 phosphorylation was detected by immunoblotting by SDS-PAGE. B) As in A, but using GST-MEK and FLAG-AKT1 immuno-precipitated from HEK293T starved cells (-), or upon EGF stimulation (+). His-tagged ERK2 WT, S>P and DK were purified from bacteria.

Furthermore, we also tested AKT1 ability to phosphorylate ERK2 at Ser284. Thus, we immunoprecipitated FLAG-tagged AKT1 from EGF-stimulated HEK293T cells and it was subsequently incubated with bacterially-purified ERK2 mutants, as indicated in fig 4.16 B. We found that AKT1 is capable of phosphorylating Ser284 in WT and DK ERK2 but not in the ERK2 S>P mutant (Fig. 4.6 B).

To further substantiate AKT involvement, we silenced AKT1 expression in A375p melanoma cells, which harbour B-RAF mutation and, as a consequence, has a high basal level of p-SER284.

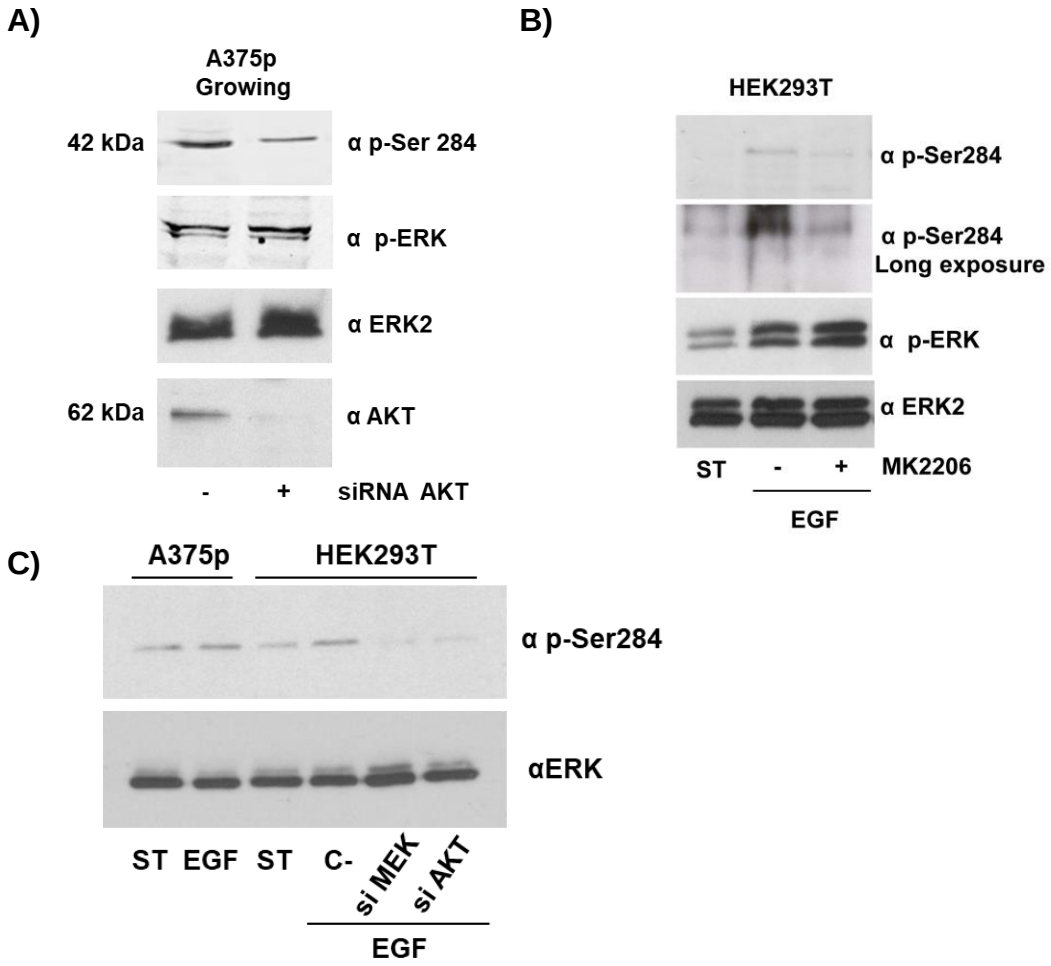

Figure 4.7. MEK and AKT downregulation reduce Ser284 phosphorylation. A) A375p melanoma cells were transfected with 50 nM of siRNA for AKT1. After 48 hours, cells were harvested during 16h and p-Ser284 and p-TEY ERK were analysed by immunoblotting. B) Starved HEK293T cells were pre-treated with the AKT allosteric inhibitor (+), MK2206 (5 μM for 1 hour). Then, cells were stimulated with EGF for 5 min and p-Ser284 and p-TEY ERK2 were analysed as in A. C) Effect of MEK and AKT downregulation on phospho- Ser284 levels in HEK 293T cells starved (ST) and under EGF stimulation; as a positive control for phopho-Ser284 levels, total lysates from A375p melanoma cells were used.

Indeed, upon AKT1 knock-down, the amount of p-Ser284 is mildly reduced in these cells (Fig. 4.7 A). We also used HEK293T cells, in which p-Ser284 is induced by EGF stimulation, and to abrogate AKT1 activity, cells were treated with MK2206, an AKT1 inhibitor. In this case, we saw a marked reduction in Ser284 phosphorylation (Fig. 4.7 B).

When MEK and AKT silencing are compared, MEK1 seems to be the principal mediator in Ser284 phosphorylation, which is conceivable due its role as the main ERK activator (Fig. 4.7 C). Overall, these evidences suggest that MEK is the main kinase devoted to phosphorylating Ser284 but AKT1 may also contribute to Ser284 total phosphorylation. Noticeably, ERK2-Ser284 phosphorylation mediated by AKT1, would add another connexion node among the two already interconnected pathways (Moelling, 1999; Procaccia et al., 2017; Zmajkovicova et al., 2013).

4.1.4 Two phosphorylated Ser284 are necessary for ERK dimerization

Having established that phosphorylation at Ser284 is required for ERK2 dimerization, we were wondering if ERK dimerization needs both oligomers to be Ser284 phosphorylated, or just one would be sufficient.

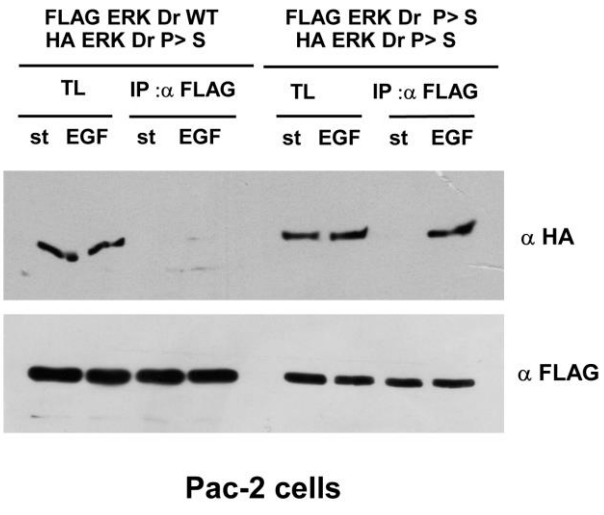

Figure 4.8. ERK2 dimerization requires Ser284 phosphorylation in both ERK2 oligomers. Co-immunoprecipitation assay of transfected PAC-2 cells (zebrafish fibroblast) with Dr ERK2 WT and P>S or two Dr ERK2 P>S, differently tagged (1 µg of each). Co-immunoprecipitation was analysed by immunoblotting using anti epitope antibody (HA).

To ascertain this, we analysed if unphosphorylatable FLAG-tagged Dr ERK2 WT could co-immunoprecipitate with HA-tagged Dr ERK2 P>S. Additionally, as a positive control, we co-transfected two Dr ERK2 P>S constructs differently tagged. We observed Co-IP only when both ERK oligomers can be phosphorylated in the Ser284, upon EGF stimulation, indicating that both ERK oligomers must be phosphorylated in order to form a dimer (Fig.4.8).

4.1.5 Phosphorylated ERK2 at Ser284 localizes at the cytoplasm.

Considering that ERK dimerization and nucleo/cytoplasmic distribution are mechanistically linked and knowing that ERK dimers are restricted to the cytoplasm (Casar et al., 2008), we wanted to gain an insight into whether Ser284 was also involved in the regulation of ERK cellular distribution. To do so, we firstly analysed the cellular distribution of S284-phosphorylated ERK. For this purpose, we performed a confocal immunofluorescence assay on HeLa cells where we observed that p-Ser284 localizes exclusively at the cytoplasm, upon EGF stimulation (Fig. 4.9), in agreement with previous findings (Casar et al., 2008).

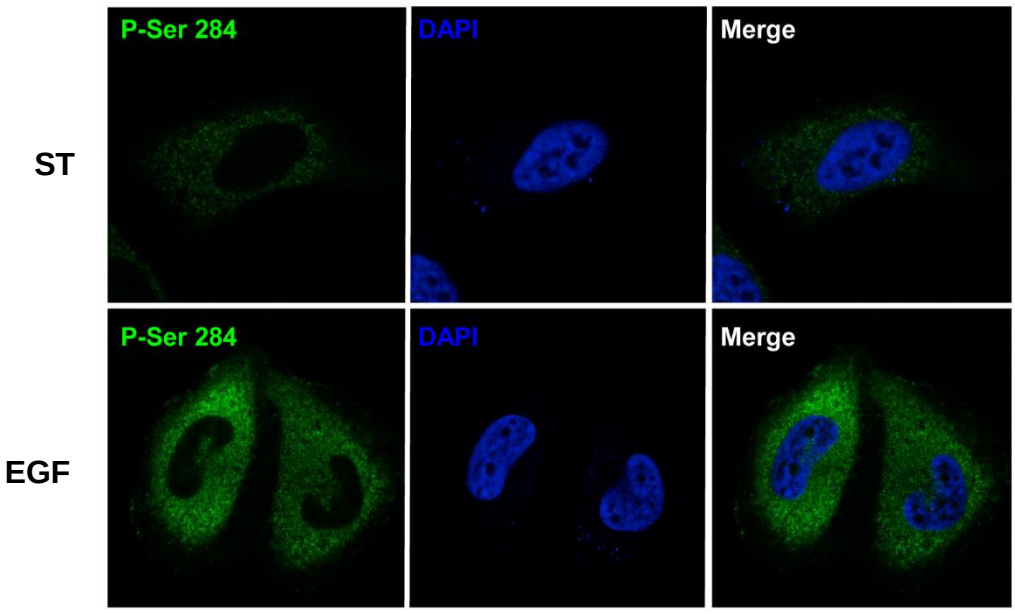

Figure 4.9. Upon EGF stimulation, p-Ser284 localized at the cytoplasm. Endogenous p-Ser284 distribution (green) was compared in starved (Overnight) and EGF (5') stimulated HeLa cells by immuno-fluorescence, using a confocal microscope. Nuclei are shown in blue.

Additionally, we compared ERK2 phosphorylation at the TEY motif and at Ser284 in Hela cells by immunofluorescence. We found that upon EGF stimulation ERK phosphorylated at the canonical TEY motif was scattered throughout the cell. Contrarily, S284-phosphorylated ERK was exclusively localized at the cytoplasm (Fig. 4.10 A), in full agreement with Ser284-phosphorylated ERK being solely in dimeric form.

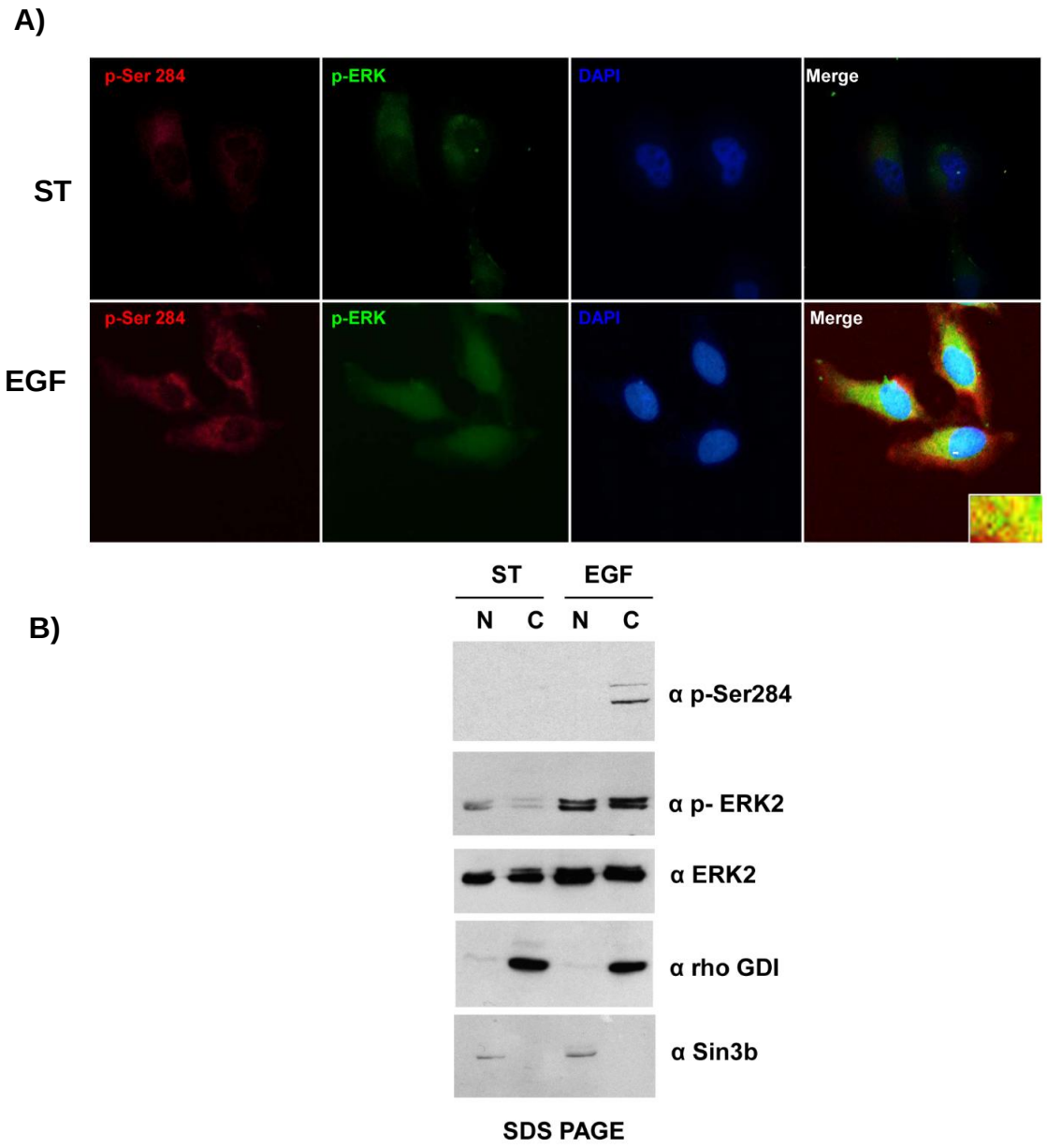

Figure 4.10. p-Ser284 is restricted to the cytoplasm of stimulated cells. A) S284-phosphorylated ERK2 localizes exclusively at the cytoplasm. HeLa cells starved (ST) or stimulated with EGF for 5 min were fixed and immunofluorescence were performed to detect endogenous ERK1/2 phosphorylated at Ser284 (red) and at the canonical TEY phosphorylation site (p-ERK green). B) Nuclear (N)-cytoplasm (C) fractionation of starved and EGF stimulated HEK293T cells. P-Ser284 and p-ERK2 distribution were analysed by immunoblotting. RhoGDI and Sin3b were used as cytoplasmic and nuclear fraction markers, respectively.

Additionally, to further demonstrate p-Ser284 localization, we performed a nucleo-cytoplasmic fractionation. Again, we observed that whereas phosphorylated ERK2 at the TEY motif was distributed in both cell compartments, p-Ser284 localization was exclusively cytoplasmic in agreement with the immunofluorescence analyses (Fig. 4.10 B).

To gain further insights into how Ser284 phosphorylation regulated ERK2 cellular distribution, we transfected HEK293T cells with exogenous FLAG-tagged ERK2 WT and S>P and analysed their nucleo-cytoplasmic distribution. We observed that, as expected, under starvation conditions ERK2 WT was exclusively cytoplasmic. Interestingly, introducing the S284P mutation evoked a remarkable redistribution, with a large amount of this mutant form accumulating in the nucleus, under resting condition (Fig.4.11).

Overall, these results point to Ser284 as a critical residue for the regulation of ERK subcellular distribution.

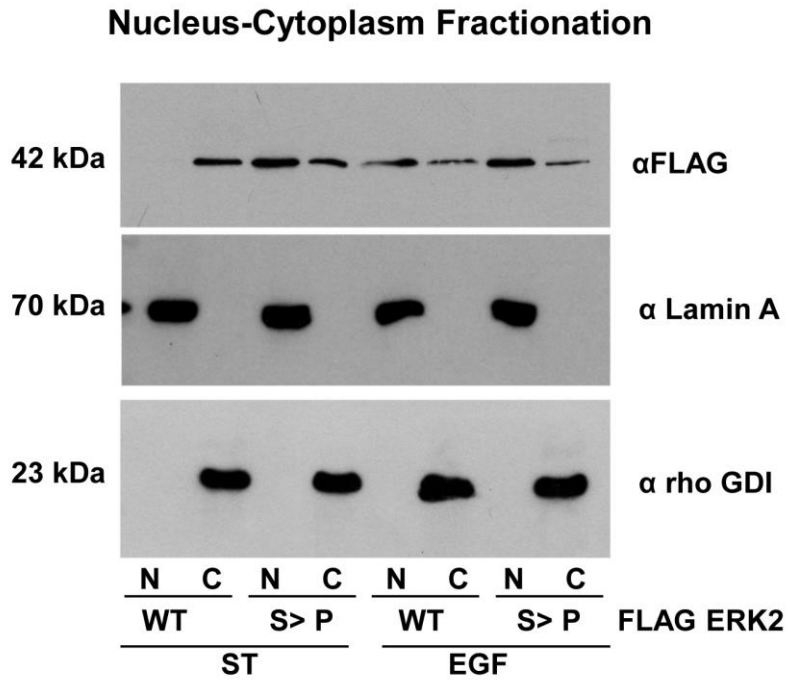

Figure 4.11. S284 regulates ERK nucleo/cytoplasmic distribution. HEK293T cells were transfected with FLAG-tagged human ERK2, wild-type and S284P. Nuclear (N) and cytoplasmic (C) fractions from starved and EGF-stimulated cells (5 min) were collected and analysed by immunoblotting. RhoGDI and Lamin A serves as a cytoplasmic and markers, respectively.

4.1.6 P-Ser284 regulates ERK2 affinity for scaffold/anchor proteins.

We have previously demonstrated that scaffold proteins function as ERK dimerization platforms as well as at cytoplasm anchors (Casar et al., 2008). Thus, being ERK p-Ser284 purely cytoplasmic, it was conceivable that S284 phosphorylation could somehow influence ERK-scaffolds affinity, thereby impacting both on its own dimerization and localization. To put this under test, we analysed by mass spectrometry ERK2 interactome in HEK293T cells transfected with ERK2 WT or ERK S>P. We found that preventing Ser284 phosphorylation inhibited ERK binding to KSR1 (Fig 4.12 A).

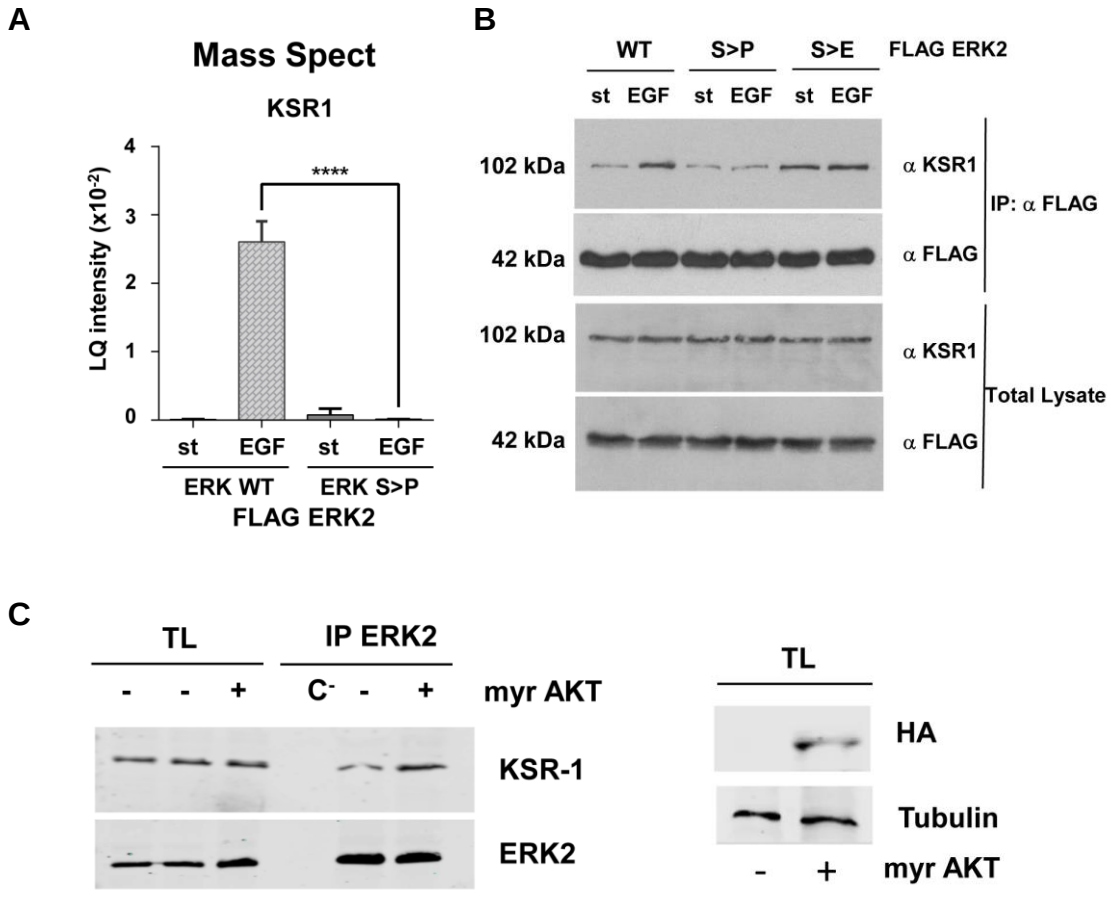

Figure 4.12. S284 phosphorylation regulates ERK binding to KSR1. A) Mass spect data indicates that human ERK2WT binds with higher affinity to KSR-1 in stimulated cells. Transfected HEK293T cells with FLAG-tagged ERK2 WT or S>P were immunoprecipitated and analysed by mass spectrometry analysis. Data represents LQ intensity of triplicated samples. B) Co-immunoprecipitation assay to analyse human FLAG-tagged ERK WT, S284P and S284E binding to KSR-1 scaffold protein. C) Constitutively activated AKT (myr-AKT) increases ERK2 and KSR1 interaction. Left panel: Endogenous ERK2 was immunoprecipitated in HEK293T cells and KSR1 interaction was detected by immunoblotting. Isogenic rabbit IgG was used for immunoprecipitation negative control (C-). Cells were transfected with myr-AKT (1µg) where shown (+). Right panel: western blot analysis of myr-AKT HA-tagged expression using anti HA antibody. Data shows Mean ± SD (n=3) using two-tailed unpaired Student T-Test (*p<0.05, **p<0.01, ***p<0.001 and ****p<0.0001).

To validate the mass spect results, the interaction of the scaffold protein KSR1 with ERK2 WT, S284P and S284E was analysed by co-immunoprecipitation (Fig. 4.12 A). According to the mass spect results, upon EGF stimulation, we observed that ERK WT binding to KSR1 increases, as expected from our previous publications (Casar et al., 2008). However, this was not the case for ERK2 S>P where no significant changes were detected among starved and stimulated cells, in line with our previous results using subcellular fractionation, being the KSR1 localization solely cytoplasmic and the S>P mutant localized mainly at the nucleus. In the same vein, S>E substitution increased ERK2-KSR1 affinity, under starvation conditions.

Similarly, since AKT1 was also capable of phosphorylating Ser284 we interrogated if AKT could contribute to enhance ERK-scaffold affinity. To test this, HEK293T cells were transfected with a AKT constitutively active form (myr-AKT), and ERK-KSR1 interaction was analysed by Co-IP. We observed that AKT enhanced endogenous ERK affinity for KSR1 (Fig. 4.12B).

In the same line, since the ERK2 mutant S284P accumulates in the nucleus under unstimulated conditions, we were wondering if it could be a consequence of its enhanced interaction with the shuttles that transport ERK to the nucleus. As it is known that importin7 functions as an ERK cytoplasmic-nuclear shuttle (Chuderland et al., 2008), we checked for the presence of Importin7 in our mass spect analyses and then analysed the interaction between ERK WT and ERK S>P with IMP7 by co-immunoprecipitation. We observed that the ERK S>P mutant, which is unable to dimerize and is nuclear under starved conditions, bound with higher affinity than ERK WT to Importin7, both in starved and in EGF stimulated cells (Fig. 4.13).

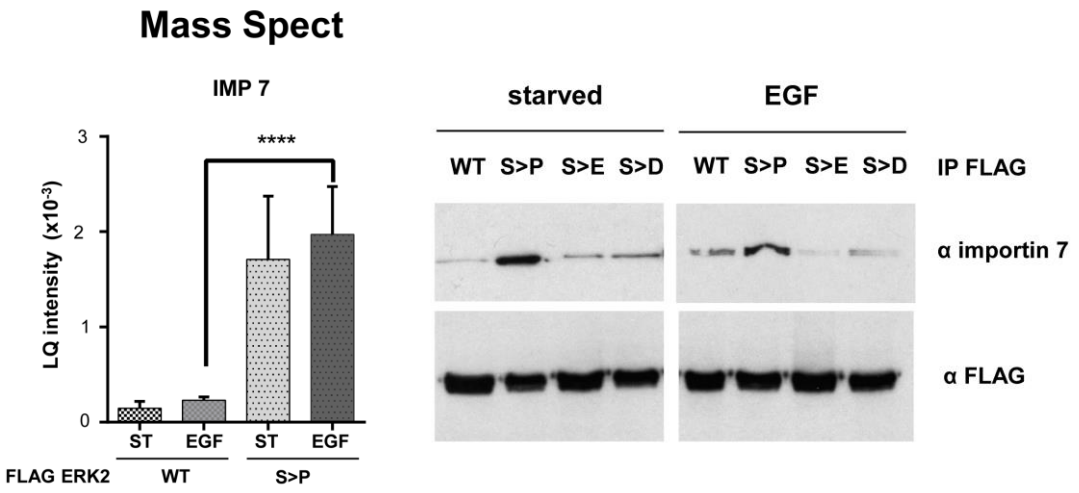

Figure 4.13. In the absence of S284 residue, ERK binds tightly to Importin7. A) Mass spec analysis indicates that human FLAG tagged ERK2 S>P mutant binds with higher affinity to Importin 7. B) Determination of human FLAG tagged ERK2 WT, S>P, S>E, and S>D binding to Importin 7 by co-immunoprecipitation assay. Data shows Mean ± SD (n=3) using two-tailed unpaired Student T-Test (*p<0.05, **p<0.01, ***p<0.001 and ****p<0.0001).

Overall, these data suggest that Ser284 is an important regulator of ERK subcellular distribution. Both by regulating ERK dimerization, augmenting scaffold binding and as a consequence retaining ERK at the cytoplasm, and also by orchestrating ERK interaction with shuttle proteins like Importin7.

In light of these findings, we hypothesized that the kinetics of ERK2 nuclear translocation could be different depending on Ser284 phopshorylation. To investigate this, we performed an *in vivo* time-lapse analysis, using HeLa cell transfected with CFP-tagged ERK2 WT and the two mutants (S284P and S284E). HA-MEK1 was also transfected to maintain the stoichiometry between ERK and its cytoplasmic anchors.

To follow ERK2 cellular distribution, images were taken at different time intervals and the CFP fluorescence of the nuclear/cytoplasm ratio was measured. Noticeably, the results (Fig. 4.14) did not show significant differences on ERK nuclear translocation rate among the different ERK mutants.

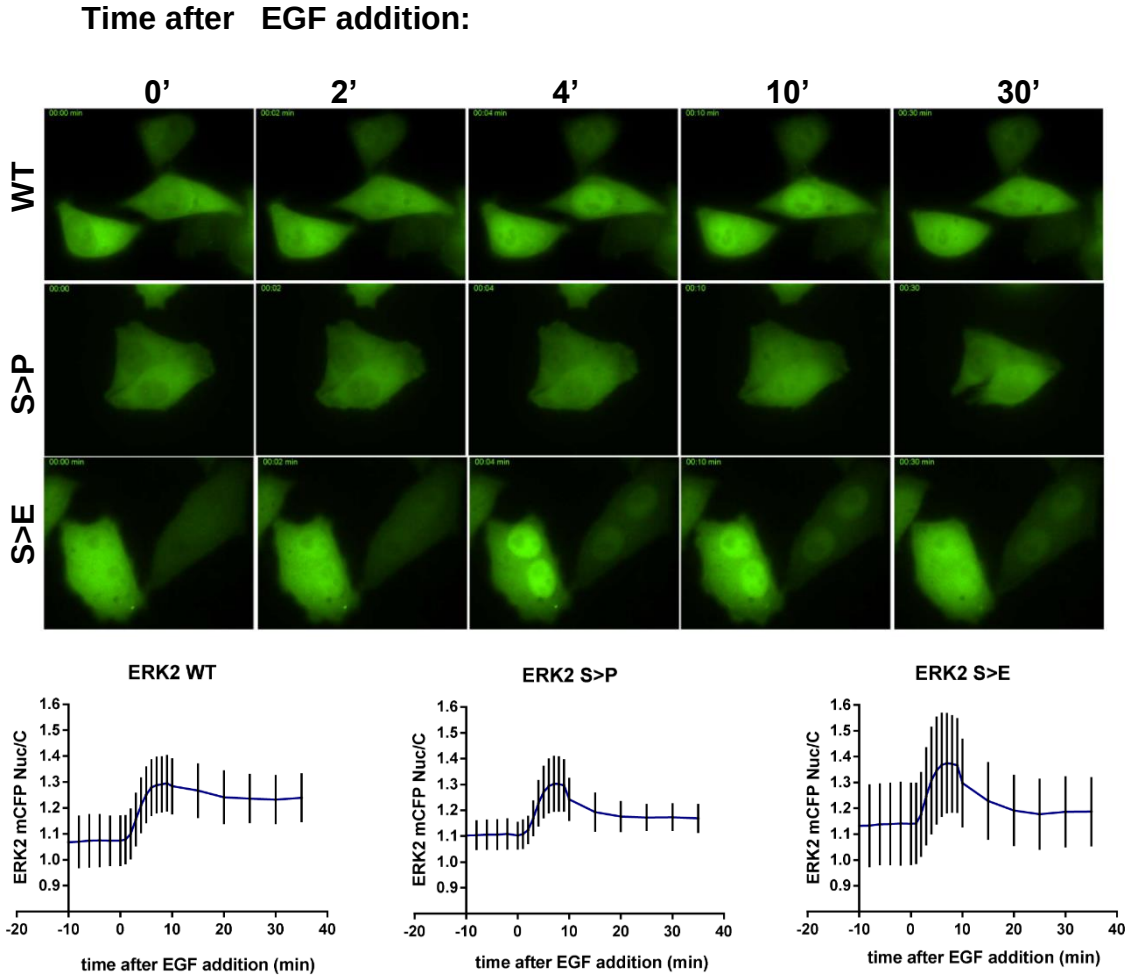

Figure 4.14. ERK2 cellular distribution by *In vivo* time lapse analysis. Hela cells were co-transfected with the three different ERK2 constructs CFP-tagged and stimulated with EGF. Photos were taken at the indicated time using confocal Leica microscope. Nuclear and cytoplasm fluorescence quantification and nuclear/cytoplasm fluorescence ratio were performed using ImageJ software. Values in the graph represent the amount of nuclear ERK at the indicated time as a result of the quantification of at least ten cells for each condition.

Thus, we conclude that Ser284 can regulate ERK basal Nuclear/cytoplasmic distribution but appears not be involved in the regulation of ERK translocation, under acute stimulation.

4.2 Biological consequence of Ser284 phosphorylation.

4.2.1 Ser284 phosphorylation effect on ERK activation kinetics

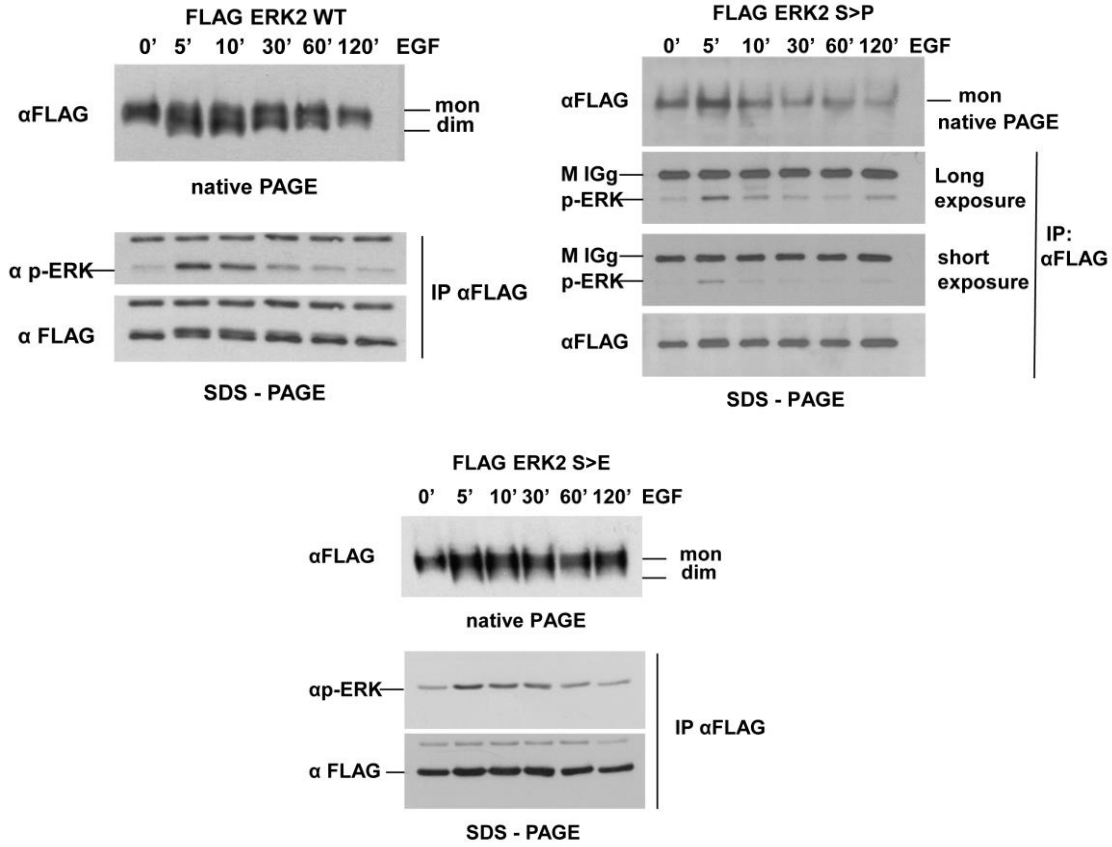

Figure 4.15 Kinetics of ERK2 phosphorylation depending on Ser284 status. HEK293T cells transfected with the different ERK2 constructs FLAG-tagged (1µg WT and 2 µg of S>P and S>E each) were stimulated for the indicated times with EGF. ERK dimerization was analysed by native page using anti-FLAG antibody. To analyse phosphorylated ERK at the canonical residues (TEY), the different constructs were immuno-precipitated using FLAG antibody and analysed by SDS-PAGE immunoblotting.

Since our results indicate that Ser 284 phosphorylation regulates ERK dimerization we sought to determine if the S284P mutation could affect ERK2 TEY motif phosphorylation in response to growth factors. We performed a time course analysis in HEK293T cells, transfected with the different FLAG-tagged Ser284 mutants, upon EGF stimulation. At the same time, ERK2 dimerization was analysed by native page, using anti-FLAG immunoblotting to detect only the transfected ERK. Our results showed the expected p-TEY phosphorylation bell-shaped kinetics, in the case of the WT and the S>E mutant, with a sustained phosphorylation between 5 and 30 min of EGF stimulation. Contrarily,

the S>P mutant showed a peak of activation after 5 min of EGF stimulation, that promptly dropped after this time (Fig. 4.15).

In the same line, we asked if S284, being close to the MAPK insert, could somehow alter ERK activity, as reflected on its ability to phosphorylate its substrates. To investigate this aspect, we performed an *in vitro* kinase assay, using HA-tagged ERK2 WT and FLAG-tagged ERK2 S>P and myelin basic protein (MBP) as a bona-fide ERK substrate, and analysed its phosphorylation by measuring MBP-P^{32} incorporation (Fig. 4.16).

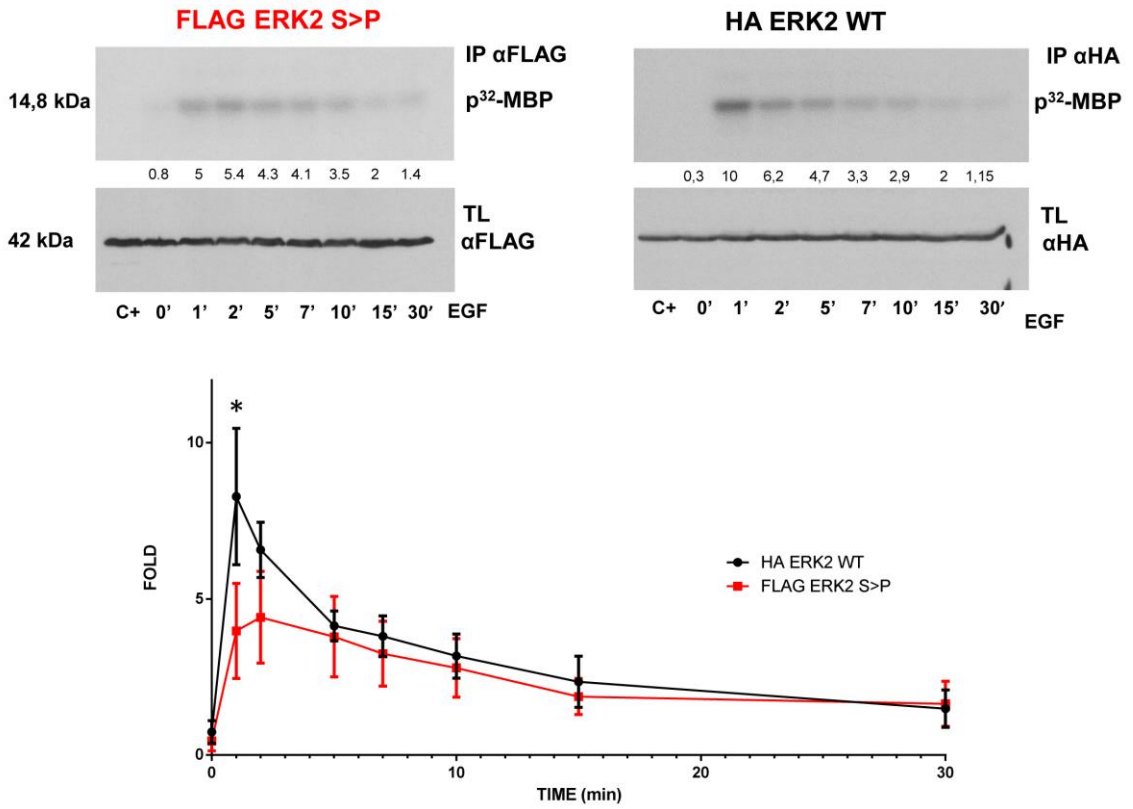

Figure 4.16. Ser284 role in ERK activity. HEK293T cells were transfected with FLAG-tagged ERK2 S>P (2 µg) and HA-tagged ERK2 WT (1 µg). After EGF stimulation, ERK constructs were immunoprecipitated using the appropriate antibody. C+ represents control transfected cells IP without antibody. At each point, immunoprecipitated ERKs were incubated with 15 µg of MBP and 1 µCi of labelled ATP (γ-^{32}P). Samples were solved by SDS-PAGE and MBP phosphorylation was measured and normalized to the t0 of ERK2 WT. Data shows Mean ± SD (n=3) using two-tailed unpaired Student T-Test (*p<0.05, **p<0.01, ***p<0.001 and ****p<0.0001).

Both ERK2 constructs were immunoprecipitated from transfected HEK293T cells, after EGF stimulation at the indicated times, and then incubated with

MBP, together with radioactive labelled ATP (γ-^{32}P). Proteins were solved by SDS-PAGE and MBP phosphorylation was analysed by autoradiography. ERK2 WT showed a significantly stronger MBP phosphorylation peak after 5 min of EGF stimulation, compared to the S>P mutant (Fig. 4.16). However, these differences almost disappear after longer periods of EGF stimulation.

4.2.2 Kinetic of Ser284 phosphorylation.

In order to understand better the role of S284 phosphorylation in the process of ERK dimerization, it was important to know the sequence of events leading to dimerization. Therefore, we tested if upon EGF stimulation the phosphorylation of the TEY motif preceded S284 phosphorylation or viceversa. To do so, we did a short-term time course experiment in HEK293T cells, analysing p-Ser284 and p-TEY correlation. Our results did not show major differences in the kinetics of ERK phosphorylation in both residues (Fig.4.17). Thus, it would indicate that the two phosphorylation events and probably dimerization occur almost simultaneously.

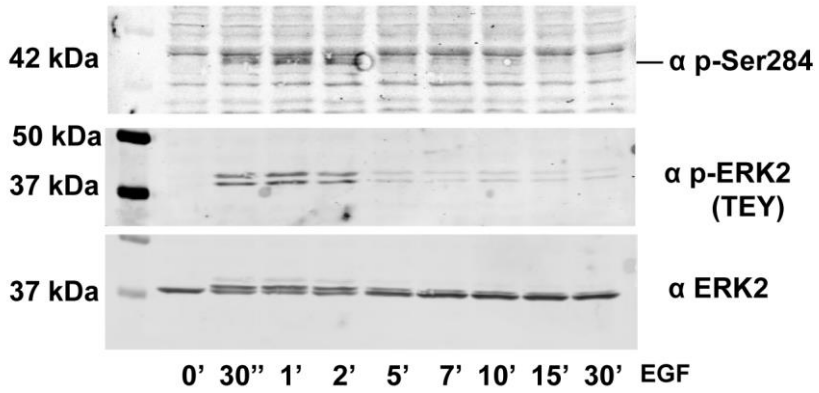

Figure 4.17 Ser284 and TEY-ERK2 phosphorylation occur simultaneously. Kinetics of Ser284 and TEY phosphorylation were analysed in starved and EGF-stimulated HEK293T cells at the indicated time points by immunoblotting.

4.2.3 Mammalian cellular viability dependence on Ser284 phosphorylation.

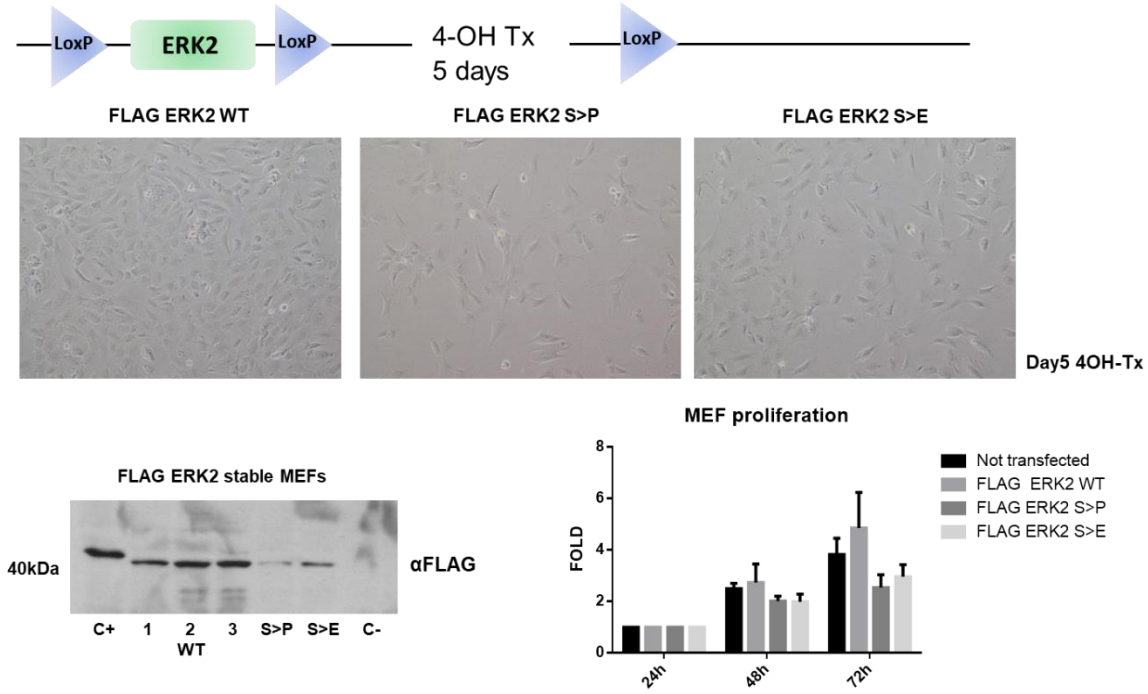

Figure 4.18. MEF viability dependence on Ser284 phosphorylation. A) Schematic representation of conditional LoxP system in mouse embryonic fibroblast. Upon hydroxy-tamoxifen treatment for at least 5 days, expression of endogenous ERK2 is completely abolished. B) Bright-field microscopy images of MEF cells stably expressing the indicated constructs. C) Expression analysis of the different FLAG-tagged constructs by immunoblotting. FLAG-ERK2 WT is represented in 3 clones. Transfected HEK293T cells were used as a positive control (C+). Similarly, untransfected cells were used as negative control (C-). D) Proliferation of the different MEF stable cell lines. The graph represents the fold increase of Alamar Blue at the indicated time points. Results show Mean ± SD (N=5).

To test the extent to which the absence of ERK dimerization by preventing Ser284 phosphorylation, could affect cell viability in a contest where ERK normally dimerizes, we used ERK-less fibroblast. These cells are constitutively devoid of ERK1 and ERK2 can be conditionally ablated by treatment with tamoxifen, resulting in cellular proliferation arrest and a senescent-like phenotype (Fig. 4.18 A) (Blasco et al., 2011). We generated stable cell lines, expressing ectopic FLAG-tagged ERK2 WT, S>P and S>E mutants.

Once endogenous ERK2 expression was eliminated, we tested the extent to which the presence of physiological levels of ectopic ERK2 S>P mutant forms could rescue cell proliferation. After 5 days of tamoxifen treatment proliferation appeared significantly reduced in the case of the non-dimerizing S>P mutant (Fig 4.18 B). The reduction in cell proliferation was also evident in the

proliferation plot analyses (Fig 4.18 D). However, when ERK2 expression was analysed, this mutant showed the lower expression levels, compared to the other two constructs (Fig. 4.18 C). Thus, in light of the expression results, it is conceivable that the lower proliferation rate in MEFs harbouring non-dimerizing ERK2 S>P could be attributed to its lower expression. However, its lower expression could also be a consequence of its inability to support cell growth as effectively as the dimerization competent forms.

4.2.4 Biological relevance of Ser284 phosphorylation and ERK dimerization in animal models.

4.2.4.1 Mouse loss-of-function model

In connection with the previous aim, we were also interested in understanding the systemic significance of ERK dimerization in animal viability. For this purpose, we are trying to generate i) a loss-of-function mouse model in which ERK2 does not dimerize and ii) a gain-of-function zebrafish model in which ERK2 dimerizes. It has been demonstrated that ERK1 knock-out results in viable animals with no overt phenotype. Contrarily, ERK2 disruption is embryonic lethal (Buscà et al., 2015; Hatano et al., 2003). Thus, we have restricted our analysis to ERK2. Using CRISPR/Cas9 editing we generated a dimerization-deficient ERK2 mouse by introducing the S284P mutation (Fig 4.19).

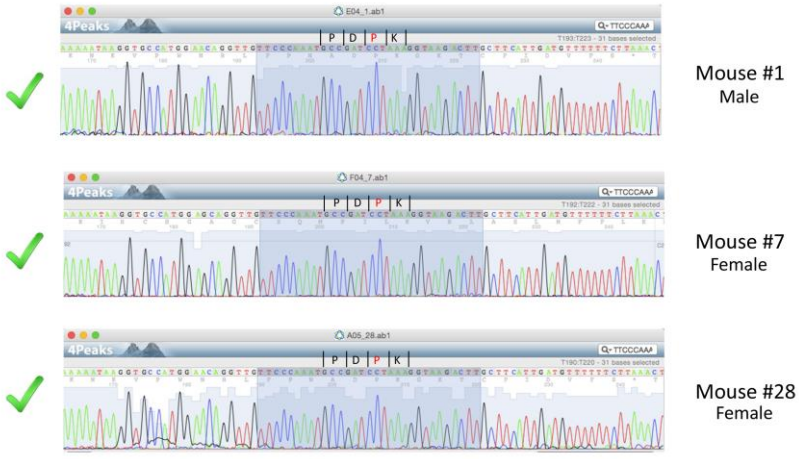

Figure 4.19. Representative sequencing of S>P mutant mice. Mouse screening genotyping. Replacement of TCC codon encoding for serine residue, by the CCT codon that encoded for proline residue.

For this purpose, we have established a collaboration with Prof. Moises Mallo (Instituto Gulbekian) who has a broad expertise in the generation of genetically-modified mice using CRISPR/Cas9 gene editing. We used FVB/N strain to keep in line with previous publications on ERK2 gene targeting. The results emerging from this editing show that this substitution is not affecting mice viability. In fact, upon crossing heterozygote animals, statistical analyses indicate a correct mendelian segregation of homozygote animals with normal phenotype and no gender segregation (Table 4.1).

Tabla 4.1 Statical analysis of heterozygous mice crosses.

Crosses				
$ERK2^{P/S}$ X $ERK2^{P/S}$	WT(S/S)	Heterozygous(P/S)	Homozygous(P/P)	Total by gender
Female	23	46	20	89
Male	22	54	23	99
Total	45	100	43	188
Percentage	**23,94%**	**53,19%**	**22,87%**	

However, it is known that ERK1 overexpression could compensate the lack of ERK2 (Frémin et al., 2015). To discard the possibility that, somehow, ERK1 is overexpressed in these animals and may rescue a ERK2 S284P phenotype, we will analyse ERK1 expression in these mice and, subsequently, we will cross homozygote ERK2 S284P animals with ERK1 knock-out mice, in order to generate $ERK1^{-/-}$/ ERK2 S284P mice. Upon crosses, homozygote animals, if viable, will be monitored for: correct mendelian segregation; gender segregation; body size; organ sizes; growth rate; overt phenotypic abnormalities and behavioural patterns. Embryo analyses will be undertaken if no homozygotes are born.

4.2.4.2 Zebrafish gain-of-function model

In a parallel approach, we are generating an ERK2 dimerization-competent zebrafish, by introducing a P293S mutation in ERK2. According to our previous results, showing that this mutant acquires the dimerization ability, we will check if ERK2 dimerization is compatible with zebrafish normal life. These experiments have been carried out in Dr.Adam Hurlstone's laboratory, in which I did a short internship to set up the initial phase of zebrafish ERK2 gene editing. As in mice, Dr ERK2 P293S gene editing has been done by knock-in mutation using CRISPR/Cas9 technology. During my internship, we identified the region of interest in the zebrafish ERK2 gene, against which we have synthesized specific single-guide RNA (sgRNA). To improve the homology-directed repair (HDR) mechanism a single-strand oligo deoxy-nucleotide (ssODN) was co-injected into single-cell embryos, together with the sgRNA, mRNA cerulean, to

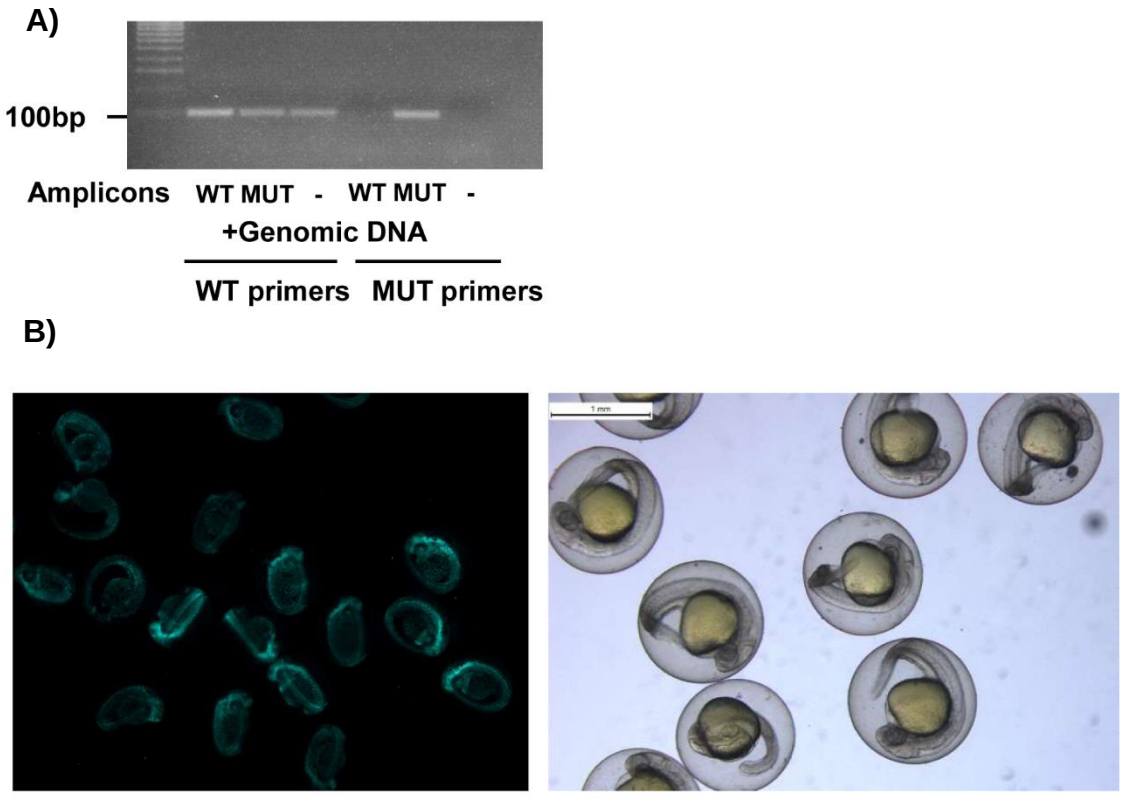

Figure 4.20. Set up of CRISP/Cas9 injection in Zebrafish. A) Analysis of primers specificity. Zebrafish genomic DNA was amplified by PCR using WT primers, which will be used to discriminate heterozygous animals, and MUT primers which specifically detect the point mutation. Amplicons string addition are represented as amplicons WT, MUT or not amplicon (-). The mutant product is displayed at 94 bp. B) Fluorescent embryos image at 24 hours post injection (hpi). Only those fluorescents embryos were selected for the subsequently analysis. Bright-field image shows normal phenotype of embryos at this stage.

track the injection efficiency, and Cas9 protein. To optimize primers recognition of the point mutation, first we designed specific primers and next, using a specific amplicon mutant string, we confirmed that the primers recognize specifically the mutation when mutant amplicon string is present (Fig. 4.20 A). After 24 hours post injection, only fluorescent embryos were selected and some of them were analysed by PCR for detecting if the mutation had occurred, in order to maintain them or not (Fig.4.20 B).

The PCR were performed using a couple of primers that amplify the region flanking the point mutation where, if the sgRNA worked properly, we expected to see a smearing band, and a couple of primers that detect de point mutation, using as positive control the mutant amplicon string. The samples were then

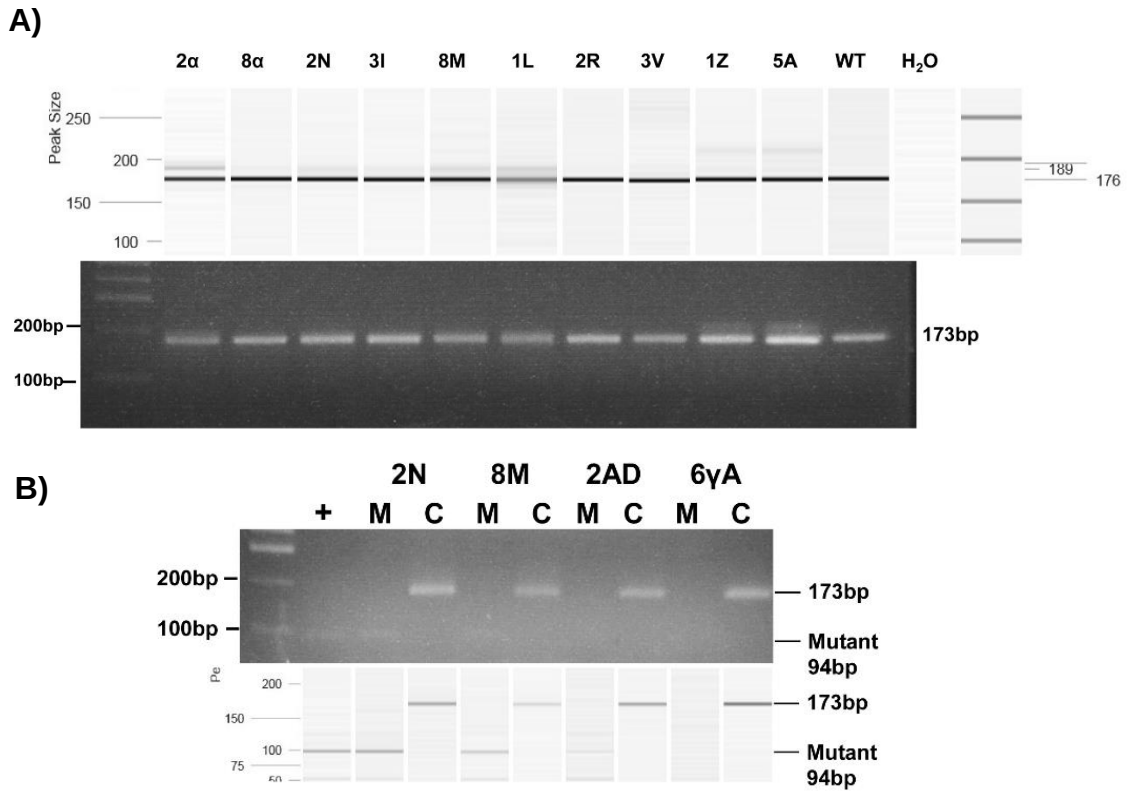

Figure 4.21. PCR analyses of CRISPR/Cas9 injected embryos. A) 24 hpi, some embryos were sacrified and PCR using primers flanking the point mutation were performed, giving a 173bp product. Samples were solved by capillary PCR (upper panel) and southern blot (lower panel). Numbers and letters serve to identify the embryos. All of numbers/letter, except from 2α and 1L, are CRISPR/Cas9 injected embryos. 2α and 1L are Cas9 and sgRNA injected only. WT indicates genomic DNA embryo used as template, whereas H_2O is the negative control. B) Like in A) PCR of some promising animals analysed by southern blot and capillary PCR using primers couple which give the 173bp product (C) and 94bp mutant product (M). Mutant string amplicon were used as positive control (+).

analysed by southern blot and by capillary PCR, being much more sensitive to detect any alteration in the PCR product, such as band size and smear (Fig. 4.21).

Adult positive fishes were genotyped (Fig 4.22), and positive fishes (number 5 and 6) were crossed to establish a founder line, in order to verify if the dimerizing-ERK2 fishes are viable or show any phenotypic alteration.

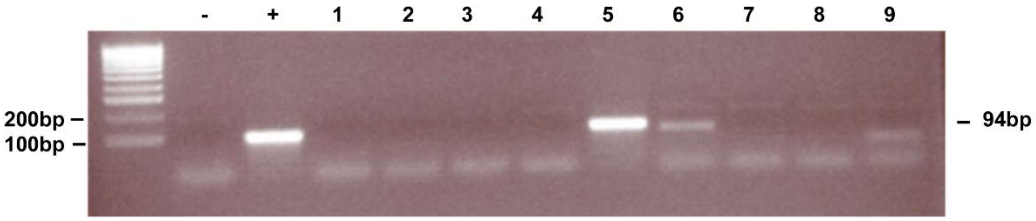

Figure 4.22. Genotype analysis of adult fishes. After being raised for 3 months, fishes (1-9) were fin clipped and genotyped using Mut primers (94bp) by nested PCR. WT genomic DNA was used as a negative control (-), and mutant amplicon string as positive control (+).

4.3 ERK2 Ser284 phosphorylation as prognostic marker in tumours.

4.3.1 Phosphorylated Ser284 levels correlation with sensitivity to Vemurafenib in melanoma cells.

As mentioned in the introduction, about 40% of human cancers harbour activating mutations in proteins involved in the RAS-ERK signalling cascade, in particular RAS and B-RAF. In cutaneous melanoma, the occurrence is even higher, with 15-20% of melanomas presenting mutant N-RAS, and oncogenic B-RAF appearing in 50-60% of the cases (Ryan and Corcoran, 2018; Yaeger and Corcoran, 2019). In order to prevent aberrant RAS-ERK signals and, as a consequence, tumour progression, several drugs have been approved, both by FDA and EMA, for clinical use in advanced melanoma cases. Among these, ATP-competitive B-RAF inhibitors, particularly Vemurafenib (PLX4032) and dabrafenib (GSK2118436), have shown remarkable, though short-lived, clinical

efficacy in melanomas harbouring B-RAFV600E/K mutations (Bollag et al., 2010; Flaherty et al., 2010; García-Gómez et al., 2018).

Although about 60% of patients with B-RAF-mutant metastatic melanoma obtain clinical benefits from Vemurafenib treatment, the remaining 40% of patients are non-respondents to the treatment (McArthur et al., 2014). Therefore, finding some predictive criterion whereby B-RAF-mutant melanoma patients could be stratified depending on their sensitivity to B-RAF inhibitors would represent an invaluable asset that could spare unnecessary burdens to patients, and a significant economic saving to health systems.

Asymmetric ERKs nucleus-cytoplasmic distribution is observed in some types of tumours, sometimes associated to distinct tumour features and/or clinical parameters. Interestingly, ERK cytoplasmic levels correlate with a better prognostic in invasive breast carcinoma (Nakopoulou et al., 2005) and in SCLC (Blackhall et al., 2003); and with high sensitivity to B-RAF inhibitors in B-RAF-mutant melanoma (Bollag et al., 2010). Since, according to our previous data, ERK phosphorylation in Ser284 is distinctive and exclusive for cytoplasmic ERK, it is quite conceivable that it could serve as a prognostic marker for these cases. Moreover, it could be much more reliable than total or TEY-phosphorylated ERK cytoplasmic levels, as they always have to be quantitated relative to the nuclear levels.

To put into test this hypothesis we analysed the phosphorylated Ser284 levels in A375p and M249 melanoma cells, harbouring B-RAF mutation (Fig.4.23). Specifically, for each of these cell lines we have analysed two clones, one sensitive to Vemurafenib treatment (parental) and another resistant (VemR), as indicated by the IC50 values.
According with previous data, in both cell lines, the clone that responds to the B-RAF inhibitor treatment showed higher levels of phosphorylated Ser284. By contrast, the insensitive clone shoed low p-Ser284 levels, as well as a reduction of phosphorylated AKT1. Total phosphorylated ERK2 was unaltered in the case of resistant cells

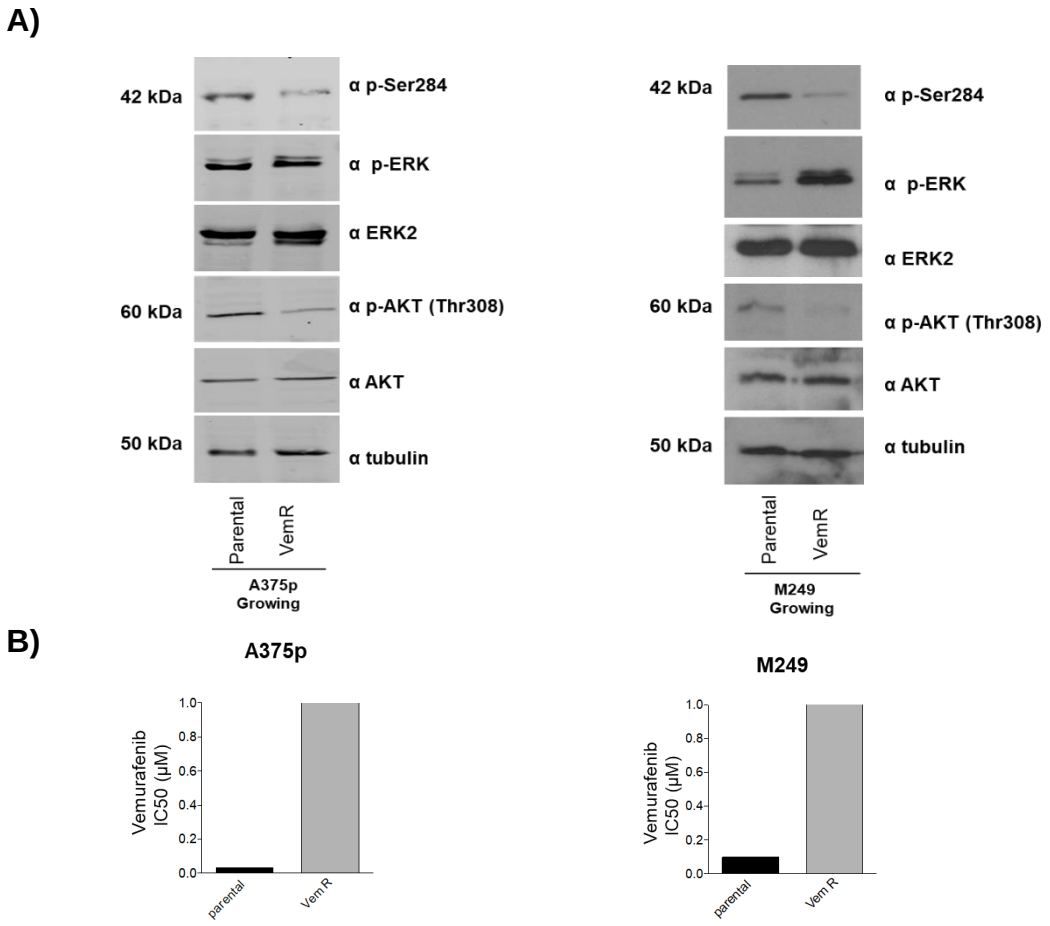

Figure 4.23. Ser284-phosphorylated ERK2 levels correlate with sensitivity to Vemurafenib. A) Growing melanoma cell lines, A375p and M249, parental and Vemurafenib resistant (VemR) were harvested and their levels of p-Ser284, p-TY ERK and p-AKT1 were analysed by immunoblotting. B) Sensitivity of the melanoma cell lines to Vemurafenib growth inhibitory effect represented by half maximal inhibitory concentration (IC50) calculated using Graph Prism software.

4.3.2 Phosphorylated Ser284 levels correlate with sensitivity to Vemurafenib in B-RAF mutant cells.

To further proof the connection between p-Ser284 levels and sensitivity to Vemurafenib, we extended our study to a broader panel of cells harbouring B-RAF and N-RAS mutations.

We observed that p-Ser284 levels were higher in those cell lines harbouring B-RAF mutations, in which treatment with Vemurafenib caused the greatest reduction in TEY-phosphorylated ERK2 and are more sensitive to Vemurafenib growth inhibitory effect, as shown in the GI 50 (Fig 4.24 A).

Moreover, this stratification may be also used for identifying B-RAF-inhibitor sensitivity in other types of tumours, in which B-RAF mutations are also common. As displayed in our panel, 8505C thyroid cancer-derived cells, being sensitive to B-RAFi, follow the same Ser284 phosphorylation pattern of melanoma cells (Fig.4.24 A).

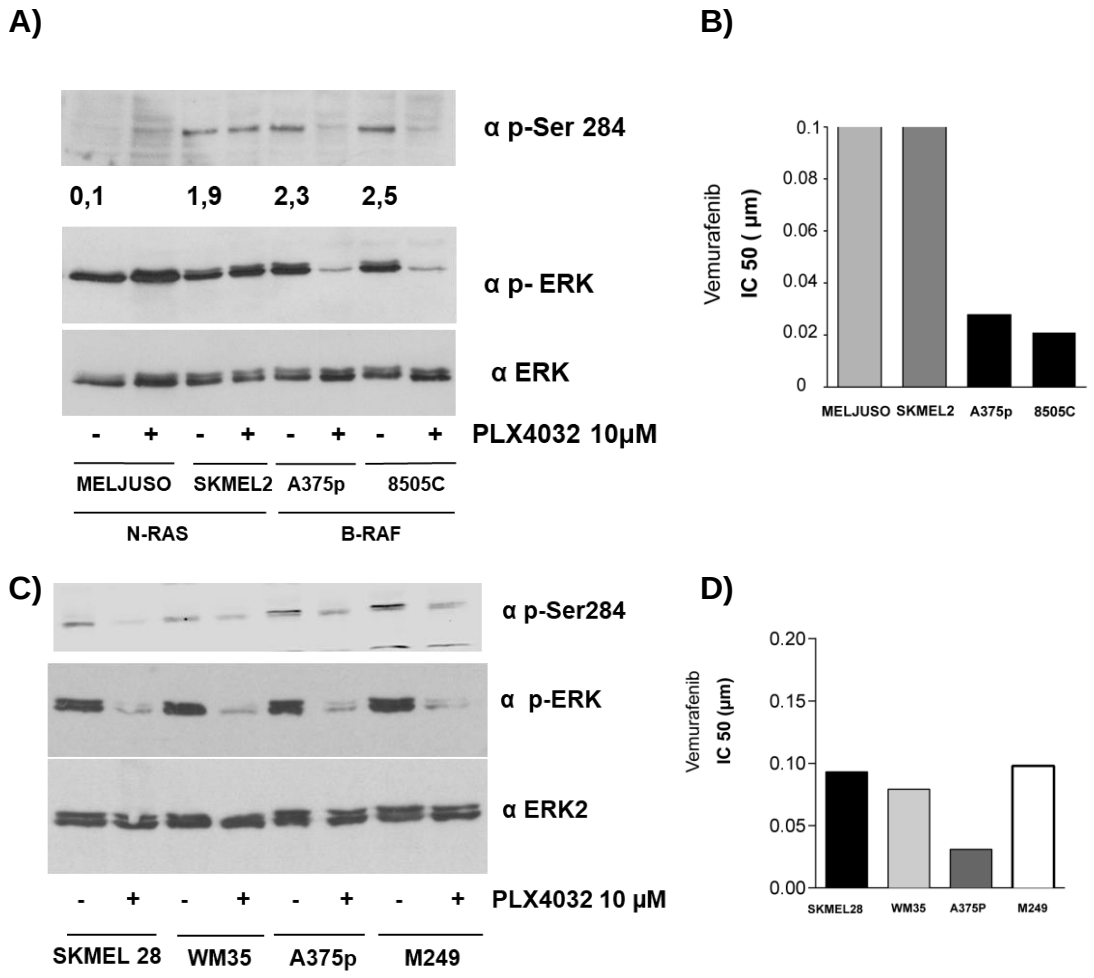

Figure 4.24. Vemurafenib response correlates with higher p-Ser284 levels in B-RAF mutant cells. A) NRAS mutant cells: MELJUSO and SKMEL2; and B-RAF mutant cells: A375p and 8505C were pre-treated (+) with PLX4032 (Vemurafenib) at 10 μM for two hours. Levels of p-Ser284 and total ERK (TEY) were analysed by immunoblotting. B) Graph showing Vemurafenib IC50 (μM) of NRAS and BRAF mutant cells. C) As in A but using a panel of melanoma cell lines harbouring BRAF mutation. D) Determination of IC50 values for Vemurafenib in the indicated melanoma cells.

High phosphorylated Ser284 levels are also present in a set of melanoma cells (Fig. 4.24 C), showing high sensitivity to PLX4032 treatment. As such, upon Vemurafenib treatment both p-Ser284 and p-TEY ERK2 levels are reduced indicating Vemurafenib efficacy, in agreement with the previous analysis.

4.3.3 Melanoma patients, harbouring B-RAF mutation, show high level of p-Ser284.

It was of interest to verify if the correlation existing between Vemurafenib response and p-Ser284 levels in cell lines, was also present in melanoma tumour samples. For this purpose, we analysed phosphorylated Ser284 in melanoma clinical samples by immunohistochemistry (Fig 4.25). We have a collection of over 50 melanoma samples, genotyped for N-RAS and B-RAF mutations, connected to fully documentated clinical records. Comparing B-RAF-mutant with B-RAF WT samples, it emerged that the antibody p-Ser284 is specifically detecting phospho-Ser284 only in the case of B-RAF mutant samples. Moreover, in agreement with our previous results, Ser284 phosphorylation is restricted exclusively to the cytoplasm. However, we need to increase the number of samples analysed in order to determine if indeed there is a correlation between p-Ser levels and tumour sensitivity to Vemurafenib. If this is so, our antibody could represent a useful clinical tool for discriminating among those melanoma patients that will respond or not to the B-RAF inhibitor treatment.

Clearly, there is a need to develop and integrate predictive biomarkers for therapeutic decision making in early stage melanoma. The ability to precisely assess and target risk treatment resistant and recurrence are at the core of precision medicine and is critical to take full advantage of the evolving tools to treat malignant cutaneous melanoma.

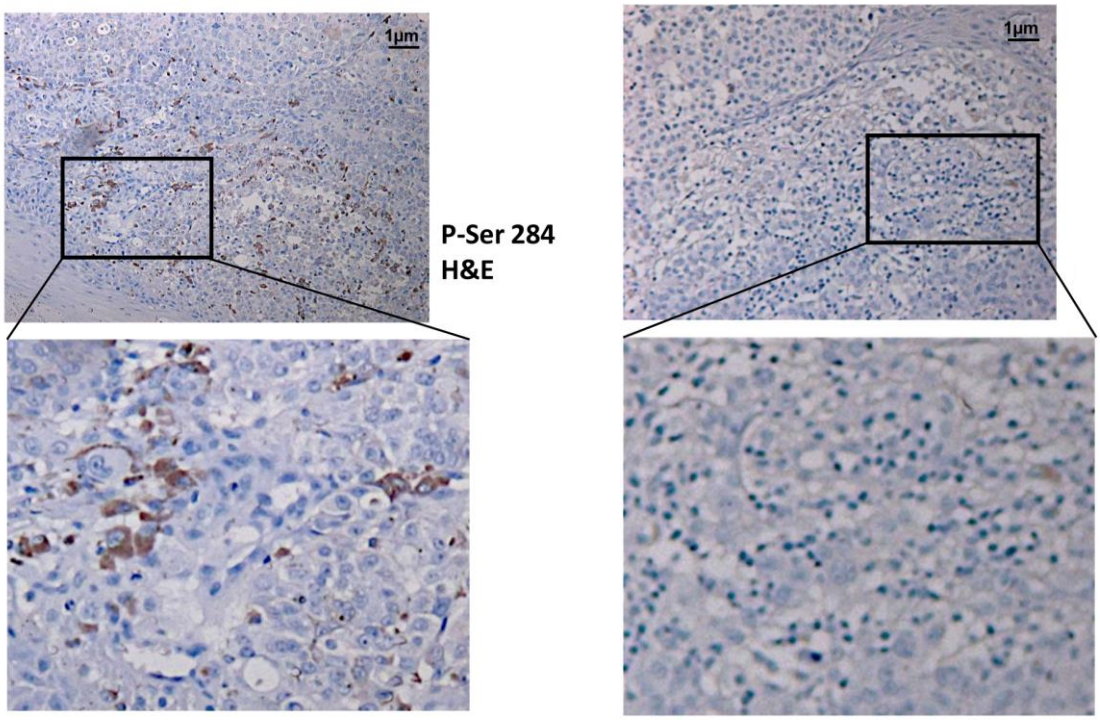

Figure 4.25. Phospho-Serine284 analysis in melanoma patients samples by Immunohistochemistry. Melanoma tumours were stained with polyclonal anti-rabbit p-Ser284 antibody (brown staining) and tissues were counterstained with hematoxylin. A) A representative sample of a BRAF mutation positive (+) melanoma showed high Ser284 phosphorylation levels at the cytoplasm. B) BRAF wild type melanoma shows low levels of phosphorylated Ser284. Control (-): consecutive sections with the omitted primary antibody were used as negative control (data not shown). Bar scale represents 1µm.

5. DISCUSSION

During the course of our experiments leading to the discovery of DEL-22379, we made the startling observation that ERK dimers were absent in fish, birds or amphibians, ERK dimerization being restricted to mammalians. Our results indicated that the capacity for dimerization resided on the ERK protein, not in the cellular context (Herrero et al., 2015). A comparison of the ERK2 sequence across the evolutionary scale unveiled that serine 284 (human) was conserved in those species in which ERK2 dimerized, mammalians in all cases. Interestingly, the corresponding residue in those species in which ERK2 did not dimerize – birds, reptiles, amphibians and insects- was either a proline or an alanine. This pattern is also evident in the case of ERK1. This unprecedented finding suggests that dimerization is a feature that ERK has attained with the advent of mammalians and that further down the evolutionary scale ERK is impaired for dimerization. Apparently at odds with our findings, Philipova and Whitaker have shown that sea urchin ERK can dimerize (Philipova and Whitaker, 2005). However, it must be noticed that this species has an ancestral form of ERK, that it is quite different from either ERK1 and 2 sequencewise. Particularly, the region around position 284 is not completely conserved, as well as the other regions involved in ERK dimerization, like the PDHD motif and the L16 helix (Buscà et al., 2016; Robinson et al., 1998). Thus, it is possible that ancestral ERK could dimerize by some distinct mechanism, and for some unknown reason, this dimerization ability was lost at subsequent evolutionary stages, to be later re-acquired in evolved species, such as in mammalians.

At this moment, we do not know the evolutive function associated to ERK dimerization. To gain an insight into this point, we have generated a loss-of-function mouse model, in which the replacement of ERK2 Ser284 by a proline prevents its dimerization. In the same direction, we are in the process of generating a gain-of-function zebrafish model, where the reciprocal substitution renders ERK2 dimerization-competent. In the case of the mouse model, our preliminary results show that, in presence of ERK1, the absence of ERK2 dimerization does not compromise normal development up to adulthood. However, a conclusion beyond doubt will only be reached when ERK2 dimerization-deficiency is tested in ERK1 -/- background. Since, it has been recently discovered that ERK1 overexpression can restore the viability of mice

deficient for ERK2 (Frémin et al., 2015). Thus, the possibility exists that an upregulation on the levels of ERK1 dimers could compensate the absence of ERK2 dimers.

Even though we don't know exactly which functions derive from the acquisition of ERK dimerization, it is logical to speculate that its spread and conservation in mammalians must have endowed this clade with some evolutionary advantage. In this respect, we are confident that our gain-of-function zebrafish model may provide us with valuable clues about this fascinating conundrum.

As we have previously demonstrated, in mammalian cells scaffold proteins serve as ERK dimerization platforms (Casar et al., 2008; Casar and Crespo, 2016). Since scaffold proteins are present throughout the evolutionary scale (Chol et al., 1994; Therrien et al., 1996; Tsang et al., 2002), it is conceivable that they originated to serve other of their various roles as regulators of RAS-ERK pathway signal flux. And that their participation in ERK dimerization is a late acquisition. In this respect, we have demonstrated that, in mammalian cells, scaffold proteins and ERK dimers are essential for the activation of cytoplasmic substrates (Casar et al., 2008; Casar and Crespo, 2016). Since in lower organisms ERK also has cytoplasmic substrates, it follows that these must be activated by monomeric ERK. In this regard, it would be interesting to understand which advantages derive from ERK dimerization in the activation of cytoplasmic substrates and its impact on mammalian evolution. Once again, our zebrafish model, could give us important clues in this respect.

Furthermore, these animal model will also represent useful models to carry out experiment to address ERK dimerization role in carcinogenesis. Our previous results indicate that ERK dimerization inhibitors exert antineoplastic effects with mild toxicity (Herrero et al., 2015), the ultimate proof for the safety of this strategy will be if ERK "dimerization-deficient" mice display no overt phenotype, which hitherto seems to be the case. Moreover, we plan to analyze the extent to which the absence of ERK dimerization prevents or attenuates carcinogenesis, by testing the response of ERK2 dimerization-deficient mice to chemical carcinogenesis protocols, namely: TPA/DMBA-induced skin cancer; urethane-induced lung cancer; and the azoxymethane/DSS colorectal carcinogenesis

model. In addition, we will also test if the absence of ERK2 dimerization can forestall the progression of tumors such as pancreatic ductal adenorcarcinoma, unreachable to most drugs due to its high fibrosis. In order to do this, we shall cross the ERK2 dimerization-deficient mice with ElasKRASV12 mice, from Dr. Barbacid's lab, in which the KRASV12 oncogene is effectively and selectively expressed in pancreatic acinar cells (Navas et al., 2012).

Similarly, if viable, we will use the ERK2 "dimerization-competent" zebrafish to test if ERK dimerization can bolster tumourigenesis. In order to do this, we will use the melanoma zebrafish models successfully utilized in our last publication (Casar et al., 2018). As such, we will test if ERK dimerization can enhance melanoma formation in transgenic "dimerization-competent" fish, expressing low penetrance BRAF oncogenic mutants, for example BRAF G466A, specifically expressed in melanocytes via the MITF promoter (Michailidou et al., 2009).

In our study we have identified Ser284 as a residue whose phosphorylation is necessary but not sufficient for ERK dimerization. As Cobb's previous studies revealed, phosphorylation at the canonical sites (TEY) is an essential requirement for ERK dimerization (Canagarajah et al., 1997; Khokhlatchev et al., 1998). In this line, we have found that phosphorylation of the canonical residues (TEY), Ser284 phosphorylation and dimerization, occur rapidly and almost simultaneously. If any differences exist, they fall beyond our range of detection. We also have found that the S284P substitution does not alter ERK phosphorylation rate. However, we speculate with the possibility that this mutation could affect the kinetics of ERK activation, changing it from a "quasi-processive" to a distributive process. The kinetics of ERK activation has been a topic that has generated a long-time controversy. However, it seems to be now well-accepted that in lower species, like in xenopus, ERK activation occurs in a distributive, switch-like, manner (Burack and Sturgill, 1997). Contrarily, in mammalian, this process follows a graded-response, or "quasi-processive" process (Aoki et al., 2011). Thus, considering that xenopus contains a proline at the equivalent position of hSer284, it is conceivable that hERK2 S284P substitution could revert the process from "quasi-processive" to distributive. In support of our hypothesis, it is known that the disruption of the regulatory

negative feedback loops reverts ERK activation from graded to switch-like manner (Lake et al., 2016; Sturm et al., 2010). Thus, it is conceivable that the S>P substitution could emulate these phenomena. Further studies and mathematical analyses and modelling would be essential to clarify this point.

We have identified the kinases responsible for phosphorylating ERK2 at Ser284. In our *in vitro* validation analyses, we have demonstrated that both MEK1 and AKT1 are able to directly phosphorylate ERK2 at Ser284. In addition to the aforementioned kinases, and to a lesser extent, other kinases such as DAPK1 and MLK1 have also been identified. We have not tested if these kinases can phosphorylate ERK at Ser284 in vitro, something that should be done as they have been described to be involved in the regulation of ERK biological outputs. This is the case of DAPK1, which has been shown to phosphorylate ERK, thereby fostering its retention at the cytoplasm, in full agreement with our results, and as a consequence, promoting apoptosis (Chen et al., 2005).

Hitherto, it was known that MEK is a dual-specificity protein kinase that phosphorylates tyrosine and then threonine in ERK1/2 canonical TEY site, being its only physiological substrate (Aoki et al., 2011; Roskoski, 2012). In our study, we have identified Ser284 as a new MEK phosphorylation site. From the structural aspect, S284 lays far away from the activation loop, where the TEY motif is found. In this respect it will be interesting to study the sequence of events that govern ERK full phosphorylation by MEK, since, as previously mentioned TEY and S284 phosphorylation occur almost simultaneously. Something that could implicate more than one MEK molecule.

Similarly, AKT is a Ser/Thr kinase that recognizes a minimal consensus motif of R-x-R-x-x-S/T-f (where x is any amino acid and f denotes a preference for large hydrophobic residues) (Manning and Toker, 2017). In ERK1/2 the sequence surrounding Ser284 ERK residue does not correspond with AKT1 canonical consensus sequence. Nevertheless, our in vitro kinase assays and cellular assays, using constitutively active AKT; down-regulating its expression and inhibiting its activity, are quite compelling in showing that, indeed, ERK Ser284 is an AKT substrate, unveiling a novel “unorthodox” phosphorylation site.

Furthermore, we have disclosed that both ERK2 oligomers need to be Ser284 phosphorylated in order to dimerize. Therefore, in light of the information available at the moment, and considering that both AKT1 and MEK1 can phosphorylate this site, we posit the following model for ERK dimerization following Ser284 phosphorylation: In response to agonist stimulation, MEK bound to the scaffold complex would phosphorylate ERK therein, both at the canonical TEY site and at Ser284. The other "free" ERK oligomer, bound to MEK previous stimulation, would be phosphorylated by MEK in the TEY motif, and after its release from MEK, it will be phosphorylated by AKT1 on Ser284, forming a dimer with the scaffold-bound phosphorylated ERK oligomer(Fig. 5.1).

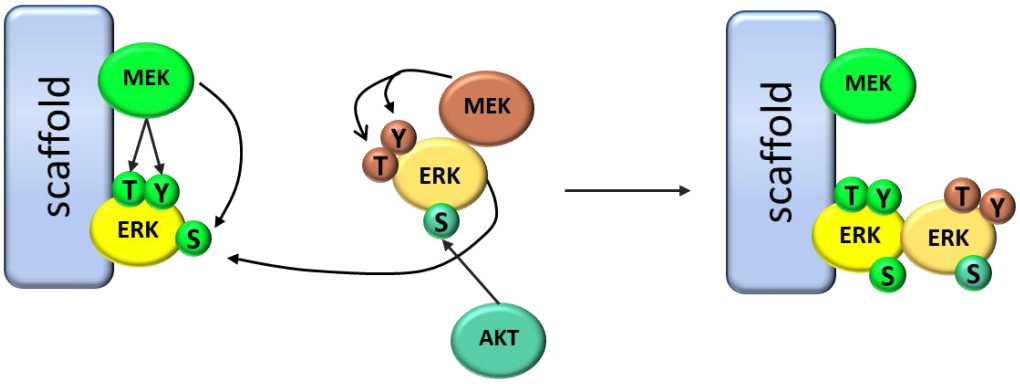

Figure 5.1. Model of ERK2 phosphorylation and dimerization mediated by MEK1 and AKT1. ERK2 would be firstly phosphorylated at TEY and Ser284 by MEK, both bound to a scaffold. The other "free" ERK2 oligomer would be phosphorylated by AKT1 on Ser284 allowing ERK2 dimerization.

Thus, the priming ERK Ser284 intra-scaffold phosphorylation would be MEK-mediated whereas the latter free ERK Ser284 phosphorylation would be mediated by AKT. To corroborate this model, we have generated a constitutively-active MEK mutant, defective for binding to the scaffold KSR1 (MEK1 F311S EE) (Lavoie et al., 2018), that will help us to elucidate the sequence of phosphorylation events leading to ERK dimerization.

With respect to ERK subcellular distribution, our fractionation and immunofluorescence assays demonstrate that ERK phosphorylated at Ser284 is localized exclusively at the cytoplasm. This is in full agreement with our findings showing that Ser284 is only phosphorylated when ERK is in its dimeric

state and that this phosphorylation enhances ERK affinity for scaffold proteins such as KSR. Conversely, when Ser284 phosphorylation is prevented, ERK interaction with the nuclear shuttle importin-7 is bolstered. Thus, Ser284 phosphorylation appears to play an important role as a mediator of ERK nucleus/cytoplasmic distribution. In support of this notion, the structure of ERK2 shows that Ser284 lays in the same plane as the S-P-S motif, whose phosphorylation facilitates ERK2 interaction with importin-7 (Chuderland et al., 2008; Flores et al., 2019). In light of this data, we propose that S-P-S phosphorylation would constitute an attractive signal for interacting with importin-7. Contrarily, Ser284 phosphorylation would generate a repulsive, and prevailing, effect on the interaction with importin7, thereby impeding ERK nuclear translocation. And, by increasing ERK concentration at the cytoplasm, bolstering the formation of ERK dimers in the scaffolded complexes (Fig. 5.2).

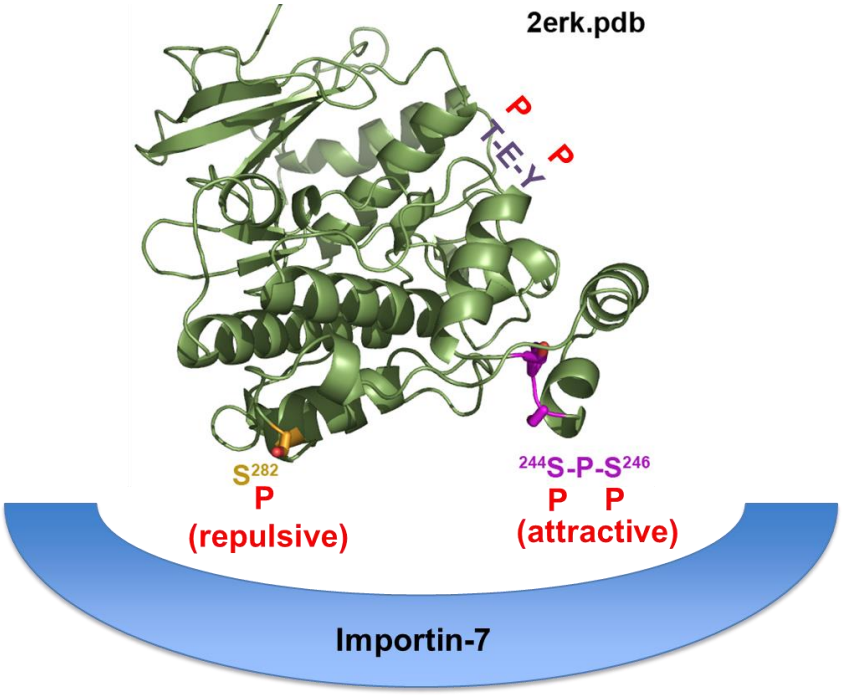

Fig. 5.2. Model of ERK2-Importin7 interaction. ERK2 model retrived by protein data bank (PDB: 2ERK2), in which is represented the TEY motif in blue; the SPS motif in purple; the Ser282 in yellow (rat numeration). The phosphorylation of Ser282 would be a repulsive force for Importin7 binding.

Noticeably, while the prevention of Ser284 phosphorylation by introducing a proline, enhances ERK nuclear levels under basal conditions, the status of Ser284 phosphorylation does not appear to affect the rate of ERK nuclear import in response to an acute stimulus. This could suggest that IMP7 would be

the shuttle determining basal ERK nuclear levels and that other IMP7-independent translocation mechanisms would prevail in ERK translocation to the nucleus under acute stimulation.

As mentioned, we didn't observe any differences in the kinetics of ERK entrance to the nucleus for the different mutants analyzed. However, in this experiment we didn't take into consideration the contribution of AKT. Being AKT capable of phosphorylating Ser284, there is the possibility that if depending on the cellular context, the basal AKT activity level is different, this would impact on the basal ERK WT Ser284 phosphorylation levels and therefore on its nuclear translocation, in comparison to the S>P and S>E mutants. To address this question, it would be necessary to test the nuclear translocation of the different ERK mutants in a cellular contest both with high and low AKT activity, in order to determine if indeed AKT is playing a determinant role in this process. Similarly, blocking AKT activation, using the AKT inhibitor MK2206, will help to definitively unravel this open question.

Regarding the dependence of mammalian cellular viability on Ser284 phosphorylation, we have analyzed how the elimination of ERK2 dimerization affects cellular proliferation. The results obtained so far, indicate that making Ser284 unphosphorylatable reduces cell viability in MEFs. However, we have found that the expression of the ERK mutant S284P is significantly lower compared to the WT ERK. The lower expression could indicate the inability of this mutant to support cell growth as a consequence of the loss of its dimerization capacity.

Additionally, in order to fully understand the role played by ERK dimerization on ERK signaling and its biological outputs, a mutant capable of being constantly in a dimerized state would be an invaluable tool. It is well known that introducing phospho-mimetic substitutions in the TEY motif does not result in ERK constitutive activity, probably due to an incorrect unfolding of the activation loop (Canagarajah et al., 1997). However, "intrinsically active" ERK1 R84S and ERK2 R65S mutants that exhibit constitutive kinase activity due to autophosphorylation of its TEY motif have been recently described. Particularly, ERK1 R84S showed all of the characteristics of a classic oncogene, which

would be the first activating mutant discovered in ERK (Atias et al., 2020; Smorodinsky-Atias et al., 2016). Thus, it would be interesting to check if by introducing on ERK2 R65S the S284D/E mutation we will obtain a constitutively dimerized form.

Finally, in light of the unquestionable localization of the phosphorylation Ser284 at the cytoplasm we have elucidate that the phosphorylation of this residue could be used as a marker of sensitivity to Vemurafenib treatment in melanoma cells. This observation arose from several study pointing that asymmetric ERKs nucleo/cytoplasmic distribution is observed in some types of tumors, sometimes associated to distinct tumoral features and/or clinical parameters. For instance, ERK nuclear but not cytoplasmic activity is associated to proliferation and transformation in fibroblasts (Robinson et al., 1998), and renal tumors exhibit ERK activity predominantly at the nucleus (Casar et al., 2007). On the other hand, ERK cytoplasmic signals are associated with anti-apoptotic signaling in myeloid leukemia (Ajenjo et al., 2004). In support of this point, interfering with cytoplasmic ERK signaling, like inhibiting ERK dimerization, evokes potent antitumoral effects (Herrero et al., 2015). Likewise, blocking ERK nuclear entrance also have similar effect (Plotnikov et al., 2015). Most importantly, ERK cytoplasmic levels correlate with a better prognostic in invasive breast carcinoma (Nakopoulou et al., 2005) and in SCLC (Blackhall et al., 2003); and are associated with high sensitivity to BRAF inhibitors in BRAF-mutant melanoma (Bollag et al., 2010). Overall, we found that Ser284 phosphorylation does correlate with sensitivity to Vemurafenib treatment in melanoma BRAF-mutant cells. In fact, those cells lines harbouring BRAF mutations, which showed higher levels of p-Ser284, were those that better respond to Vemurafenib treatment. By contrast, in Vemurafenib resistant melanoma cells we have also observed a reduction of AKT phosphorylation, that would explain the lower levels of p-Ser284. Although very often AKT activation is associated to an adaptive mechanism derived from BRAF inhibition that leads to a paradoxical activation of IGF-PI3K pathway (Burotto et al., 2014; Villanueva et al., 2010), AKT plays an important role in the regulation of ERK cytoplasmic signals. As mentioned in the introduction, RAS-ERK and PI3K-AKT pathways are intimately interconnected. in this regard, AKT-mediated PEA15

phosphorylation reduces ERK nuclear activity via the retention of ERK at the cytoplasm, preventing proliferation (Gervais et al., 2006; Von Kriegsheim et al., 2009). Thus, all of these studies are in full agreement with our findings pointing to AKT1 as one of the kinase responsible for phosphorylating Ser284, it is possible that its contribution to retaining ERK at the cytoplasm occurs through different mechanisms.

In addition, we have also tested our S284 phosphospecific antibody in melanoma clinical samples and we have found that, indeed, those samples from BRAF positive melanoma patients exhibited a marked staining in the cytoplasm. This opens the possibility to use our antibody as a detection tool, in order to stratify patients that will respond to Vemurafenib treatment, from those that will likely be non-respondents. However, at this point our studies are at a preliminary stage. To address this question, we have a collection of more than 50 clinical samples, fully connected with the clinical history. If successful, ERK p-ser284 levels could turn out to be useful tool to spare patients from unnecessary secondary effects resulting from useless BRAF inhibitors treatment, and also sparing health system from a pointless economic burden. Moreover, our antibodies could be also utilized in liquid biopsies in order to detect Ser284 phosphorylation in circulant cells.

Finally, since ERK p-ser284 levels could serve as a prognostic marker of sensitivity to Vemurafenib, contrarily the levels of the phosphatase responsible of dephosphorylating such residue could turn out to be a marker of resistance to BRAF-inhibitors treatments. Thus, it would be interesting to identify the phosphatases responsible for inactivating Ser284 in order to check its impacts on the response to vemurafenib in melanoma cell lines.

6. CONCLUSIONS

1. Ser284 phosphorylation is necessary but not sufficient for ERK2 dimerization
2. Phosphorylation at Ser284 in both ERK2 molecules is required for dimerization
3. AKT1 and MEK1 are the main kinases responsible for the phosphorylation of ERK2 at Ser284
4. ERK2 phosphorylated at Ser284 is localized exclusively at the cytoplasm
5. Ser284 phosphorylation enhances ERK2 affinity for scaffold proteins like KSR1. Contrarily, it diminishes ERK2 affinity for nuclear shuttles like importin 7.
6. The sensitivity of BRAF-mutant melanoma cells to vemurafenib treatment correlates with higher levels of p-Ser284. Thus, p-Ser284 levels could be used as a predictive biomarker for the response to Vemurafenib in BRAF positive melanoma patients

7. BIBLIOGRAPHY

Adachi M, Fukuda M, Nishida E. 2000. Nuclear export of MAP kinase (ERK) involves a MAP kinase kinase (MEK)-dependent active transport mechanism. *J Cell Biol* **148**:849–856. doi:10.1083/jcb.148.5.849

Adachi M, Fukuda M, Nishida E. 1999. Two co-existing mechanisms for nuclear import of MAP kinase: Passive diffusion of a monomer and active transport of a dimer. *EMBO J* **18**:5347–5358. doi:10.1093/emboj/18.19.5347

Ahmad MK, Abdollah NA, Shafie NH, Yusof NM, Razak SRA. 2018. Dual-specificity phosphatase 6 (DUSP6): a review of its molecular characteristics and clinical relevance in cancer. *Cancer Biol Med* **15**:14–28. doi:10.20892/j.issn.2095-3941.2017.0107

Ajenjo N, Canoñón E, Sánchez-Pérez I, Matallanas D, León J, Perona R, Crespo P. 2004. Subcellular localization determines the protective effects of activated ERK2 against distinct apoptogenic stimuli in myeloid leukemia cells. *J Biol Chem* **279**:32813–32823. doi:10.1074/jbc.M313656200

Alessi DR, Gomez N, Moorhead G, Lewis T, Keyse SM, Cohen P. 1995. Inactivation of p42 MAP kinase by protein phosphatase 2A and a protein tyrosine phosphatase, but not CL100, in various cell lines. *Curr Biol* **5**:283–95. doi:10.1016/s0960-9822(95)00059-5

Alessi DR, Saito Y, Campbell DG, Cohen P, Sithanandam G, Rapp U, Ashworth A, Marshall CJ, Cowley S. 1994. Identification of the sites in MAP kinase kinase-1 phosphorylated by p74raf-1. *EMBO J* **13**:1610–1619. doi:10.1002/j.1460-2075.1994.tb06424.x

Alexa A, Gógl G, Glatz G, Garai Á, Zeke A, Varga J, Dudás E, Jeszenoi N, Bodor A, Hetényi C, Reményi A. 2015. Structural assembly of the signaling competent ERK2-RSK1 heterodimeric protein kinase complex. *Proc Natl Acad Sci U S A* **112**:2711–2716. doi:10.1073/pnas.1417571112

Anastas JN, Kulikauskas RM, Tamir T, Rizos H, Long G V., Von Euw EM, Yang PT, Chen HW, Haydu L, Toroni RA, Lucero OM, Chien AJ, Moon RT. 2014. WNT5A enhances resistance of melanoma cells to targeted BRAF inhibitors. *J Clin Invest* **124**:2877–2890. doi:10.1172/JCI70156

Anderson NG, Maller JL, Tonks NK, Sturgill TW. 1990. Requirement for integration of signals from two distinct phosphorylation pathways for activation of MAP kinase. *Nature* **343**:651–653. doi:10.1038/343651a0

Aoki K, Yamada M, Kunida K, Yasuda S, Matsuda M. 2011. Processive phosphorylation of ERK MAP kinase in mammalian cells. *Proc Natl Acad Sci U S A* **108**:12675–12680. doi:10.1073/pnas.1104030108

Asem MS, Buechler S, Wates RB, Miller DL, Stack MS. 2016. Wnt5a signaling in cancer. *Cancers (Basel)* **8**. doi:10.3390/cancers8090079

Askari N, Diskin R, Avitzour M, Yaakov G, Livnah O, Engelberg D. 2006. MAP-quest: Could we produce constitutively active variants of MAP kinases? *Mol Cell Endocrinol* **252**:231–240. doi:10.1016/j.mce.2006.03.015

Atias KS, Soudah N, Engelberg D. 2020. Mutations That Confer Drug - Resistance , Oncogenicity and Intrinsic Activity on the ERK MAP Kinases — Current State of the Art 1–33. doi:10.3390/cells9010129

Baljuls A, Schmitz W, Mueller T, Zahedi RP, Sickmann A, Hekman M, Rapp UR. 2008. Positive regulation of A-RAF by phosphorylation of isoform-specific hinge segment and identification of novel phosphorylation sites. *J Biol Chem* **283**:27239–27254. doi:10.1074/jbc.M801782200

Banerjee A, Gugasyan R, McMahon M, Gerondakis S. 2006. Diverse Toll-like receptors utilize Tpl2 to activate extracellular signal-regulated kinase (ERK) in hemopoietic cells. *Proc Natl Acad Sci U S A* **103**:3274–3279. doi:10.1073/pnas.0511113103

Bardwell AJ, Abdollahi M, Bardwell L. 2003. Docking sites on mitogen-activated protein kinase (MAPK) kinases, MAPK phosphatases and the Elk-1 transcription factor compete for MAPK binding and are crucial for enzymic activity. *Biochem J* **370**:1077–1085. doi:10.1042/BJ20021806

Blackhall FH, Pintilie M, Michael M, Cell S, Cancer L, Leighl N, Feld R, Tsao M, Shepherd FA. 2003. Expression and Prognostic Significance of Kit , Protein Kinase B , and Mitogen-activated Protein Kinase in Patients with Small Cell lung cancer **9**:2241–2247.

Blasco RB, Francoz S, Santamaría D, Cañamero M, Dubus P, Charron J, Baccarini M, Barbacid M. 2011. C-Raf, but Not B-Raf, Is Essential for Development of K-Ras Oncogene-Driven Non-Small Cell Lung Carcinoma. *Cancer Cell* **19**:652–663. doi:10.1016/j.ccr.2011.04.002

Bollag G, Hirth P, Tsai J, Zhang J, N. P, Ibrahim HC, Al. E. 2010. Clinical efficacy of a RAF inhibitor needs broad target blockade in BRAF-mutant melanoma. *Nature* **467**:596–599. doi:10.1038/nature09454.Clinical

Bondeva T, Balla A, Varnai P, Balla T. 2002. Structural Determinants of Ras-Raf Interaction Analyzed in Live Cells. *Mol Biol Cell* **13**:2323–2333. doi:www.molbi-olcell.org/cgi/doi/10.1091/mbc.E02–01–0019

Boulton TG, Nye SH, Robbins DJ, Ip NY, Radzlejewska E, Morgenbesser SD, DePinho RA, Panayotatos N, Cobb MH, Yancopoulos GD. 1991. ERKs: A family of protein-serine/threonine kinases that are activated and tyrosine phosphorylated in response to insulin and NGF. *Cell* **65**:663–675. doi:10.1016/0092-8674(91)90098-J

Boulton TG, Yancopoulos GD, Gregory JS, Slaughter C, Moomaw C, Hsu J, Cobb MH. 1990. An insulin-stimulated protein kinase similar to yeast kinases involved in cell cycle control. *Science (80-)* **249**:64–67. doi:10.1126/science.2164259

Brenan L, Andreev A, Cohen O, Pantel S, Kamburov A, Cacchiarelli D, Persky NS, Zhu C, Bagul M, Goetz EM, Burgin AB, Garraway LA, Getz G, Mikkelsen TS, Piccioni F, Root DE, Johannessen CM. 2016. Phenotypic Characterization of a Comprehensive Set of MAPK1/ERK2 Missense Mutants. *Cell Rep* **17**:1171–1183. doi:10.1016/j.celrep.2016.09.061

Brunner D, Oellers N, Szabad J, Biggs WH, Zipursky SL, Hafen E. 1994. A gain-of-function mutation in Drosophila MAP kinase activates multiple receptor tyrosine kinase signaling pathways. *Cell* **76**:875–888. doi:10.1016/0092-8674(94)90362-X

Burack WR, Sturgill TW. 1997. The activating dual phosphorylation of MAPK by MEK is nonprocessive. *Biochemistry* **36**:5929–5933. doi:10.1021/bi970535d

Buscà R, Christen R, Lovern M, Clifford AM, Yue JX, Goss GG, Pouysségur J, Lenormand P. 2015. ERK1 and ERK2 present functional redundancy in tetrapods despite higher evolution rate of ERK1. *BMC Evol Biol* **15**:1–15. doi:10.1186/s12862-015-0450-x

Buscà R, Pouysségur J, Lenormand P. 2016. ERK1 and ERK2 map kinases: Specific roles or functional redundancy? *Front Cell Dev Biol* **4**:1–23. doi:10.3389/fcell.2016.00053

Canagarajah BJ, Khokhlatchev A, Cobb MH, Goldsmith EJ. 1997. Activation mechanism of the MAP kinase ERK2 by dual phosphorylation. *Cell* **90**:859–869. doi:10.1016/S0092-8674(00)80351-7

Cao Z, Liao Q, Su M, Huang K, Jin J, Cao D. 2019. AKT and ERK dual inhibitors: The way forward? *Cancer Lett* **459**:30–40. doi:10.1016/j.canlet.2019.05.025

Cargnello M, Roux PP. 2011. Activation and Function of the MAPKs and Their Substrates, the MAPK-Activated Protein Kinases. *Microbiol Mol Biol Rev* **75**:50–83. doi:10.1128/mmbr.00031-10

Casar B, Arozarena I, Sanz-Moreno V, Pinto A, Agudo-Ibanez L, Marais R, Lewis RE, Berciano MT, Crespo P. 2009. Ras Subcellular Localization Defines Extracellular Signal-Regulated Kinase 1 and 2 Substrate Specificity through Distinct Utilization of Scaffold Proteins. *Mol Cell Biol* **29**:1338–1353. doi:10.1128/mcb.01359-08

Casar B, Badrock AP, Jiménez I, Arozarena I, Colón-Bolea P, Lorenzo-Martín LF, Barinaga-Rementería I, Barriuso J, Cappitelli V, Donoghue DJ, Bustelo XR, Hurlstone A, Crespo P. 2018. RAS at the Golgi antagonizes malignant transformation through PTPRκ-mediated inhibition of ERK activation. *Nat Commun* **9**:3595. doi:10.1038/s41467-018-05941-8

Casar B, Crespo P. 2016. ERK Signals: Scaffolding scaffolds? *Front Cell Dev Biol* **4**:1–11. doi:10.3389/fcell.2016.00049

Casar B, Pinto A, Crespo P. 2008. Essential Role of ERK Dimers in the Activation of Cytoplasmic but Not Nuclear Substrates by ERK-Scaffold Complexes. *Mol Cell* **31**:708–721. doi:10.1016/j.molcel.2008.07.024

Casar B, Sanz-Moreno V, Yazicioglu MN, Rodríguez J, Berciano MT, Lafarga M, Cobb MH, Crespo P. 2007. Mxi2 promotes stimulus-independent ERK nuclear translocation. *EMBO J* **26**:635–646. doi:10.1038/sj.emboj.7601523

Catalanotti F, Reyes G, Jesenberger V, Galabova-Kovacs G, De Matos Simoes R, Carugo O, Baccarini M. 2009. A Mek1-Mek2 heterodimer determines the strength and duration of the Erk signal. *Nat Struct Mol Biol* **16**:294–303. doi:10.1038/nsmb.1564

Caunt CJ, Keyse SM. 2013. Dual-specificity MAP kinase phosphatases (MKPs): Shaping the outcome of MAP kinase signalling. *FEBS J* **280**:489–504. doi:10.1111/j.1742-4658.2012.08716.x

Chen CH, Wang WJ, Kuo JC, Tsai HC, Lin JR, Chang ZF, Chen RH. 2005. Bidirectional signals transduced by DAPK-ERK interaction promote the apoptotic effect of DAPK. *EMBO J* **24**:294–304. doi:10.1038/sj.emboj.7600510

Chen M, Wan L, Zhang Jiangwen, Zhang Jinfang, Mendez L, Clohessy JG, Berry K, Victor J, Yin Q, Zhu Y, Wei W, Pandolfi PP. 2018. Deregulated PP1α phosphatase activity towards MAPK activation is antagonized by a tumor suppressive failsafe mechanism. *Nat Commun* **9**. doi:10.1038/s41467-017-02272-y

Choi S, Hedman AC, Sayedyahossein, Samar Thapa N, Sacks DB, Anderson RA. 2016. Agonist-stimulated phosphatidylinositol-3,4,5-trisphosphate generation by scaffolded phosphoinositide kinases. *Nat Cell Biol* **18**:1324–1335. doi:10.1016/j.physbeh.2017.03.040

Chol KY, Satterberg B, Lyons DM, Elion EA. 1994. Ste5 tethers multiple protein kinases in the MAP kinase cascade required for mating in S. cerevisiae. *Cell* **78**:499–512. doi:10.1016/0092-8674(94)90427-8

Chong H, Lee J, Guan KL. 2001. Positive and negative regulation of Raf kinase activity and function by phosphorylation. *EMBO J* **20**:3716–3727. doi:10.1093/emboj/20.14.3716

Chuderland D, Konson A, Seger R. 2008. Identification and Characterization of a General

Nuclear Translocation Signal in Signaling Proteins. *Mol Cell* **31**:850–861. doi:10.1016/j.molcel.2008.08.007

Chuderland D, Seger R. 2005. Protein-protein interactions in the regulation of the extracellular signal-regulated kinase. *Mol Biotechnol* **29**:57–74. doi:10.1385/MB:29:1:57

Costa M, Marchi M, Cardarelli F, Roy A, Beltram F, Maffei L, Ratto GM. 2006. Dynamic regulation of ERK2 nuclear translocation and mobility in living cells. *J Cell Sci* **119**:4952–4963. doi:10.1242/jcs.03272

Cowley S, Paterson H, Kemp P, Marshall CJ. 1994. Activation of MAP kinase kinase is necessary and sufficient for PC12 differentiation and for transformation of NIH 3T3 cells. *Cell* **77**:841–852. doi:10.1016/0092-8674(94)90133-3

Cox J, Mann M. 2008. MaxQuant enables high peptide identification rates, individualized p.p.b.-range mass accuracies and proteome-wide protein quantification. *Nat Biotechnol* **26**:1367–1372. doi:10.1038/nbt.1511

Crews CM, Alessandrini A, Erikson RL. 1992. The primary structure of MEK, a protein kinase that phosphorylates the ERK gene product. *Science (80-)* **258**:478–480. doi:10.1126/science.1411546

Dang A, Frost JA, Cobb MH. 1998. The MEK1 proline-rich insert is required for efficient activation of the mitogen-activated protein kinases ERK1 and ERK2 in mammalian cells. *J Biol Chem* **273**:19909–19913. doi:10.1074/jbc.273.31.19909

Davis RJ. 1994. MAPKs: new JNK expands the group. *Trends Biochem Sci* **19**:470–473. doi:10.1016/0968-0004(94)90132-5

De Araújo MEG, Stasyk T, Taub N, Ebner HL, Fürst B, Filipek P, Weys SR, Hess MW, Lindner H, Kremser L, Huber LA. 2013. Stability of the endosomal scaffold protein lAMTOR3 depends on heterodimer assembly and proteasomal degradation. *J Biol Chem* **288**:18228–18242. doi:10.1074/jbc.M112.349480

Deakin NO, Pignatelli J, Turner CE. 2012. Diverse Roles for the Paxillin Family of Proteins in Cancer. *Genes and Cancer* **3**:362–370. doi:10.1177/1947601912458582

Dhanasekaran DN, Kashef K, Lee CM, Xu H, Reddy EP. 2007. Scaffold proteins of MAP-kinase modules. *Oncogene* **26**:3185–3202. doi:10.1038/sj.onc.1210411

Dhillon AS, Pollock C, Steen H, Shaw PE, Mischak H, Kolch W. 2002. Cyclic AMP-Dependent Kinase Regulates Raf-1 Kinase Mainly by Phosphorylation of Serine 259. *Mol Cell Biol* **22**:3237–3246. doi:10.1128/mcb.22.10.3237-3246.2002

Dhillon AS, Yip YY, Grindlay GJ, Pakay JL, Dangers M, Hillmann M, Clark W, Pitt A, Mischak H, Kolch W. 2009. The C-terminus of Raf-1 acts as a 14-3-3-dependent activation switch. *Cell Signal* **21**:1645–1651. doi:10.1016/j.cellsig.2009.07.001

Douville E, Downward J. 1997. EGF induced SOS phosphorylation in PC12 cells involves P90 RSK-2. *Oncogene* **15**:373–383. doi:10.1038/sj.onc.1201214

Eblen ST. 2018. Extracellular Regulated Kinases: Signaling from Ras to ERK Substrates to Control Biological Outcomes. *Adv Cancer Res* **138**:99–142. doi:10.1016/bs.acr.2018.02.004.Extracellular

Eblen ST, Slack-Davis JK, Tarcsafalvi A, Parsons JT, Weber MJ, Catling AD. 2004. Mitogen-Activated Protein Kinase Feedback Phosphorylation Regulates MEK1 Complex Formation

and Activation during Cellular Adhesion. *Mol Cell Biol* **24**:2308–2317. doi:10.1128/mcb.24.6.2308-2317.2004

Emrick MA, Hoofnagle AN, Miller AS, Ten Eyck LF, Ahn NG. 2001. Constitutive Activation of Extracellular Signal-regulated Kinase 2 by Synergistic Point Mutations. *J Biol Chem* **276**:46469–46479. doi:10.1074/jbc.M107708200

Farooq A, Chaturvedi G, Mujtaba S, Plotnikova O, Zeng L, Dhalluin C, Ashton R, Zhou MM. 2001. Solution structure of ERK2 binding domain of MAPK phosphatase MKP-3: Structural insights into MKP-3 activation by ERK2. *Mol Cell* **7**:387–399. doi:10.1016/S1097-2765(01)00186-1

Farooq A, Zhou MM. 2004. Structure and regulation of MAPK phosphatases. *Cell Signal* **16**:769–779. doi:10.1016/j.cellsig.2003.12.008

Ferrell JE, Bhatt RR. 1997. Mechanistic studies of the dual phosphorylation of mitogen-activated protein kinase. *J Biol Chem* **272**:19008–19016. doi:10.1074/jbc.272.30.19008

Flaherty K, Puzanov I, Kim K, Ribas A, McArthur G, Sosman J, O'Dwyer P, Lee R, Grippo J, Nolop K, Chapman P. 2010. Inhibition of Mutated, Activated BRAF in Metastatic Melanoma. *NIH* **363**:809–19. doi:10.1056/NEJMoa1002011.Inhibition

Flores K, Seger R. 2013. Stimulated nuclear import by β-like importins. *F1000Prime Rep* **5**:1–7. doi:10.12703/P5-41

Flores K, Yadav SS, Katz AA, Seger R. 2019. The nuclear translocation of mitogen-activated protein kinases: Molecular mechanisms and use as novel therapeutic target. *Neuroendocrinology* **108**:121–131. doi:10.1159/000494085

Frémin C, Meloche S. 2010. From basic research to clinical development of MEK1/2 inhibitors for cancer therapy. *J Hematol Oncol* **3**:1–11. doi:10.1186/1756-8722-3-8

Frémin C, Saba-El-Leil MK, Lévesque K, Ang SL, Meloche S. 2015. Functional redundancy of ERK1 and ERK2 MAP kinases during development. *Cell Rep* **12**:913–921. doi:10.1016/j.celrep.2015.07.011

Frost JA, Steen H, Shapiro P, Lewis T, Ahn N, Shaw PE, Cobb MH. 1997. Cross-cascade activation of ERKs and ternary complex factors by Rho family proteins. *EMBO J* **16**:6426–6438. doi:10.1093/emboj/16.21.6426

Fukuda M, Asano S, Nakamura T, Adachi M, Yoshida M, Yanagida M, Nishida E. 1997a. CRM1 is responsible for intracellular transport mediated by the nuclear export signal. *Nature* **390**:308–311. doi:10.1038/36894

Fukuda M, Gotoh I, Adachi M, Gotoh Y, Nishida E. 1997b. A novel regulatory mechanism in the mitogen-activated protein (MAP) kinase cascade. Role of nuclear export signal of MAP kinase kinase. *J Biol Chem* **272**:32642–32648. doi:10.1074/jbc.272.51.32642

Fürthauer M, Lin W, Ang SL, Thisse B, Thisse C. 2002. Sef is a feedback-induced antagonist of RAs/MAPK-mediated FGF signalling. *Nat Cell Biol* **4**:170–174. doi:10.1038/ncb750

Gao Y, Chang MT, Mckay D, Na N, Zhou B, Yaeger RD, Torres NM, Muniz K, Drosten M, Barbacid M, Stuart D, Moebitz H, Solit DB, Abdel-wahab OI, Taylor BS, Yao Z, Rosen N. 2018. Allele-specific mechanisms of activation of MEK1 mutants determine their properties **8**:648–661. doi:10.1158/2159-8290.CD-17-1452.Allele-specific

Garbett D, Bretscher A. 2014. The surprising dynamics of scaffolding proteins. *Mol Biol Cell*

25:2315–2319. doi:10.1091/mbc.E14-04-0878

García-Gómez R, Bustelo XR, Crespo P. 2018. Protein–Protein Interactions: Emerging Oncotargets in the RAS-ERK Pathway. *Trends in Cancer* **xx**. doi:10.1016/j.trecan.2018.07.002

Germann UA, Furey BF, Markland W, Hoover RR, Aronov AM, Roix JJ, Hale M, Boucher DM, Sorrell DA, Martinez-Botella G, Fitzgibbon M, Shapiro P, Wick MJ, Samadani R, Meshaw K, Groover A, DeCrescenzo G, Namchuk M, Emery CM, Saha S, Welsch DJ. 2017. Targeting the MAPK signaling pathway in cancer: Promising preclinical activity with the novel selective ERK1/2 inhibitor BVD-523 (ulixertinib). *Mol Cancer Ther* **16**:2351–2363. doi:10.1158/1535-7163.MCT-17-0456

Gervais M, Dugourd C, Muller L, Ardidie C, Canton B, Loviconi L, Corvol P, Chneiweiss H, Monnot C. 2006. Akt Down-Regulates ERK1/2 Nuclear Localization and Angiotensin II-induced Cell Proliferation through PEA-15. *Mol Biol Cell* **17**:3940–3951. doi:10.1091/mbc.E06

Goetz EM, Ghandi M, Treacy DJ, Wagle N, Garraway LA. 2014. ERK Mutations Confer Resistance to Mitogen-Activated Protein Kinase Pathway Inhibitors. *Cancer Res* **85**:11–16. doi:10.1038/jid.2014.371

Haccard O, Jessus C. 2006. Oocyte maturation, mos and cyclins: A matter of synthesis. *Cell Cycle* **5**:1152–1159. doi:10.4161/cc.5.11.2800

Han J, Ulevitch J. 1994. Targeted by **2**:1–4.

Hannen R, Hauswald M, Bartsch JW. 2017. A rationale for targeting extracellular regulated kinases ERK1 and ERK2 in glioblastoma. *J Neuropathol Exp Neurol* **76**:838–847. doi:10.1093/jnen/nlx076

Hatano N, Mori Y, Oh-hora M, Kosugi A, Fujikawa T, Nakai N, Niwa H, Miyazaki JI, Hamaoka T, Ogata M. 2003. Essential role for ERK2 mitogen-activated protein kinase in placental development. *Genes to Cells* **8**:847–856. doi:10.1046/j.1365-2443.2003.00680.x

Heidorn SJ, Milagre C, Whittaker S, Nourry A, Niculescu-Duvas I, Dhomen N, Hussain J, Reis-Filho JS, Springer CJ, Pritchard C, Marais R. 2010. Kinase-Dead BRAF and Oncogenic RAS Cooperate to Drive Tumor Progression through CRAF. *Cell* **140**:209–221. doi:10.1016/j.cell.2009.12.040

Herrero A, Pinto A, Colón-Bolea P, Casar B, Jones M, Agudo-Ibáñez L, Vidal R, Tenbaum SP, Nuciforo P, Valdizán EM, Horvath Z, Orfi L, Pineda-Lucena A, Bony E, Keri G, Rivas G, Pazos A, Gozalbes R, Palmer HG, Hurlstone A, Crespo P. 2015. Small Molecule Inhibition of ERK Dimerization Prevents Tumorigenesis by RAS-ERK Pathway Oncogenes. *Cancer Cell* **28**:170–182. doi:10.1016/j.ccell.2015.07.001

Hu J, Yu H, Kornev AP, Zhao J, Filbert EL, Taylor SS, Shaw AS. 2011. Mutation that blocks ATP binding creates a pseudokinase stabilizing the scaffolding function of kinase suppressor of Ras, CRAF and BRAF. *Proc Natl Acad Sci U S A* **108**:6067–6072. doi:10.1073/pnas.1102554108

Huebner K, Ar-Rushdi A, Griffin CA, Isobe M, Kozak C, Emanuel BS, Nagarajan L, Cleveland JL, Bonner TI, Goldsborough MD. 1986. Actively transcribed genes in the raf oncogene group, located on the X chromosome in mouse and human. *Proc Natl Acad Sci U S A* **83**:3934–3938. doi:10.1073/pnas.83.11.3934

Ikawa S, Fukui M, Ueyama Y, Tamaoki N, Yamamoto T, Toyoshima K. 1988. B-raf, a new member of the raf family, is activated by DNA rearrangement. *Mol Cell Biol* **8**:2651–2654.

doi:10.1128/mcb.8.6.2651

Ishibe S, Joly D, Liu ZX, Cantley LG. 2004. Paxillin serves as an ERK-regulated scaffold for coordinating FAK and Rac activation in epithelial morphogenesis. *Mol Cell* **16**:257–267. doi:10.1016/j.molcel.2004.10.006

Jaiswal BS, Durinck S, Stawiski EW, Yin J, Wang W, Lin E, Moffat J, Martin SE, Modrusan Z, Seshagiri S. 2018. ERK Mutations and amplification confer resistance to ERK-inhibitor therapy. *Clin Cancer Res* **24**:4044–4055. doi:10.1158/1078-0432.CCR-17-3674

Jaumot M, Hancock JF. 2001. Protein phosphatases 1 and 2A promote Raf-1 activation by regulating 14-3-3 interactions. *Oncogene* **20**:3949–3958. doi:10.1038/sj.onc.1204526

Jha S, Morris EJ, Hruza A, Mansueto MS, Schroeder GK, Arbanas J, McMasters D, Restaino CR, Dayananth P, Black S, Elsen NL, Mannarino A, Cooper A, Fawell S, Zawel L, Jayaraman L, Samatar AA. 2016. Dissecting therapeutic resistance to ERK inhibition. *Mol Cancer Ther* **15**:548–559. doi:10.1158/1535-7163.MCT-15-0172

Johannessen CM, Boehm JS, Kim SY, Thomas SR, Wardwell L, Johnson LA, Emery CM, Stransky N, Cogdill AP, Barretina J, Caponigro G, Hieronymus H, Murray RR, Salehi-Ashtiani K, Hill DE, Vidal M, Zhao JJ, Yang X, Alkan O, Kim S, Harris JL, Wilson CJ, Myer VE, Finan PM, Root DE, Roberts TM, Golub T, Flaherty KT, Dummer R, Weber BL, Sellers WR, Schlegel R, Wargo JA, Hahn WC, Garraway LA. 2010. COT drives resistance to RAF inhibition through MAP kinase pathway reactivation. *Nature* **468**:968–972. doi:10.1038/nature09627

Kaoud TS, Johnson WH, Ebelt ND, Piserchio A, Zamora-olivares D, Ravenstein SX Van, Pridgen JR, Edupuganti R, Sammons R, Cano M, Warthaka M, Harger M, Tavares CDJ, Park J, Radwan MF, Ren P, Anslyn E V, Tsai KY, Ghose R, Dalby KN. 2019. Modulating multi-funtional ERK complexes by covalent targeting of a recruitment site in vivo. *Nat Commun* 1–15. doi:10.1038/s41467-019-12996-8

Karlsson M, Mathers J, Dickinson RJ, Mandl M, Keyse SM. 2004. Both nuclear-cytoplasmic shuttling of the dual specificity phosphatase MKP-3 and its ability to anchor MAP kinase in the cytoplasm are mediated by a conserved nuclear export signal. *J Biol Chem* **279**:41882–41891. doi:10.1074/jbc.M406720200

Khokhlatchev A V., Canagarajah B, Wilsbacher J, Robinson M, Atkinson M, Goldsmith E, Cobb MH. 1998. Phosphorylation of the MAP kinase ERK2 promotes its homodimerization and nuclear translocation. *Cell* **93**:605–615. doi:10.1016/S0092-8674(00)81189-7

Kidger AM, Rushworth LK, Stellzig J, Davidson J, Bryant CJ, Bayley C, Caddye E, Rogers T, Keyse SM, Caunt CJ. 2017. Dual-specificity phosphatase 5 controls the localized inhibition, propagation, and transforming potential of ERK signaling. *Proc Natl Acad Sci U S A* **114**:E317–E326. doi:10.1073/pnas.1614684114

Kluba M, Engelborghs Y, Hofkens J, Mizuno H. 2015. Inhibition of receptor dimerization as a novel negative feedback mechanism of EGFR signaling. *PLoS One* **10**:1–21. doi:10.1371/journal.pone.0139971

Kolch W. 2005. Coordinating ERK/MAPK signalling through scaffolds and inhibitors. *Nat Rev Mol Cell Biol* **6**:827–837. doi:10.1038/nrm1743

Kozar I, Margue C, Rothengatter S, Haan C, Kreis S. 2019. Many ways to resistance: How melanoma cells evade targeted therapies. *Biochim Biophys Acta - Rev Cancer* **1871**:313–322. doi:10.1016/j.bbcan.2019.02.002

Krens SFG, He S, Lamers GEM, Meijer AH, Bakkers J, Schmidt T, Spaink HP, Snaar-Jagalska

BE. 2008. Distinct functions for ERK1 and ERK2 in cell migration processes during zebrafish gastrulation. *Dev Biol* **319**:370–383. doi:10.1016/j.ydbio.2008.04.032

Lake D, Corrêa SAL, Müller J. 2016. Negative feedback regulation of the ERK1/2 MAPK pathway. *Cell Mol Life Sci* **73**:4397–4413. doi:10.1007/s00018-016-2297-8

Lavoie H, Sahmi M, Maisonneuve P, Marullo SA, Thevakumaran N, Jin T, Kurinov I, Sicheri F, Therrien M. 2018. MEK drives BRAF activation through allosteric control of KSR proteins. *Nature* **554**:549–553. doi:10.1038/nature25478

Lavoie H, Therrien M. 2015. Regulation of RAF protein kinases in ERK signalling. *Nat Rev Mol Cell Biol* **16**:281–298. doi:10.1038/nrm3979

Lechtenberg BC, Mace PD, Sessions EH, Williamson R, Stalder R, Wallez Y, Roth GP, Riedl SJ, Pasquale EB. 2017. Structure-Guided Strategy for the Development of Potent Bivalent ERK Inhibitors. *ACS Med Chem Lett* **8**:726–731. doi:10.1021/acsmedchemlett.7b00127

Lee JC, Laydon JT, McDonnell PC, Gallagher TF, Kumar S, Green D, McNulty D, Blumenthal MJ, Keys JR, Land Vatter SW, Strickler JE, McLaughlin MM, Siemens IR, Fisher SM, Livi GP, White JR, Adams JL, Young PR. 1994. A protein kinase involved in the regulation of inflammatory cytokine biosynthesis. *Nature*. doi:10.1038/372739a0

Lee JD, Ulevitch RJ HJ. 1995. Primary structure of BMK1: a new mammalian MAP kinase.

Lefloch R, Pouysségur J, Lenormand P. 2009. Total ERK1/2 activity regulates cell proliferation. *Cell Cycle* **8**:705–711. doi:10.4161/cc.8.5.7734

Levchenko A, Bruck J, Sternberg PW. 2000. Scaffold proteins may biphasically affect the levels of mitogen-activated protein kinase signaling and reduce its threshold properties. *Proc Natl Acad Sci* **97**:5818–5823. doi:10.1073/pnas.97.11.5818

Lidke DS, Huang F, Post JN, Rieger B, Wilsbacher J, Thomas JL, Pouysségur J, Jovin TM, Lenormand P. 2010. ERK nuclear translocation is dimerization-independent but controlled by the rate of phosphorylation. *J Biol Chem* **285**:3092–3102. doi:10.1074/jbc.M109.064972

Lin LL, Wartmann M, Lin AY, Knopf JL, Seth A, Davis RJ. 1993. cPLA2 is phosphorylated and activated by MAP kinase. *Cell* **72**:269–278. doi:10.1016/0092-8674(93)90666-E

Liu F, Yang X, Geng M, Huang M. 2018. Targeting ERK, an Achilles' Heel of the MAPK pathway, in cancer therapy. *Acta Pharm Sin B* **8**:552–562. doi:10.1016/j.apsb.2018.01.008

Locasale JW, Shaw AS, Chakraborty AK. 2007. Scaffold proteins confer diverse regulatory properties to protein kinase cascades. *Proc Natl Acad Sci U S A* **104**:13307–12. doi:10.1073/pnas.0706311104

Longo PA, Jennifer KM, Min-Sung K, Daniel LJ. 2013. Transient mammilian cell transfection with Polyethylenimine (PEI). *NIH* **529**:227–240. doi:10.1016/j.biotechadv.2011.08.021.Secreted

Lorenz K, Schmitt JP, Schmitteckert EM, Lohse MJ. 2009. A new type of ERK1/2 autophosphorylation causes cardiac hypertrophy. *Nat Med* **15**:75–83. doi:10.1038/nm.1893

Luebker SA, Koepsell SA. 2019. Diverse mechanisms of BRAF inhibitor resistance in melanoma identified in clinical and preclinical studies. *Front Oncol* **9**:1–8. doi:10.3389/fonc.2019.00268

Mace PD, Wallez Y, Egger MF, Dobaczewska M k., Robisnson H, Pasquale EB, Riedl SJ. 2013. Structure of ERK2 bound to PEA-15 reveals a mechanism for rapid release of activated MAPK. *Nat Cell Biol* **5**:1–23. doi:10.1038/ncomms2687.Structure

Manning BD, Toker A. 2017. AKT/PKB Signaling: Navigating the Network. *Cell* **169**:381–405. doi:10.1016/j.cell.2017.04.001

Marusiak AA, Edwards ZC, Hugo W, Trotter EW, Girotti MR, Stephenson NL, Kong X, Gartside MG, Fawdar S, Hudson A, Breitwieser W, Hayward NK, Marais R, Lo RS, Brognard J. 2014. Mixed lineage kinases activate MEK independently of RAF to mediate resistance to RAF inhibitors. *Nat Commun* **5**:1–11. doi:10.1038/ncomms4901

Matheny SA, Chen C, Kortum RL, Razidlo GL, Lewis RE, White MA. 2004. Ras regulates assembly of mitogenic signalling complexes through the effector protein IMP. *Nature* **427**:256–260. doi:10.1038/nature02237

Matsubayashi Y, Fukuda M, Nishida E. 2001. Evidence for Existence of a Nuclear Pore Complex-mediated, Cytosol-independent Pathway of Nuclear Translocation of ERK MAP Kinase in Permeabilized Cells. *J Biol Chem* **276**:41755–41760. doi:10.1074/jbc.M106012200

Mauricio Burotto1, 3, Victoria L. Chiou1, Jung-Min Lee1 and ECK. 2014. The MAPK pathway across different malignancies: A new perspective. *Cancer* **120**:3446–3456. doi:10.1002/cncr.28864.The

McArthur GA, Chapman PB, Robert C, Larkin J, Haanen JB, Dummer R, Ribas A, Hogg D, Hamid O, Ascierto PA, Garbe C, Testori A, Maio M, Lorigan P, Lebbé C, Jouary T, Schadendorf D, O'Day SJ, Kirkwood JM, Eggermont AM, Dréno B, Sosman JA, Flaherty KT, Yin M, Caro I, Cheng S, Trunzer K, Hauschild A. 2014. Safety and efficacy of vemurafenib in BRAFV600E and BRAFV600K mutation-positive melanoma (BRIM-3): Extended follow-up of a phase 3, randomised, open-label study. *Lancet Oncol* **15**:323–332. doi:10.1016/S1470-2045(14)70012-9

McKay MM, Morrison DK. 2007. Integrating signals from RTKs to ERK/MAPK. *Oncogene* **26**:3113–3121. doi:10.1038/sj.onc.1210394

McKay MM, Ritt DA, Morrison DK. 2009. Signaling dynamics of the KSR1 scaffold complex. *Proc Natl Acad Sci U S A* **106**:11022–11027. doi:10.1073/pnas.0901590106

McReynolds. A, Karra AS, Yan L, Lopez ED, Turjanski, Adrian G. Dioum E, Lorenz K, Zaganjor E, Stippec S, McGlynn, Kathleen Earnest S, Cobb MH. 2016. Phosphorylation or mutation of the ERK2 activation loop alters oligonucleotide binding. *HHS* **55**:1909–1917. doi:10.1016/j.physbeh.2017.03.040

Michailidou C, Jones M, Walker P, Kamarashev J, Kelly A, Hurlstone AFL. 2009. Dissecting the roles of Raf- and PI3K-signalling pathways in melanoma formation and progression in a zebrafish model. *DMM Dis Model Mech* **2**:399–411. doi:10.1242/dmm.001149

Michaud NR, Fabian JR, Mathes KD, Morrison DK. 1995. 14-3-3 is not essential for Raf-1 function: identification of Raf-1 proteins that are biologically activated in a 14-3-3- and Ras-independent manner. *Mol Cell Biol* **15**:3390–3397. doi:10.1128/mcb.15.6.3390

Migliaccio N, Sanges C, Ruggiero I, Martucci NM, Rippa E, Arcari P, Lamberti A. 2013. Raf kinases in signal transduction and interaction with translation machinery. *Biomol Concepts* **4**:391–399. doi:10.1515/bmc-2013-0003

Miyamoto Y, Yamada K, Yoneda Y. 2016. Importin α: a key molecule in nuclear transport and non-transport functions. *J Biochem* **160**:69–75. doi:10.1093/jb/mvw036

Moelling K, Heimann B, Beimling P, Rapp UR, Sander T. 1984. Serine- and threonine-specific protein kinase activities of purified gag-mil and gag-raf proteins. *Nature* **312**:558–561. doi:10.1038/312558a0

Moelling SZ and Ka. 1999. Phosphorylation and Regulation of Raf by Akt (Protein Kinase B). *Science (80-)*.

Morris EJ, Jha S, Restaino CR, Dayananth P, Zhu H, Cooper A, Carr D, Deng Y, Jin W, Black S, Long B, Liu J, DiNunzio E, Windsor W, Zhang R, Zhao S, Angagaw MH, Pinheiro EM, Desai J, Xiao L, Shipps G, Hruza A, Wang J, Kelly J, Paliwal S, Gao X, Babu BS, Zhu L, Daublain P, Zhang L, Lutterbach BA, Pelletier MR, Philippar U, Siliphaivanh P, Witter D, Kirschmeier P, Robert Bishop W, Hicklin D, Gary Gillil D, Jayaraman L, Zawel L, Fawell S, Samatar AA. 2013. Discovery of a novel ERK inhibitor with activity in models of acquired resistance to BRAF and MEK inhibitors. *Cancer Discov* **3**:742–750. doi:10.1158/2159-8290.CD-13-0070

Morrison DK. 2001. KSR: A MAPK scaffold of the Ras pathway? *J Cell Sci* **114**:1609–1612.

Moschos SJ, Sullivan RJ, Hwu WJ, Ramanathan RK, Adjei AA, Fong PC, Shapira-Frommer R, Tawbi HA, Rubino J, Rush TS, Zhang D, Miselis NR, Samatar AA, Chun P, Rubin EH, Schiller J, Long BJ, Dayananth P, Carr D, Kirschmeier P, Bishop WR, Deng Y, Cooper A, Shipps GW, Moreno BH, Robert L, Ribas A, Flaherty KT. 2018. Development of MK-8353, an orally administered ERK1/2 inhibitor, in patients with advanced solid tumors. *JCI insight* **3**. doi:10.1172/jci.insight.92352

Murphy LO, Smith S, Chen RH, Fingar DC, Blenis J. 2002. Molecular, interpretation of ERK signal duration by immediate early gene products. *Nat Cell Biol* **4**:556–564. doi:10.1038/ncb822

Nakopoulou L, Mylona E, Rafailidis P, Alexandrou P, Giannopoulou I, Keramopoulos A. 2005. Effect of different ERK2 protein localizations on prognosis of patients with invasive breast carcinoma. *Apmis* **113**:693–701. doi:10.1111/j.1600-0463.2005.apm_236.x

Nguyen A, Burack WR, Stock JL, Kortum R, Chaika O V, Afkarian M, Muller WJ, Murphy KM, Morrison DK, Lewis RE, McNeish J, Shaw AS. 2002. Kinase suppressor of Ras (KSR) is a scaffold which facilitates mitogen-activated protein kinase activation in vivo. *Mol Cell Biol* **22**:3035–45. doi:10.1128/MCB.22.9.3035

Oppermann FS, Gnad F, Olsen J V., Hornberger R, Greff Z, Kéri G, Mann M, Daub H. 2009. Large-scale proteomics analysis of the human kinome. *Mol Cell Proteomics* **8**:1751–1764. doi:10.1074/mcp.M800588-MCP200

Pagès G, Guérin S, Grall D, Bonino F, Smith A, Anjuere F, Auberger P, Pouysségur J. 1999. Defective thymocyte maturation in p44 MAP kinase (Erk 1) knockout mice. *Science (80-)* **286**:1374–1378.

Pan C, Jin X, Zhao Y, Pan Y, Yang J, Karnes RJ, Zhang J, Wang L, Huang H. 2017. AKT - phosphorylated FOXO 1 suppresses ERK activation and chemoresistance by disrupting IQGAP 1- MAPK interaction. *EMBO J* **36**:995–1010. doi:10.15252/embj.201695534

Pegram LM, Liddle JC, Xiao Y, Hoh M, Rudolph J, Iverson DB, Vigers GP, Smith D, Zhang H, Wang W, Moffat JG, Ahn NG. 2019. Activation loop dynamics are controlled by conformation-selective inhibitors of ERK2. *Proc Natl Acad Sci U S A* **116**:15463–15468. doi:10.1073/pnas.1906824116

Philipova R, Whitaker M. 2005. Active ERK1 is dimerized in vivo: Bisphosphodimers generate peak kinase activity and monophosphodimers maintain basal ERK1 activity. *J Cell Sci* **118**:5767–5776. doi:10.1242/jcs.02683

Piserchio A, Ramakrishan V, Wang H, Kaoud TS, Arshava B, Dutta K, Dalby KN, Ghose R. 2015. Structural and dynamic features of F-recruitment site driven substrate phosphorylation by ERK2. *Sci Rep* **5**:1–18. doi:10.1038/srep11127

Piserchio A, Warthaka M, Devkota AK, Kaoud TS, Lee S, Abramczyk O, Ren P, Dalby KN, Ghose R. 2011. Solution NMR insights into docking interactions involving inactive ERK2. *Biochemistry* **50**:3660–3672. doi:10.1021/bi2000559

Plotnikov A, Chuderland D, Karamansha Y, Livnah O, Seger R. 2019. Nuclear ERK translocation is mediated by protein kinase CK2 and accelerated by autophosphorylation. *Cell Physiol Biochem* **53**:366–387. doi:10.33594/000000144

Plotnikov A, Flores K, Maik-Rachline G, Zehorai E, Kapri-Pardes E, Berti DA, Hanoch T, Besser MJ, Seger R. 2015. The nuclear translocation of ERK1/2 as an anticancer target. *Nat Commun* **6**:1–11. doi:10.1038/ncomms7685

Plotnikov A, Zehorai E, Procaccia S, Seger R. 2011. The MAPK cascades: Signaling components, nuclear roles and mechanisms of nuclear translocation. *Biochim Biophys Acta - Mol Cell Res* **1813**:1619–1633. doi:10.1016/j.bbamcr.2010.12.012

Procaccia S, Ordan M, Cohen I, Bendetz-Nezer S, Seger R. 2017. Direct binding of MEK1 and MEK2 to AKT induces Foxo1 phosphorylation, cellular migration and metastasis. *Sci Rep* **7**:1–16. doi:10.1038/srep43078

Pulido R, Zúñiga Á, Ullrich A. 1998. PTP-SL and STEP protein tyrosine phosphatases regulate the activation of the extracellular signal-regulated kinases ERK1 and ERK2 by association through a kinase interaction motif. *EMBO J* **17**:7337–7350. doi:10.1093/emboj/17.24.7337

Pullikuth A, McKinnon E, Schaeffer H, Catling AD. 2005. The MEK1 scaffolding protein MP1 regulates cell spreading by integrating PAK1 and Rho signals. *Mol Cell Biol* **25**:5119–33. doi:10.1128/MCB.25.12.5119-5133.2005

Rajakulendran T, Sahmi M, Lefrançois M, Sicheri F, Therrien M. 2009. A dimerization-dependent mechanism drives RAF catalytic activation. *Nature* **461**:542–545. doi:10.1038/nature08314

Ray LB, Sturgill TW. 1987. Rapid stimulation by insulin of a serine/threonine kinase in 3T3-L1 adipocytes that phosphorylates microtubule-associated protein 2 in vitro (ribosomal protein S6 kinase/phosphatase inhibitors). *Proc Natl Acad Sci U S A* **84**:1502–1506. doi:10.1073/pnas.84.6.1502

Rian H, Krens SFG, Spaink HP, Snaar-Jagalska BE. 2013. Generation of Constitutive Active ERK Mutants as Tools for Cancer Research in Zebrafish. *ISRN Cell Biol* **2013**:1–11. doi:10.1155/2013/867613

Ritt DA, Monson DM, Specht SI, Morrison DK. 2010. Impact of Feedback Phosphorylation and Raf Heterodimerization on Normal and Mutant B-Raf Signaling. *Mol Cell Biol* **30**:806–819. doi:10.1128/mcb.00569-09

Robbins DJ, Zhen E, Cheng M, Xu S, Vanderbilt CA, Ebert D, Garcia C, Dang A, Cobb MH. 1993. Regulation and properties of extracellular signal-regulated protein kinases 1 and 2 in vitro. *J Am Soc Nephrol* **4**:1104–1110.

Robinson FL, Whitehurst AW, Raman M, Cobb MH. 2002. Identification of Novel Point Mutations in ERK2 That Selectively Disrupt Binding to MEK1. *J Biol Chem* **277**:14844–14852. doi:10.1074/jbc.M107776200

Robinson MJ, Stippec SA, Goldsmith E, White MA, Cobb MH. 1998. A constitutively active and nuclear form of the MAP kinase ERK2 is sufficient for neurite outgrowth and cell transformation. *Curr Biol* **8**:1141–1152. doi:10.1016/s0960-9822(07)00485-x

Roskoski R. 2012a. ERK1/2 MAP kinases: Structure, function, and regulation. *Pharmacol Res* **66**:105–143. doi:10.1016/j.phrs.2012.04.005

Roskoski R. 2012b. MEK1/2 dual-specificity protein kinases: Structure and regulation. *Biochem Biophys Res Commun* **417**:5–10. doi:10.1016/j.bbrc.2011.11.145

Rossomando AJ, Wu J, Michel H, Shabanowitz J, Hunt DF, Weber MJ, Sturgill TW. 1992. Identification of Tyr-185 as the site of tyrosine autophosphorylation of recombinant mitogen-activated protein kinase p42(mapk). *Proc Natl Acad Sci U S A* **89**:5779–5783. doi:10.1073/pnas.89.13.5779

Rouse J, Cohen P, Trigon S, Morange M, Alonso-Llamazares A, Zamanillo D, Hunt T, Nebreda AR. 1994. A novel kinase cascade triggered by stress and heat shock that stimulates MAPKAP kinase-2 and phosphorylation of the small heat shock proteins. *Cell* **78**:1027–1037. doi:10.1016/0092-8674(94)90277-1

Roy M, Li Z, Sacks DB. 2005. IQGAP1 Is a Scaffold for Mitogen-Activated Protein Kinase Signaling. *Mol Cell Biol* **25**:7940–7952. doi:10.1128/mcb.25.18.7940-7952.2005

Rushworth LK, Hindley AD, O'Neill E, Kolch W. 2006. Regulation and Role of Raf-1/B-Raf Heterodimerization. *Mol Cell Biol* **26**:2262–2272. doi:10.1128/mcb.26.6.2262-2272.2006

Ryan MB, Corcoran RB. 2018. Therapeutic strategies to target RAS-mutant cancers. *Nat Rev Clin Oncol* **15**:709–720. doi:10.1038/s41571-018-0105-0

Ryan MB, Der CJ, Wang-Gillam A, Cox AD. 2015. Targeting RAS-mutant Cancers: Is ERK the Key? *Trends in Cancer* **1**:183–198. doi:10.1016/j.trecan.2015.10.001

Saba-El-Leil MK, Frémin C, Meloche S. 2016. Redundancy in the world of MAP kinases: All for one. *Front Cell Dev Biol* **4**:1–9. doi:10.3389/fcell.2016.00067

Saba-El-Leil MK, Vella FDJ, Vernay B, Voisin L, Chen L, Labrecque N, Ang SL, Meloche S. 2003. An essential function of the mitogen-activated protein kinase Erk2 in mouse trophoblast development. *EMBO Rep* **4**:964–968. doi:10.1038/sj.embor.embor939

Saei, Eichhorn. 2019. Adaptive Responses as Mechanisms of Resistance to BRAF Inhibitors in Melanoma. *Cancers (Basel)* **11**:1176. doi:10.3390/cancers11081176

Samatar AA, Poulikakos PI. 2014. Targeting RAS-ERK signalling in cancer: Promises and challenges. *Nat Rev Drug Discov* **13**:928–942. doi:10.1038/nrd4281

Sang D, Pinglay S, Wiewiora RP, Selvan ME, Lou HJ, Chodera JD, Turk BE, Gümüş ZH, Holt LJ. 2019. Ancestral reconstruction reveals mechanisms of erk regulatory evolution. *Elife* **8**:1–28. doi:10.7554/eLife.38805

Sanz-Moreno V, Casar B, Crespo P. 2003. p38 Isoform Mxi2 Binds to Extracellular Signal-Regulated Kinase 1 and 2 Mitogen-Activated Protein Kinase and Regulates Its Nuclear Activity by Sustaining Its Phosphorylation Levels. *Mol Cell Biol* **23**:3079–3090. doi:10.1128/mcb.23.9.3079-3090.2003

Schaeffer HJ. 1998. MP1: A MEK Binding Partner That Enhances Enzymatic Activation of the MAP Kinase Cascade. *Science (80-)* **281**.

Schevzov G, Kee AJ, Wang B, Sequeira VB, Hook J, Coombes JD, Lucas CA, Stehn JR, Musgrove EA, Cretu A, Assoian R, Fath T, Hanoch T, Seger R, Pleines I, Kile BT, Hardeman EC, Gunning PW. 2015. Regulation of cell proliferation by ERK and signal-dependent nuclear translocation of ERK is dependent on Tm5NM1-containing actin filaments. *Mol Biol Cell* **26**:2475–2490. doi:10.1091/mbc.E14-10-1453

Shaul YD, Seger R. 2007. The MEK/ERK cascade: From signaling specificity to diverse functions. *Biochim Biophys Acta - Mol Cell Res* **1773**:1213–1226. doi:10.1016/j.bbamcr.2006.10.005

Smorodinsky-Atias K, Goshen-Lago T, Goldberg-Carp A, Melamed D, Shir A, Mooshayef N, Beenstock J, Karamansha Y, Darlyuk-Saadon I, Livnah O, Ahn NG, Admon A, Engelberg D. 2016. Intrinsically active variants of Erk oncogenically transform cells and disclose unexpected autophosphorylation capability that is independent of TEY phosphorylation. *Mol Biol Cell* **27**:1026–1039. doi:10.1091/mbc.E15-07-0521

Sturm OE, Orton R, Grindlay J, Birtwistle M, Vyshemirsky V, Gilbert D, Calder M, Pitt A, Kholodenko B, Kolch W. 2010. The mammalian MAPK/ERK pathway exhibits properties of a negative feedback amplifier. *Sci Signal* **3**:1–8. doi:10.1126/scisignal.2001212

Takekawa M, Tatebayashi K, Saito H. 2005. Conserved docking site is essential for activation of mammalian MAP kinase kinases by specific MAP kinase kinase kinases. *Mol Cell* **18**:295–306. doi:10.1016/j.molcel.2005.04.001

Taylor CA, Cormier KW, Keenan SE, Earnest S, Stippec S, Wichaidit C, Juang YC, Wang J, Shvartsman SY, Goldsmith EJ, Cobb MH. 2019. Functional divergence caused by mutations in an energetic hotspot in ERK2. *Proc Natl Acad Sci U S A* **116**:15514–15523. doi:10.1073/pnas.1905015116

Teis D, Taub N, Kurzbauer R, Hilber D, De Araujo ME, Erlacher M, Offterdinger M, Villunger A, Geley S, Bohn G, Klein C, Hess MW, Huber LA. 2006. p14-MP1-MEK1 signaling regulates endosomal traffic and cellular proliferation during tissue homeostasis. *J Cell Biol* **175**:861–868. doi:10.1083/jcb.200607025

Teis D, Wunderlich W, Huber LA. 2002. Localization of the MP1-MAPK scaffold complex to endosomes is mediated by p14 and required for signal transduction. *Dev Cell* **3**:803–814. doi:10.1016/S1534-5807(02)00364-7

Therrien M, Michaud NR, Rubin GM, Morrison DK. 1996. KSR modulates signal propagation within the MAPK cascade. *Genes Dev* **10**:2684–2695. doi:10.1101/gad.10.21.2684

Torii S, Kusakabe M, Yamamoto T, Maekawa M, Nishida E. 2004. Sef is a spatial regulator for Ras/MAP kinase signaling. *Dev Cell* **7**:33–44. doi:10.1016/j.devcel.2004.05.019

Traverse S, Gomez N, Paterson H, Marshall C, Cohen P. 1992. Sustained activation of the mitogen-activated protein (MAP) kinase cascade may be required for differentiation of PC12 cells. Comparison of the effects of nerve growth factor and epidermal growth factor. *Biochem J* **288**:351–355. doi:10.1042/bj2880351

Tsang M, Friesel R, Kudoh T, Dawid IB. 2002. Identification of sef, a novel modulator of FGF signalling. *Nat Cell Biol* **4**:165–169. doi:10.1038/ncb749

Turjanski AG, Vaqué JP, Gutkind JS. 2007. MAP kinases and the control of nuclear events. *Oncogene* **26**:3240–3253. doi:10.1038/sj.onc.1210415

Turriziani B, Garcia-Munoz A, Pilkington R, Raso C, Kolch W, von Kriegsheim A. 2014. On-beads digestion in conjunction with data-dependent mass spectrometry: A shortcut to quantitative and dynamic interaction proteomics. *Biology (Basel)* **3**:320–332.

doi:10.3390/biology3020320

Ünal EB, Uhlitz F, Blüthgen N. 2017. A compendium of ERK targets. *FEBS Lett* **591**:2607–2615. doi:10.1002/1873-3468.12740

Vdzina C, Czerkawski H, Saucier R, Vdzina C, Higashide E, Shibata M, Horii S, Mizuno K, Nakano H, Matsuda Y, Ito K, Ohkubo S, Tomita F, Horii S, Fukase H, Mizuta E, Hatano K, Yoshida M, Tomita F, Radics L, Rakhit S, Yoshihira K, Highet RJ, Wei TT, Okubo S, Tomita F, Flon H, Asheshov IN, Wei T, Byrne KM, Tamaoki T, Yarmolinsky MB. 1984. The Human Homologs of the raf (mil) Oncogene Are located on Human Chromosomes 3 and 4. *Science (80-)* **223**:71–74.

Villanueva J, Vultur A, Lee JT, Somasundaram R, Cipolla AK, Wubbenhorst B, Xu X, Phyllis A, Kee D, Santiago-walker AE, Letrero R, Andrea KD, Pushparajan A, Hayden JE, Brown KD, Laquerre S, Mcarthur GA, Sosman JA, Nathanson KL, Herlyn M. 2010. Acquired resistance to BRAF inhibitors mediated by a RAF kinase switch in melanoma can be overcome by co-targeting MEK and IGF-1R/PI3K. *Cancer Cell* **18**:683–695. doi:10.1016/j.ccr.2010.11.023.Acquired

Voisin L, Saba-El-Leil MK, Julien C, Fremin C, Meloche S. 2010. Genetic Demonstration of a Redundant Role of Extracellular Signal-Regulated Kinase 1 (ERK1) and ERK2 Mitogen-Activated Protein Kinases in Promoting Fibroblast Proliferation. *Mol Cell Biol* **30**:2918–2932. doi:10.1128/mcb.00131-10

Vomastek T, Schaeffer HJ, Tarcsafalvi A, Smolkin ME, Bissonette EA, Weber MJ. 2004. Modular construction of a signaling scaffold: MORG1 interacts with components of the ERK cascade and links ERK signaling to specific agonists. *Proc Natl Acad Sci U S A* **101**:6981–6986. doi:10.1073/pnas.0305894101

Von Kriegsheim A, Baiocchi D, Birtwistle M, Sumpton D, Bienvenut W, Morrice N, Yamada K, Lamond A, Kalna G, Orton R, Gilbert D, Kolch W. 2009. Cell fate decisions are specified by the dynamic ERK interactome. *Nat Cell Biol* **11**:1458–1464. doi:10.1038/ncb1994

Wang X, Finegan KG, Robinson AC, Knowles L, Khosravi-Far R, Hinchliffe KA, Boot-Handford RP, Tournier C. 2006. Activation of extracellular signal-regulated protein kinase 5 downregulates FasL upon osmotic stress. *Cell Death Differ* **13**:2099–2108. doi:10.1038/sj.cdd.4401969

White CD, Brown MD, Sacks DB. 2009. IQGAPs in cancer: A family of scaffold proteins underlying tumorigenesis. *FEBS Lett* **583**:1817–1824. doi:10.1016/j.febslet.2009.05.007

Whitehurst AW, Wilsbacher JL, You Y, Luby-Phelps K, Moore MS, Cobb MH. 2002. ERK2 enters the nucleus by a carrier-independent mechanism. *Proc Natl Acad Sci U S A* **99**:7496–7501. doi:10.1073/pnas.112495999

Wilsbacher JL, Juang Y, Khokhlatchev A V, Gallagher E, Binns D, Goldsmith EJ, Cobb MH, May R V, Re V, Recei M, September V. 2006. Characterization of Mitogen-Activated Protein Kinase (MAPK) Dimers **2**:13175–13182.

Wortzel I, Seger R. 2011. The ERK cascade: Distinct functions within various subcellular organelles. *Genes and Cancer* **2**:195–209. doi:10.1177/1947601911407328

Wu PK, Hong SK, Yoon SH, Park JI. 2015. Active ERK2 is sufficient to mediate growth arrest and differentiation signaling. *FEBS J* **282**:1017–1030. doi:10.1111/febs.13197

Xiao Y, Al. E. 2014. Phosphorylation releases constraints to domain motion in ERK2. *PNAS* **98**:956–961. doi:10.1073/pnas.98.3.956

Xiong S, Zhao Q, Rong Z, Huang G, Huang Y, Chen P, Zhang S, Liu L, Chang Z. 2003. hSef Inhibits PC-12 Cell Differentiation by Interfering with Ras-Mitogen-activated Protein Kinase MAPK Signaling. *J Biol Chem* **278**:50273–50282. doi:10.1074/jbc.M306936200

Yaeger R, Corcoran RB. 2019. Targeting alterations in the RAF–MEK pathway. *Cancer Discov* **9**:329–341. doi:10.1158/2159-8290.CD-18-1321

Yang JY, Zong CS, Xia W, Yamaguchi H, Ding Q, Xie X, Lang JY, Lai CC, Chang CJ, Huang WC, Huang H, Kuo HP, Lee DF, Li LY, Lien HC, Cheng X, Chang KJ, Hsiao CD, Tsai FJ, Tsai CH, Sahin AA, Muller WJ, Mills GB, Yu D, Hortobagyi GN, Hung MC. 2008. ERK promotes tumorigenesis by inhibiting FOXO3a via MDM2-mediated degradation. *Nat Cell Biol* **10**:138–148. doi:10.1038/ncb1676

Yang L, Zheng L, Chng WJ, Ding JL. 2019. Comprehensive Analysis of ERK1/2 Substrates for Potential Combination Immunotherapies. *Trends Pharmacol Sci* **40**:897–910. doi:10.1016/j.tips.2019.09.005

Yao Z, Seger R. 2009. The ERK signaling cascade-views from different subcellular compartments. *BioFactors* **35**:407–416. doi:10.1002/biof.52

Yao Z, Yaeger R, Rodrik-Outmezguine VS, Tao A, Torres, Neilawattie M. Chang, Matthew T. Drosten M, Zhao H, Cecchi F, Hembrough T, Michels J, Baumert H, Miles L, Campbell NM, Stanchina E, Solit DB, Barbacid M, Barry S. T, Rosen N. 2017. Tumours with class 3 BRAF mutants are sensitive to the inhibition of activated RAS. *Nature* **548**:234–238. doi:10.1038/nature23291

Yoon S, Seger R. 2006. The extracellular signal-regulated kinase: Multiple substrates regulate diverse cellular functions. *Growth Factors* **24**:21–44. doi:10.1080/02699050500284218

Yuan J, Ng WH, Tian Z, Yap J, Baccarini M, Chen Z, Hu J. 2018. Activating mutations in MEK1 enhance homodimerization and promote tumorigenesis. *Sci Signal* **11**. doi:10.1126/scisignal.aar6795

Zaballos MA, Acuña-Ruiz A, Morante M, Crespo P, Santisteban P. 2019. Regulators of the RAS-ERK pathway as therapeutic targets in thyroid cancer. *Endocr Relat Cancer* **26**:R319–R344. doi:10.1530/ERC-19-0098

Zehorai E, Yao Z, Plotnikov A, Seger R. 2010. The subcellular localization of MEK and ERK-A novel nuclear translocation signal (NTS) paves a way to the nucleus. *Mol Cell Endocrinol* **314**:213–220. doi:10.1016/j.mce.2009.04.008

Zeke A, Bastys T, Alexa A, Garai Á, Mészáros B, Kirsch K, Dosztányi Z, Kalinina O V, Reményi A. 2015. Systematic discovery of linear binding motifs targeting an ancient protein interaction surface on MAP kinases . *Mol Syst Biol* **11**:837. doi:10.15252/msb.20156269

Zervos AS, Faccio L, Gatto JP, Kyriakis JM, Brent R. 1995. Mxi2, a mitogen-activated protein kinase that recognizes and phosphorylates Max protein. *Proc Natl Acad Sci U S A* **92**:10531–10534. doi:10.1073/pnas.92.23.10531

Zhang B-H. 2000. Activation of B-Raf kinase requires phosphorylation of the conserved residues Thr598 and Ser601. *EMBO J* **19**:5429–5439. doi:10.1093/emboj/19.20.5429

Zhang C, Spevak W, Zhang Y, Burton EA, Ma Y, Habets G, Zhang J, Lin J, Ewing T, Matusow B, Tsang G, Marimuthu A, Cho H, Wu G, Wang W, Fong D, Nguyen H, Shi S, Womack P, Nespi M, Shellooe R, Carias H, Powell B, Light E, Sanftner L, Walters J, Tsai J, West BL, Visor G, Rezaei H, Lin PS, Nolop K, Ibrahim PN, Hirth P, Bollag G. 2015. RAF inhibitors that evade paradoxical MAPK pathway activation. *Nature* **526**:583–586. doi:10.1038/nature14982

Zhang F, Strand A, Robbins D, Cobb MH, Goldsmith EJ. 1994. Atomic structure of the MAP kinase ERK2 at 2.3 Å resolution. *Nature* **367**:704–711. doi:10.1038/367704a0

Zheng CF, Guan KL. 1994. Activation of MEK family kinases requires phosphorylation of two conserved Ser/Thr residues. *EMBO J* **13**:1123–1131. doi:10.1002/j.1460-2075.1994.tb06361.x

Zmajkovicova K, Jesenberger V, Catalanotti F, Baumgartner C, Reyes G, Baccarini M. 2013. MEK1 Is Required for PTEN Membrane Recruitment, AKT Regulation, and the Maintenance of Peripheral Tolerance. *Mol Cell* **50**:43–55. doi:10.1016/j.molcel.2013.01.037

Zuo Q, Liu J, Huang L, Qin Y, Hawley T, Seo C, Yu Y, Cancer N, Institutes NC, Hospital N, Province G. 2019. AXL/AKT axis mediated-resistance to BRAF inhibitor depends on PTEN status in melanoma. *HHS Public Access* **37**:3275–3289. doi:10.1038/s41388-018-0205-4.AXL/AKT